Università degli Studi di Palermo
Facoltà di Medicina e Chirurgia

Dottorato di Ricerca in Oncopatologia Cellulare e Molecolare Clinica
(SSD Med 06)
XXII Ciclo
Coordinatore: ***Prof. E. Fiorentino***

Genetic and functional dissection of the miR-17~92 cluster of miRNAs

Ph.D. Thesis by:

Dr. Aleco D'Andrea

Tutor

Prof. A. Russo

Course Coordinator

Prof. E. Fiorentino

Co-Tutor

Prof. A. Ventura

A.A. 2008-2010

ABSTRACT

Background: The miR-17~92 cluster was among the first cluster of miRNAs to be linked to cancer. It is directly activated by the members of the MYC family of transcription factors and acts as a *bona fide* oncogene in several types of cancer, including lymphomas. miR-17~92 is essential for mammalian development. Knock-out mice die *in utero* or at birth with cardiovascular defects and impaired B-cell maturation.

Aims: Although miR-17~92 is important for tumorigenesis and development both the molecular mechanisms and the prominent miRNAs acting in different contexts are still unknown. The main aim of our study was to identify the role played by different members of the miR-17~92 cluster in B-cell lymphomas and vascular development.

Materials and Methods: A mouse model of B-cell lymphomas and a conditional *miR-17~92* KO mouse strain were employed to investigate the role of miR-17~92 in Myc-induced cancers. A GFP-based in vitro assay allowed us to rapidly verify the oncogenic potential of each miRNA family and to determine how mutations in the seed/non seed sequence affect miRNA function. Gene-expression profiling, computational prediction and an shRNA-mediated validation screening were used to identify miR-19 targets. miR-17~92 involvement in vascular development was studied by means of Real time, western blot, ELISA and the CD-31 (PECAM) vascular staining.

Results and Conclusions : Our results suggest that the expression of two members of the cluster, miR-19a and miR-19b, is necessary and largely sufficient to recapitulate the oncogenic potential of the full miR-17~92 cluster in Myc-driven B cell lymphomas. A systematic mutational analysis of miR-19b showed that single point mutation in the seed sequence impaired miR-19b anti-apoptotic activity. Finally, a chimeric miRNA (miR-19b seed/miR-20 non-seed) acted as effectively as miR-19b, suggesting that the specific sequence of non-seed region of miR-19 provides little additional substrate specificity. We identified the tumor suppressor PTEN as the critical miR-19b target and the principal mediator of its pro-survival activity. We also showed that miR-17~92–null embryos have upregulation of VEGF, although it is unclear at this time whether miR-17~92 suppresses VEGF expression directly or indirectly.

Introduction

miRNAs: functions and mechanism of action

MicroRNAs (miRNAs) are a group of non-coding regulatory RNAs, 20-22 nucleotides in length, which have been shown to regulate several cellular processes such as proliferation, differentiation, apoptosis, cell metabolism and angiogenesis [1].

MiRNAs are transcribed by the RNA Pol-II as pri-miRNAs and then processed into mature miRNAs by the sequential action of Drosha and Dicer ribonucleases [1] (Fig.1). Upon maturation, miRNAs are incorporated into the RNA-induced silencing complex (RISC). The key components of the RISC are the Argonaute (Ago) proteins. All Argonaute proteins share two main, highly conserved, structural features: the PAZ domain and the PIWI domain. The PAZ domain binds dsRNA while the PIWI domain has extensive homology to the RNAse H catalytic domain [2]. In humans, only Ago2 (slicer) has endonucleolitic activity [3].

miRNAs are able to coordinate the expression of entire sets of genes, thus finely tuning the mammalian transcriptome [1]. MiRNAs can regulate gene expression by recognizing specific binding sites in the 3′ untranslated region (UTR) of target mRNA molecules mainly through their seed sequence (nt.2-8). Additional complementary regions are often found in the non-seed sequence (nt.9-22) [1]. MiRNAs binding leads the degradation of the target mRNAs, to the inhibition of their translation, or both [1, 4]. In animals, it has been recently proposed that downregulation of target genes mostly occurs through mRNA destabilization, with only a very modest effect on translational efficiency [5].

To date over 1000 of miRNAs have been identified in humans. Interestingly, about 30% of miRNAs in both humans and mouse are organized in cluster [6-8]. They are transcribed as a single polycistronic unit that is rapidly processed in order to obtain the single mature miRNAs. Evolutionary, this organization facilitates functional overlap and cooperativity among miRNAs. This would allow several miRNAs to coordinately regulate multiple nodes belonging to the same pathway or different pathways in a timely fashion [7], although this hypothesis has not been formally tested yet.

In the last few years miRNAs have been shown to have a great impact in both normal cellular processes and cancer. They are highly conserved across vertebrates and have a fundamental role in controlling developmental pathways. Genes controlling developmental processes such as cell proliferation, cell death and differentiation are commonly associated with cancer, and many microRNAs are implicated in tumour development and progression [9]. In fact, a significant number of miRNAs is located in tumour susceptibility loci in mice [10]. miRNA ''signatures'' of human cancer have been found of great help for tumor classification and clinical outcome predictions [11, 12].

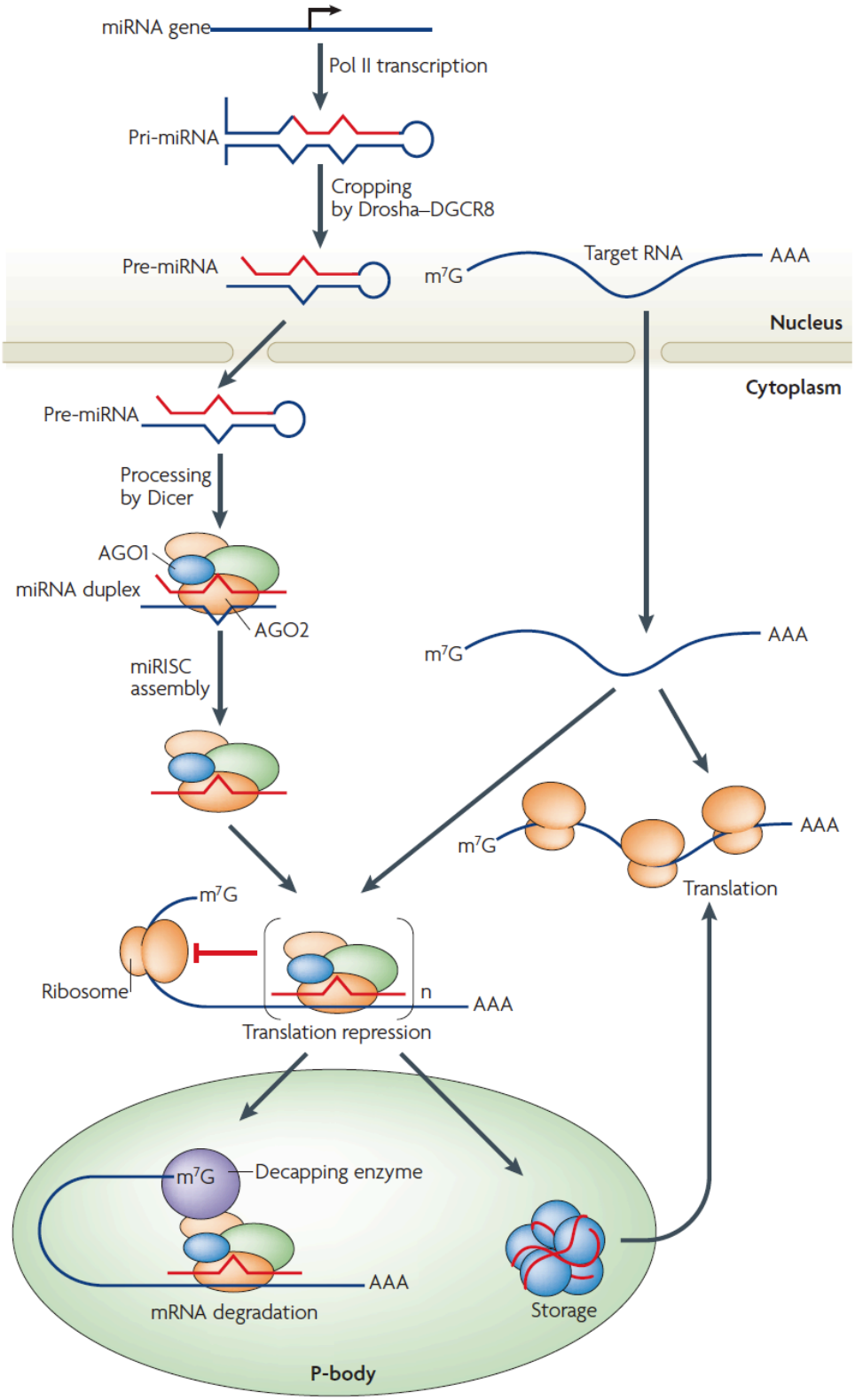

Fig. 1 miRNAs processing mechanism. miRNAs are transcribed in the nucleus as pri-miRNAs and subsequently processed by Drosha into pre-miRNAs. The pre-miRNA is exported to the cytoplasm and cleaved by dicer to produce the mature miRNA. Upon assembly into the RISC complex miRNAs are able to act on their targets through degradation of the messenger RNA, repression of translation or both (from *Rana et al*., 2007).

miR-17~92: The prototype of clustered miRNAs

miR-17~92 is a polycistronic miRNA cluster that encodes for 6 different miRNAs. It was first identified in 2004 as part of a frequent amplified region in diffuse large B cell lymphomas (13q31-q32) [13]. Based on their seed sequence, the miRNAs belonging to the cluster can be grouped into 4 different families: miR-17, miR-18, miR-19 and miR-92 (Fig.2). Each of these miRNAs can potentially regulate hundreds of target mRNAs. Moreover, coordinate expression of multiple miRNAs from the same locus allows them to cooperate in regulating several biological processes [14]. miR-17~92 known functions include regulation of cell cycle, proliferation, apoptosis and angiogenesis, and several targets have been identified to date including the tumor suppressor PTEN [15-17], the antiapoptotic protein Bim [18-21], and well-known cell cycle regulators such as p21 and E2F1[20, 22-25].
Moreover two paralog clusters, miR-106b~25 and miR-106a~363, have been identified on human chromosomes 7 and X respectively (Fig.2). The three clusters originated from a series of duplication and deletion events occurred during early vertebrate evolution [26]. The sequence of each miRNA component, as well as the spatial organization of these miRNAs within the mir-17~92 family, is highly conserved across species and among all three paralogs [26]. Because of their high homology they are likely to have overlapping functions and regulate a similar set of genes. In fact, members of the miR106b~25 cluster regulate cell cycle and promote proliferation by targeting E2F1 and p21/CDKN1A [20, 23, 27]. Unlike the miR-17~92 and miR-106b~25 clusters, which are both abundantly expressed across many tissues and cell types, mir-106a~363 cluster is expressed at very low or often undetectable level in both normal or cancer cells and tissue [18, 24]. Two recent reports have underlined the oncogenic potential of the miR-106a~363 cluster by showing that its promoter region is a frequent site of retroviral integration site [28, 29]. To date it remains unclear whether expression of this miRNA cluster is restricted to a specific cell type or it simply represents a non-functional pseudogene [30].

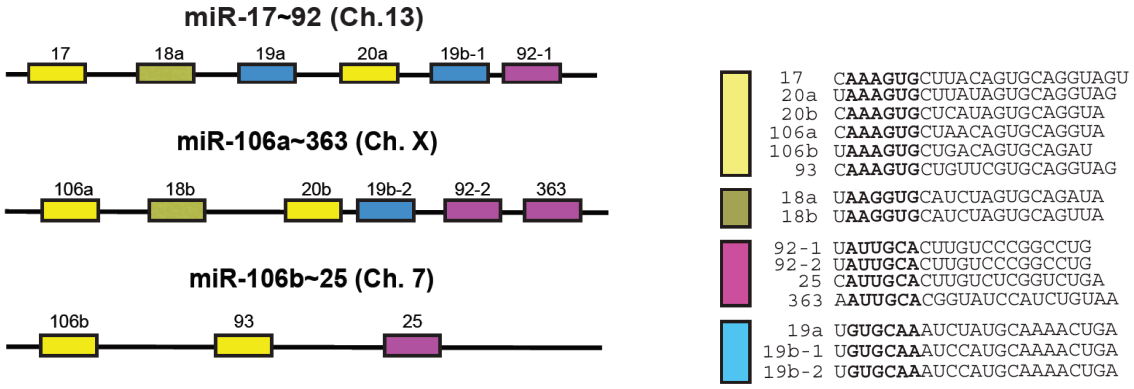

Fig.2 The miR-17 family of miRNA clusters. Spatial organization and seed families. (adapted from *Ventura et al.*, 2008).

miRNAs and development

The most striking evidence that miRNAs are absolutely required during mammalian development comes from the observation that the miRNA-processing factors Dicer, Drosha, Dgcr-8 and Ago-2 are essential for mouse viability [31]. Knock out mice individually lacking one of these factors die at early stages with multiple developmental defects [32-35].
More recently deletion of either single miRNAs or entire cluster have been performed to elucidate their role during development [31]. miR-155 was among the first miRNAs to be deleted in vivo [36, 37]. It was shown to have a prominent role in the mammalian immune system. Genetic ablation of this miRNA determines impaired B and T-cell response possibly due to deregulation of cytokine production [36, 37] and AID [38, 39].
The embryonic lethality of Dicer knockout mice was partially attributed to defective angiogenesis [32]. Several miRNAs are indeed able to regulate vascular development [40]. miR-126 was the first vascular miRNA to be knocked out in mice. Loss-of-function studies in mice and zebrafish revealed an important function of miR-126 in governing vascular integrity and angiogenesis [41, 42]. Targeted deletion of miR-126 was also associated with partial embryonic lethality and defective response of endothelial cells to angiogenic factors [41, 42].

miR-17~92 role in development

miR-17~92 is essential for mammalian development. The miR-17~92 knockout embryos die perinatally and are characterized by small size, defective ventricular septation in the heart, and hypoplastic lungs [18] (Fig. 3A, B, C). B-cell development is also strongly impaired in the absence of the cluster at the pro-B to pre-B transition stage [18] (Fig. 3D). Surprisingly, deletion of the miR-106b~25 and miR106a~363 paralogs, either alone or in combination, has no effects on mouse viability while compound mutants mice (miR-17~92$^{\Delta/\Delta}$; miR-106b~25$^{\Delta/\Delta)}$ and miR-17~92$^{\Delta/\Delta}$; miR-106b~25$^{\Delta/\Delta}$; miR-106a~363$^{\Delta/y}$) die at earlier stages (~E13.5-14.5) with increased apoptosis, extensive hemorrhages and edemas throughout the body [18](Fig. 3E). Interestingly, in 2000 *Miquerol et al*. described a similar phenotype linking cardiovascular defects and increased vascular permeability to elevated levels of the angiogenic factor VEGF-A [43]. VEGF signaling is essential during cardiovascular development; therefore its levels are tightly regulated from embryo development to adult life [44]. The importance of this gene is underlined by the finding that deletion of even a single VEGF allele causes embryonic lethality at early stages due to impaired angiogenesis [45, 46]. Deletion of the VEGF receptor flk-1, also leads to early embryonic lethality due to defective blood vessels formation [47]. Moreover VEGF is the most prominent angiogenic factor promoting tumor progression and a recognized therapeutic target [48]. Indeed, a link between the miR-17~92 family of microRNAs and VEGF has been recently established [49-51]. Members of the miR-17/20 family were shown to directly target VEGF and its major activator under hypoxia, Hif-1α, in tumor cells, thus finely tuning cell adaptation to low oxygen concentration [49-51].

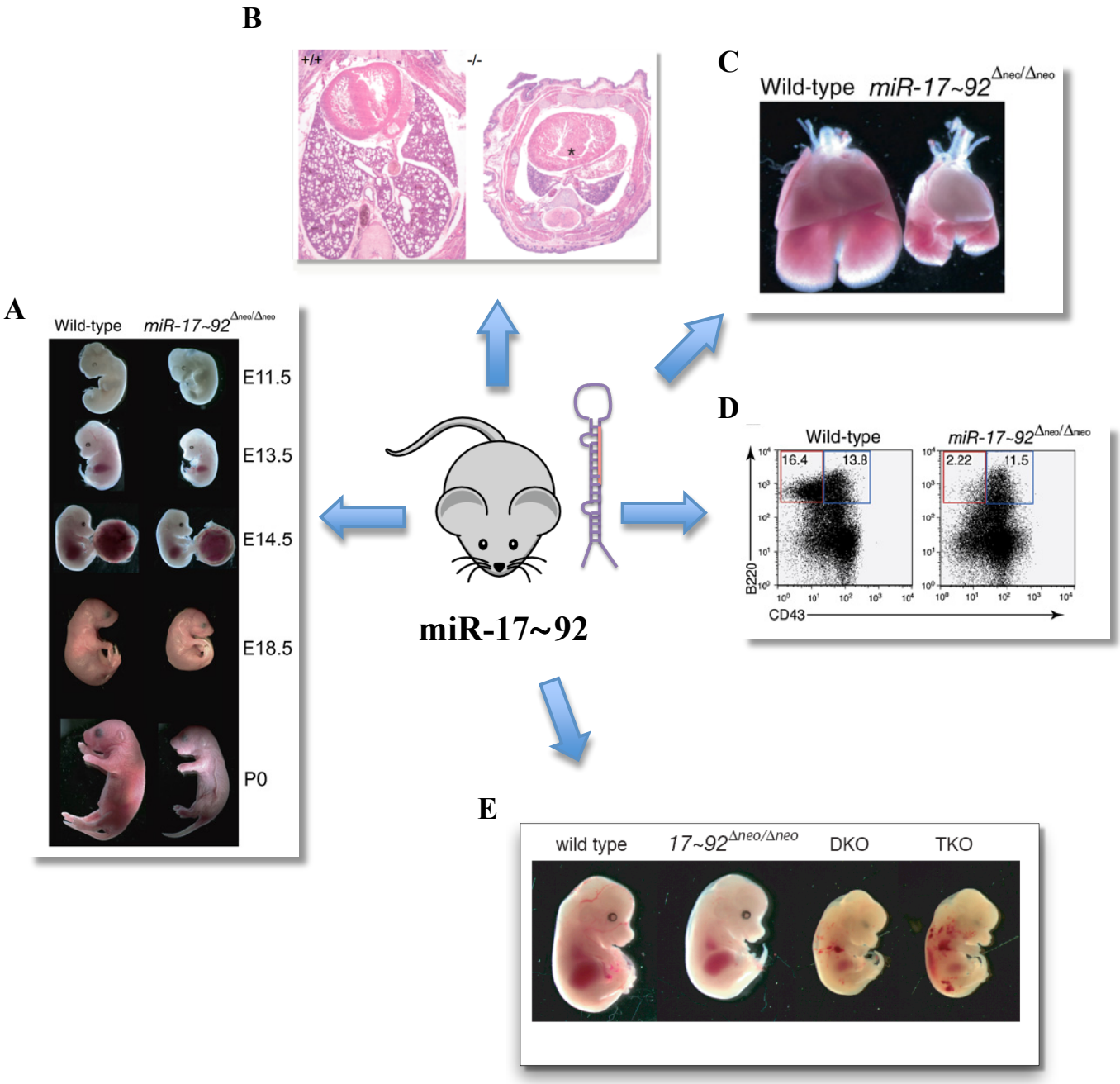

Fig. 3 miR-17~92 pleiotropic roles in development. (A) Wild Type and Knock Out embryos at various developmental stages. (B) Hematoxylin-eosin staining of transversal sections of Wild Type and miR-17~92 $^{\Delta neo/\Delta neo}$ hearts at E18.5. The asterisk indicates the ventricular septal defect. (C) Hypoplastic lungs in miR-17~92 $^{\Delta neo/\Delta neo}$ embryos. (D) Flow cytometry plots of E18.5 Fetal liver cells showing a dramatic reduction in the number of pre-B cells in The miR-17~92$^{\Delta neo/\Delta neo}$ embryos. (E) Macroscopic appearance of double (miR-17~92$^{\Delta/\Delta}$; miR-106b~25$^{\Delta/\Delta}$) and triple (miR-17~92$^{\Delta/\Delta}$; miR-106b~25$^{\Delta/\Delta}$; miR-106a~363$^{\Delta/y}$) Knock Out embryos at E14.5. Notice the hemorrhagic and edematous area in the body. (Adapted from *Ventura et al.*, 2008)

miRNAs and cancer

miRNAs have been classified as oncogene or tumor suppressor according to their ability to influence cancer-related pathways [52] (Tab. 1). The first miRNAs implicated in cancer were miR-15a and miR-16-1, which are often deleted or downregulated in B-cell chronic lymphocytic leukemia [53]. They were both classified as tumor suppressor miRNAs, giving their ability to target the antiapoptotic protein Bcl-2 [54]. More recently their tumor suppressor activity was confirmed in vivo [55].

Among the miRNAs that have been identified as oncogenes, miR-155 overexpression alone in the B-cell compartment was shown to be sufficient to determine acute lymphoblastic leukemia and high-grade lymphoma *in vivo* [56]. Noteworthy is also miR-21, an oncogenic miRNA frequently overexpressed in a variety of human cancers [57]. By using loss and gain of function in a mouse model *Medina et al*. showed that miR-21 overexpression alone promotes lymphoma onset. Moreover shutting down miR-21 expression leads to a complete tumor regression partly due to increased apoptosis, a mechanism known as "onco-miR addiction" [58].

miR-17~92 and cancer

miR-17~92, also known as oncomiR-1 [59], is among the most potent oncogenic miRNAs. It was originally identified as a potential oncogene due to its genomic amplification and elevated expression in multiple hematopoietic malignancies, including diffuse large B-cell lymphomas, mantle cell lymphomas, and Burkitt's lymphomas [13, 59-62]. Over-expression of miR-17~92 has been observed in multiple tumor types [63] including gastric [20], lung and thyroid cancer [64-66]. The miR-17~92 oncogenic role is supported by evidences of its involvement in multiple key biological processes such as cell proliferation, differentiation, apoptosis (reviewed in *Mendell, 2008*)

In 2005 *O'Donnell et al.* showed that the transcription of miR-17~92 is directly activated by the c-Myc oncogene [24]. This finding was further confirmed by several reports that have shown a synergistic cooperation between c-Myc and miR-17~92 in malignant lymphoma development [59, 60]. Other studies additionally demonstrated that the c-Myc homologue N-Myc is able to activate the expression of the cluster in neuroblastoma e medulloblastoma [67, 68]. In 2008 *Xiao et al.* showed that a moderate miR-17~92 overexpression (2-3 fold) *in vivo* determines a lymphoproliferative disorder, autoimmunity, enhances B-cell proliferation and reduce apoptosis-induced cell death [21]. We and others have recently investigated the relative contribution of each member of the cluster in a mouse model of myc-driven lymphoma [15, 16]. miR-19a and miR-19b were identified as the key component of the miR-17~92 cluster in this specific context. In fact, it was found that they largely mediate the pro-survival activity of the cluster by targeting the tumor suppressor protein PTEN, thus suppressing apoptosis [15, 16].

More controversial is the role played by miR-17~92 during angiogenesis. In 2006 *Dews et al*. reported that miR-17~92 over-expression increases angiogenesis in a mouse model of colon cancer. This pro-angiogenic function has been attributed to the down-regulation of two anti-angiogenic molecules thrombospondin-1 (TSP-1) and connective tissue growth factor (CTGF) by miR-18 and miR-19 respectively [69].

Conversely *Doebele et al.* have recently demonstrated a cell-intrinsic antiangiogenic function mediated by individual members of this cluster in endothelial cells [70]. The apparent discrepancy between these two findings might lie in the different context in which miR-17~92 is acting (e.g. Tumor *vs* endothelial cells). A tentative model is shown in fig. 4 [71].

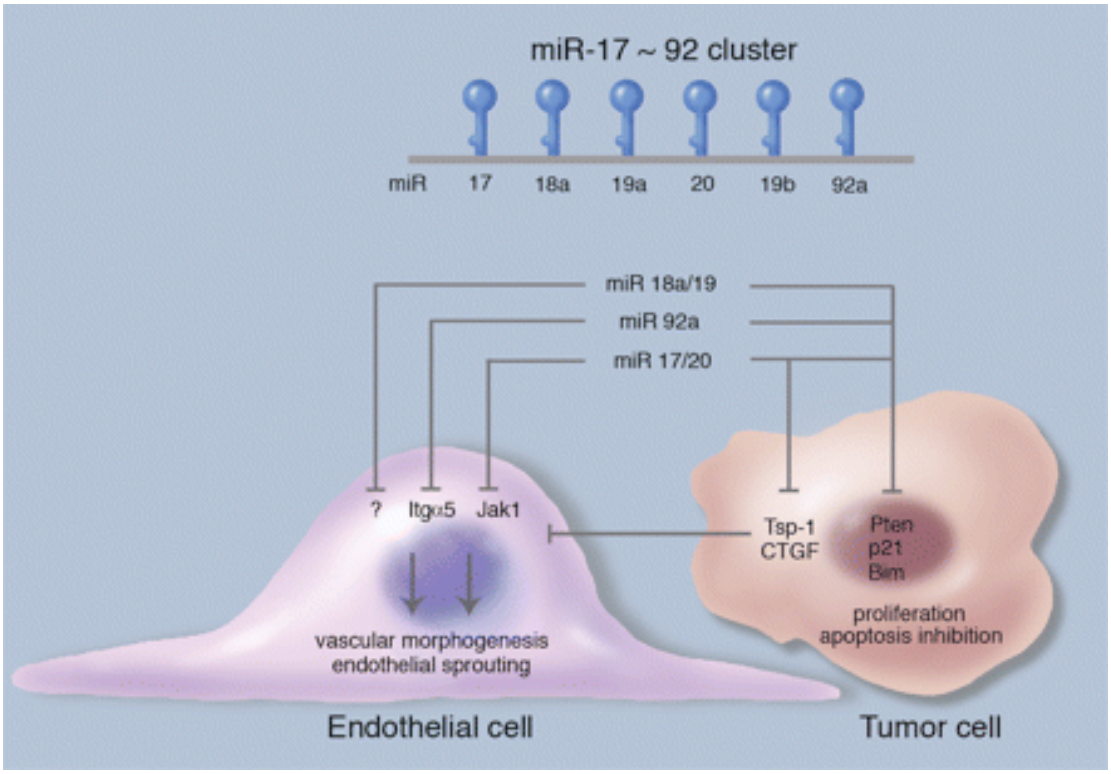

Fig. 4 Proposed roles of miR-17~92 in angiogenesis (from *Kuhnert and Kuo*, 2010)

MicroRNA	Dysregulation	Function	Validated targets	Oncogene (ONC) or tumour suppressor (TS)	Refs
miR-15a and *miR-16-1*	Loss in CLL, prostate cancer and multiple myeloma	Induces apoptosis and inhibits tumorigenesis	BCL2, WT1 RAB9B and MAGE83	TS	15,20,23, 30,52,69
let-7 (*a*, *b*, *c*, *d*, *e*, *f*, *g* and *i*)	Loss in lung and breast cancer and in various solid and haematopoietic malignancies	Induces apoptosis and inhibits tumorigenesis	RAS, MYC and HMGA2	TS	22,26, 42,70
miR-29 (*a*, *b* and *c*)	Loss in aggressive CLL, AML (11q23), MDS lung and breast cancers and cholangocarcinoma	Induces apoptosis and inhibits tumorigenicity. Reactivates silenced tumour suppressor genes	TCL1, MCL1 and DNMTs	TS	30,64, 71,72
miR-34	Loss in pancreatic, colon, breast and liver cancers	Induces apoptosis	CDK4, CDK6, cyclin E2, EZF3 and MET	TS	56–58
miR-145	Loss in breast cancer	Inhibits proliferation and induces apoptosis of breast cancer cells	ERG	TS	31
miR-221 and *miR-222*	Loss in erythroblastic leukaemia	Inhibits proliferation in erythroblasts	KIT	TS	30
miR-221 and *miR-222*	Overexpression in aggressive CLL, thyroid carcinoma and hepatocellular carcinoma	Promotes cell proliferation and inhibits apoptosis in various solid malignancies	p27, p57, PTEN and TIMP3	ONC	43,51,73
miR-155	Upregulated in aggressive CLL, Burkitt's lymphoma and lung, breast and colon cancers	Induces cell proliferation and leukaemia or lymphoma in mice	MAF and SHIP1	ONC	32–34, 36,37
miR-17–92 cluster	Upregulated in lymphomas and in breast, lung, colon, stomach and pancreatic cancers	Induces proliferation	E2F1, BIM and PTEN	ONC	19,34,35, 40,41
miR-21	Upregulated in glioblastomas, AML (11q23), aggressive CLL and breast, colon, pancreatic, lung, prostate, liver and stomach cancers	Inhibits apoptosis and increases tumorigenicity	PTEN, PDCD4, TPM1 and TIMP3	ONC	31,37–39, 44–50
miR-372 and *miR-373*	Upregulated in testicular tumours	Promotes tumorigenicity in cooperation with RAS	LATS2	ONC	74

Tab. 1 microRNA that function as oncogenes and tumor suppressor genes in human cancers (From *Croce, 2009)*

B-cell lymphoma: the Eμ-Myc mouse model

About 95% of all lymphomas are of B-cell origin while the remaining 5% originate from T-cell [72]. B cell development occurs through several stages during which their Ig heavy and light chain genes undergo profound genomic rearrangements to produce a functional B-cell receptor (BCR) (Fig. 5). A hallmark of all B-cell lymphomas is a reciprocal chromosomal translocation involving one of the Ig loci and a proto-oncogene. As a consequence, the oncogene comes under the control of the Ig promoter that determines its deregulated or constitutive expression [72]. Such translocations often occur as a result of errors during somatic recombination events [73]. Among several oncogenes whose deregulated expression is known to be relevant for tumorigenesis, oncogenic activation of c-Myc, following a chromosomal translocation event, play a major role in Burkitt's B-cell lymphomas [74] (Fig. 6).
c-Myc was originally identified as the cellular counterpart of the viral oncogene v-Myc [75].
It is broadly expressed during embryogenesis and in high proliferative adult tissues; furthermore is rapidly induced upon mitogenic stimuli. C-Myc roles comprise control of cell growth and proliferation, inhibition of cell differentiation, cells sensitization to apoptosis [76]. Myc overexpression alone is not sufficient to transform cells that often need to acquire additional mutations such as loss of tumor suppressor (e.g. PTEN) to overcome the apoptotic stimulus triggered by high levels c-Myc [72]. PTEN is a haploinsufficent tumor suppressor gene. Loss of a single PTEN allele is a frequent event in human cancer that leads to abnormal activation of the pro-survival AKT/PI3K pathway [77, 78] (Fig. 7).
In order to study the role of c-myc in B-cell lymphomagenesis, in 1985 *Adams et al.* developed a transgenic mouse model based on overexpression of c-Myc in the B-cell compartment under the control of the B-cell specific Ig heavy chain enhancer. Mice carrying the transgene invariably develop lymphomas and die within 4-6 months [79].

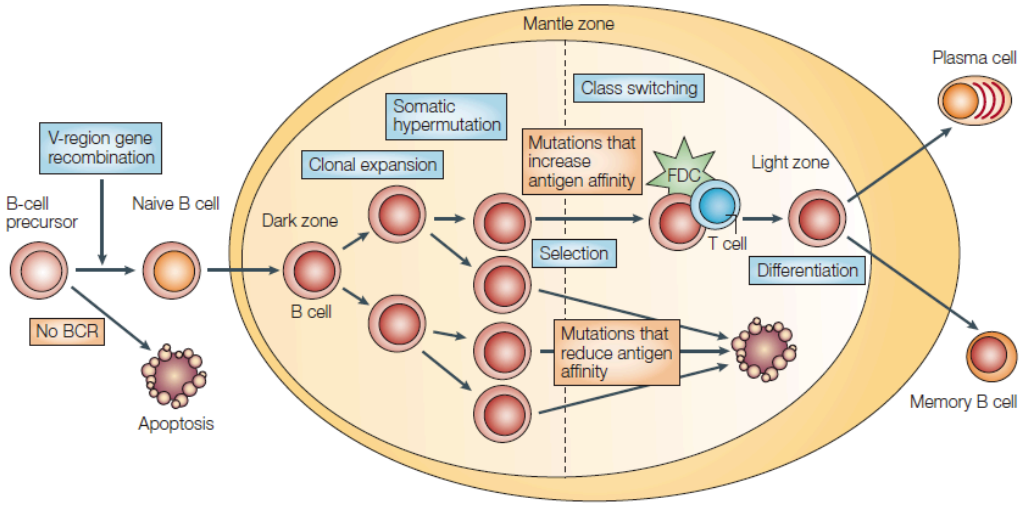

Fig. 5 B-cell development stages. Mature (naive) antigen-activated B cells that receive signals known as 'T-cell help' are driven into primary B-cell follicles in secondary lymphoid organs such as lymph nodes, where they establish germinal centers. Here they rapidly proliferate (clonal expansion) and undergo somatic hypermutation that leads to the introduction of mutations at a high rate into the rearranged Ig variable (V)-region genes of the B cells. Mutations that lead to reduced affinity of the BCR for antigen cause cells to undergo apoptosis. A few B cells will acquire mutations in the BCR that increase their affinity for antigen. A fraction of these B cells undergo class-switch recombination and finally differentiate into memory B cells or plasma cells (from *Kuppers*, 2005).

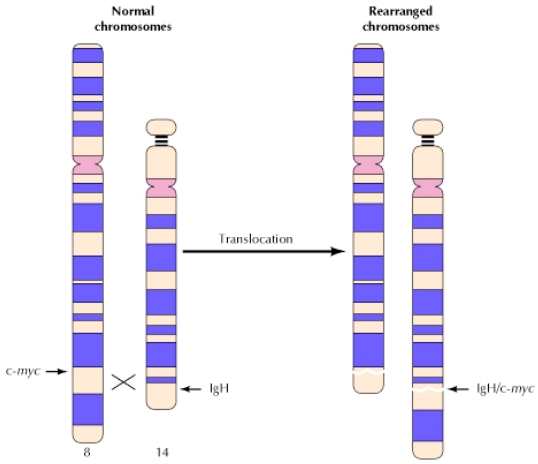

Fig. 6 Translocation of c-*myc*. The c-*myc* proto-oncogene is translocated from chromosome 8 to the immunoglobulin heavy-chain locus (IgH) on chromosome 14 in Burkitt's lymphomas, resulting in abnormal c-*myc* expression (From The Cell: A Molecular Approach. 2nd edition.Cooper GM. Sunderland (MA): Sinauer Associates; 2000).

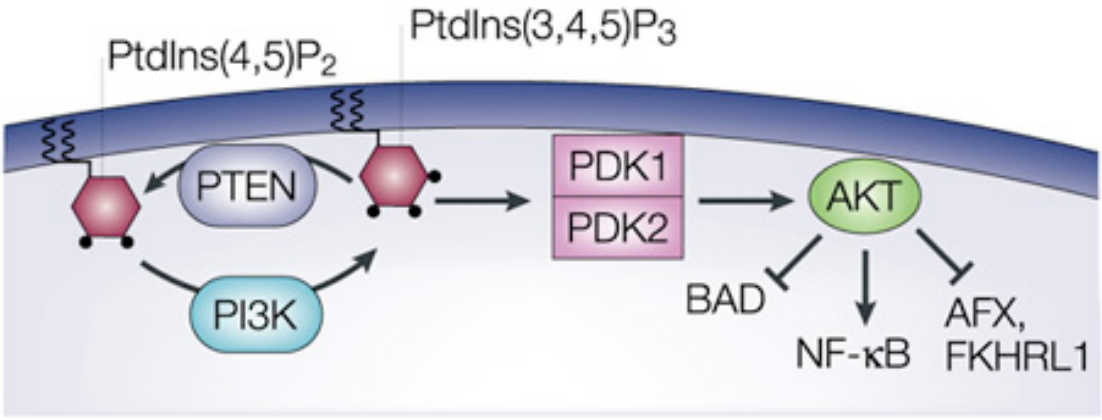

Fig. 7 Survival signalling through PI3K/AKT. Survival signals (e.g. EGF, PDGF) activate phosphatidylinositol 3-kinase (PI3K).Active PI3K generates the 3-phosphorylated lipid phosphatidylinositol-3,4,5-trisphosphate (PtdIns(3,4,5)P3). This leads to recruitment of the kinases PDK1, PDK2 and AKT to the plasma membrane. Active AKT interferes with the apoptotic machinery by phosphorylating, and thus inhibiting, the proapoptotic BCL2 family protein BAD. Survival signalling by AKT is counteracted by the tumour suppressor PTEN, a lipid phosphatase that antagonizes the action of PI3K by removing the 3-phosphate from PtdIns(3,4,5)P3. (From *Igney and Krammer, 2002*)

Aims of the Thesis

In this study we focused our attention on the miR-17~92 cluster of miRNAs that is often overexpressed or amplified in human cancers and has been shown to have an essential function in mammalian development.

Our main aim was to identify the role played by the different members of the miR-17~92 cluster in pathological (B-cell lymphomas) and physiological (embryonic angiogenesis) events. Previous reports have shown that miR-17~92 is a direct target of the transcriptional activator c-Myc and cooperatively acts with it during cancerogenesis. In this study we used a mouse model of Myc-driven B-cell lymphoma to shed light on the role of each member of the cluster on tumor maintenance, identify the critical targets and clarify the molecular mechanism responsible for the enhanced tumorigenicity.

Mature miRNA sequences are highly conserved among vertebrates. Although it has been shown that the interaction between a miRNA and its targets is mainly mediated by the seed sequence, very little is known about the role played by the non-seed region during the target recognition process. Our in vitro model provided an excellent opportunity to gain insight into the relative importance of the seed and non-seed sequences in respect to miRNA function and target(s) specificity. A second aim of our project was to verify how and to what extent mutations in the mature miRNA sequence impair the ability of a miRNA to modulate gene expression.

Several reports have shown that miR-17~92 has also an important role in regulating angiogenesis in a context-dependent manner. In fact, a ectopic expression of this cluster in colon cancer cells, has shown to exhibit pro-angiogenic activity while other reports have stated that individual members of the cluster exhibit antiangiogenic activity when expressed in endothelial cells. We and others have showed that hypoxia is able, in vitro, to repress expression of members of the miR-17~92 and its paralog cluster miR-106a~363, thus contributing to elevate the levels of the pro-angiogenic factor VEGF, a target of the miR-17/20 family. Here we hypothesized that VEGF deregulation could contribute to the early embryonic lethality observed in double (miR-17~92 and miR-106a~363/miR-106b~25) and triple (miR-17~92/miR-106b~25/miR-106a~363) knock out embryos and, with a lower penetrance, in miR-17~92 knockout embryos. By using a genetic loss-of-function approach we sought to clarify the role played by miR-17~92 during physiological angiogenesis and verify whether deregulation of VEGF is responsible for the defects in the heart and vasculature pattern development observed in the knock out embryos and could contribute to explain their embryonic lethality.

Materials and Methods

Mouse husbandry

Animal studies and procedures were approved by the Memorial Sloan Kettering Cancer Center Institutional Animal Care and Use Committee. Mice were maintained in a mixed 129SvJae and C57/B6 background. The Rosa26-Cre-ER^{T2} and miR-17-92$^{fl/fl}$ mice have been described previously (Ventura et al. 2007, 2008). The Eu-Myc mice were generated and described by Adams et al. (1985). For the in vivo tumorigenicity studies, 4- to 8-wk-old athymic (nu/nu) mice were injected intravenously with 10^5 lymphoma cells and monitored daily. Mice were euthanized when moribund. Kaplan-Meier curves were plotted using PRISM software, and the log-rank Mantel-Cox test was used to determine statistical significance. In vivo fluorescent GFP imaging was performed with the Maestro Imaging system (CRI, Woburn, MA USA)

Antibodies and immunohistochemistry

The following antibodies (Abs) were used for WB: PTEN antibody (1:2000, Cell Signaling, 138G6, cat #9559), tubulin antibody (1:5000, Sigma cat #T9026). VEGF (147) rabbit polyclonal Antibody (1:1000, Santa Cruz Biotechnology), GAPDH (6C5) mouse monoclonal antibody (1:1000, Santa Cruz Biotechnology)
Immunohistochemical staining was performed on 5μm sections of formalin fixed paraffin-embedded tissues, using an automated staining processor (Discovery XT, Ventana Medical Systems, Inc.). The PTEN antibody was diluted 1:100 in PBS 2%BSA. 20X images from each tumor were acquired with a Nikon Eclipse E400 microscope connected to a Nikon Digital Slight camera using identical acquisition settings for all samples.

RNA blotting

RNA blotting was performed as described [80] using Express-hyb™ Buffer (Clontech, Moutain view, CA) and DNA oligonucleotide probes complementary to the mature miRNA sequences. Blots were washed once in 2X SSC plus 0.5% SDS, and a second time in 0.2XSSC plus 0.5% SDS at 42 °C such that less than 10% cross-hybridization was observed.

Cell culture and retroviral transduction

The Eμ-Myc; miR-17~92$^{fl/fl}$; Cre-ER^{T2} lymphoma lines were cultured on a feeder of irradiated NIH-3T3 cells in a medium composed of 50% DMEM and 50% IMDM, supplemented with 10% fetal bovine serum. To induce deletion of the miR-17~92 cluster, cells were incubated for 4 days with 250 nM 4-OHT. During our initial set of experiments with 4-OHT-treated lymphoma cells, we noticed that, upon prolonged passages, the few cells that had escaped full miR-17~92 deletion (miR-17~92$^{fl/fl}$ and miR-17~92$^{fl/\Delta}$) invariably outcompeted the miR-17~92$^{\Delta/\Delta}$ cells, eventually becoming the majority within a couple of weeks. To avoid this limitation and allow the execution of long-term in vivo experiments, 4 days after 4-OHT treatment, subclones were isolated by plating 10 cells per well into a 96-well plate using a MoFlo fluorescence-activated cell sorter. After expansion, clones composed solely of fully recombined cells were isolated and used for further manipulation. Retroviruses were generated in Phoenix packaging cells. When required, transduced cells were selected by adding puromycin (2 mg/mL) to the culture medium for 4 d.
MCF-7 cells were routinely grown in Gibco DMEM:F12 (Invitrogen, Carlsbad, CA) supplemented with 10% fetal bovine serum (FBS), 100 U/ml penicillin, and 50mg/ml streptomycin. Seventy percent confluent cells were stimulated with 300 mM CoCl2 for 4 or 24 h.

Primary Mouse Embryo fibroblasts (MEFs) were isolated from E13.5 following a standard protocol. MEF were cultured in DME-HG supplemented with 10% fetal bovine serum under standard or hypoxic (5%O_2) condition in the hypoxia incubator HERA cell 150 (Thermo scientific).

Plasmids and shRNA library

A 1.2-kb fragment encompassing the entire miR-17~92 cluster was PCR amplified from mouse genomic DNA and cloned into the MSCV-PIG retroviral vector (a gift from Mike Hemann, Massachusetts Institute of Technology). Deletion mutants were by site-directed PCR and verified by sequencing. The shRNA library was cloned in the MLP retroviral vector (a gift from Michael Hemann, Massachusetts Institute of Technology). For each gene, three shRNA directed against the coding sequence were designed using the RNAi Central resource created by the laboratory of Greg Hannon (http://katahdin.cshl.org:9331/ siRNA/RNAi.cgi?type=shRNA). Each construct was sequence-verified.

Luciferase assays

The luciferase reporters constructs containing portion of the PTEN 3'UTR and carrying mutations of the miR-19 seed matches were a gift of Joshua Mendell (Johns Hopkins University, Baltimore, Maryland) and their generation is described in O'Donnell et al., 2005. For transfection, HeLa cells were seeded at a density of 150,000 cells/well in 24-well plates. The next day, cells were transfected with 100 ng pGL3-PTEN reporter (wild-type or mutant), 20 ng of pRL-SV40 (expressing the Renilla luciferase under the control of the SV40 promoter) and 4ul of a pre-miR-control or pre-miR-19b (6.25 µM, Ambion). Transfections were performed using the siPORT NeoFX reagent (Ambion) following manufacturer's instructions. Early-passages primary miR-17~92 $^{+/+}$ and miR-17~92 $^{\Delta/\Delta}$ MEFs (described in Ventura et al., 2008), plated at 60% confluency in 24-well plates, were transfected with 100 ng pGL3-PTEN reporter (wild-type or mutant), 20 ng of pRL-SV40, and 100 ng of MSCVPIG constructs using FUGENE 6 (Roche) and following manufacturer's instructions. The luciferase reporters constructs containing a portion of the VEGF 3'UTR with a wildtype or mutated miR-17 binding site were generated according to a standard cloning protocol (Promega). Early-passages primary miR-17~92$^{\Delta/\Delta}$ MEFs were plated at a density of 30,000 cell/well in 24 well plates. The next day cells were transfected with 100ng psiCHECK-2-VEGF3'UTR reporter (wild type or mutant) and 100 nM pre-miR or a negative control (Ambion). Transfections were performed using the siPORT NeoFX reagent (Ambion) following manufacturer's instructions. Firefly and Renilla Luciferase activities were measured 48 hours after transfection using the Dual Reporter Luciferase kit (Promega) and a Glomax 96 luminometer (Promega).

Apoptosis assays

Apoptosis was measured using the Caspase Detection Kit (Red-VAD-FMK or FITC-VAD-FMK, Calbiochem) and confirmed using the TUNEL assay (In Situ Cell Death Detection Kit, TMR red, Roche) following the manufacturer's instructions.

Gene expression analysis

Total RNA extracted from three technical replicates was hybridized to the Affymetrix 430 A2.0 gene chip, following the manufacturer's instruction. Gene expression was normalized using the GCRMA Bioconductor package, and log expression values were computed using the limma package.

For genes with multiple probes, the probe with lowest adjusted P-value was selected. Genes with a log expression change of <_0.2 in all three comparisons and with an adjusted P-value < 0.05 in at least one comparison were considered for subsequent overlap analysis.

Pre-miR and anti-miR transfections

Transfections were performed with either pre-miR or antimiR (Ambion, Austin, TX). MCF-7 cells were seeded at 4*10^5 cells/well in six-well plates. MEFs were seeded at 3*10^4 cells/well in 24-well plates. After 24 h (30–40% confluency), the cells were transfected with the pre-miR (50 nM) or the anti-miR (100 nM) using siPort Neo Fx transfection agent (Ambion), according to manufacturer's instructions. Non-specific pre-miR and anti-miR (Ambion) were used as negative controls together with mock control. The success of transfection was confirmed by quantitative real-time PCR.

CD-31 (PECAM) whole mount staining

For the PECAM whole mount immunostaining the following protocol was used. Embryos were dissected, fixed in 4% cold PBS overnight, dehydrated in increasing methanol concentration and stored at -20°C. The day of use, embryos were treated with 6% H_20_2 to inactivate endogenous preoxidases and rehydrated in decreasing methanol concentration. Following blocking in 10% goat serum in PBST, embryos were incubated o.n. at 4°C with the anti-CD31(PECAM) Rat anti-mouse IgG (BD pharmingen) diluted in blocking solution. The second day embryos were washed 3 times for 2hrs with PBS and incubated o.n. at 4°C with a biotynilated goat anti-rat IgG (Vectastain kit, Vectorlab). The third day embryos were washed again 3 times for 2hrs in PBS and then incubated with streptavidin-HRP (TSA kit, Invitrogen) o.n at 4°C. After a final wash in PBS for 6hrs, signal was dected using the DAB chromogenic substrate. Embryos were cleared in 80% glycerol o.n. at 4°C. Alternatively glycerol was washed off with PBS and embryos were cleared with a mixture 1:2 of Benzyl alcohol/Benzyl Benzoate.

Real Time PCR

Total cellular RNA was isolated using TRIZOL (invitrogen) according to manufacturer's protocol. For VEGF mRNA detection, 1 μg of total RNA was reverse transcribed using the high capacity cDNA archive kit (Applied Biosystems), according to vendor's instructions. VEGF mRNA sequence was detected using the Mm01281449_m1 VEGF TaqMan gene expression assay (Applied Biosystems). To normalize quantitative real-time PCR reactions, parallel reactions were run on each sample for β-Actin. Changes in the target mRNA content relative to β-Actin were determined using the comparative Ct method to calculate changes in Ct, and ultimately fold and percent change. An average Ct value for each RNA was obtained for replicate reactions.

VEGF detection by ELISA

Human and Mouse VEGF protein was measured in conditioned medium or whole organ lysates using the VEGF Quantikine ELISA kit (R&D, Systems, Minneapolis, MN) with the lowest detection limit of 5 pg/ml, with intra-assay precision of<4.8% (or better than 2.5% and<4.8%) and inter-assay precision of<7.2% (or better than 4.7% and<7.2%). All points were done in triplicate, and the all the experiments were repeated three times. The range of curve standards was 0, 15.6, 31.2, 62.5, 125, 250, 500 pg/ml; all VEGF concentrations in samples were within the range of curve standard. Linear regression analysis was performed to create the standard curve.

miRNA target predictions

miRNA targets were predicted using miRanda (http://www.microrna. org) and TargetScan (http://www.targetscan.org). For the cumulative distribution function (CDF) plots, target sites were restricted to perfect seed complementarity between positions 2 and 7 of the miRNA. Empirical cumulative distributions were computed using R ecdf function for the set of predicted gene of the transduced miRNAs and for the genes with no target sites (background). P-values were computed using the Kolmogorov-Smirnov two-sample test.

Statistical analysis

The correlations were studied by Student's t-test or the one-way ANOVA test for multiple group comparison. P-values <0.05 were considered statistically significant.

Results – Part I

Generation of miR-17~92 $^{flox/flox}$; Eμ-Myc ; CRE-ER^{T2} mice

In order to generate an in vivo model where the deletion of the miR17~92 cluster can be temporary controlled, Eμ-Myc mice [79] were crossed to mice carrying a conditional miR17~92 knockout (KO) allele (Fig. 1A). The resulting mice were further crossed to CRE-ER^{T2} mice carrying a modified version of the CRE recombinase linked to the estrogen receptor T2 (**ER^{T2}**) that was targeted to the ubiquitously expressed ROSA26 locus [81]. The **ER^{T2}** moiety fused to CRE retains the recombinase in the cytosol until 4-hydroxy-tamoxifen (4-OHT) administration releases this inhibition (Fig. 1B). Upon 4-OHT binding the CRE recombinase translocates to the nucleus where it can catalyze the recombination between the two loxP sites and thus deleting the miR-17~92 cluster. Compared to the previously published studies based on the overexpression of the miR-17~92 cluster, our approach is based on the removal of the endogenous miR-17~92 locus and thus is more likely to identify physiologically relevant functions of this cluster of miRNAs.
A lymphoma cell line (named AV4182) was generated and propagated in vitro from these mice. When injected into immunocompromised mice those cells were able to form tumors (data not shown). Cells were treated with 250nM 4-OHT for 4 days to verify efficiency of recombination. Results from genotyping and realtime PCR are shown in Fig. 3C and D, confirming efficient deletion of both miR17~92 alleles and concomitant loss of miR-17~92 expression.

miR-17~92 suppresses apoptosis in Eμ-Myc lymphomas

Next we sought to determine whether removal of the cluster had an effect on the growth of the Eμ-Myc B-lymphoma cells. Following 4-days of 4-OHT treatment, cells were allowed to recover for 4 additional days to exclude any possible adverse effects of sustained CRE expression on the growth of lymphoma cells [82]. As shown in Fig. 2A deletion of the miR17~92 cluster drastically reduced the cell growth over the course of 6 days. Moreover restoration of miR-17~92 expression was sufficient to rescue this phenotype (Fig. 2A). Additional experiments were conducted to further understand whether a reduction in cell proliferation, an increase in cell death or a combination of both were responsible for the different growth kinetics between miR17~92$^{fl/fl}$ and miR17~92$^{\Delta/\Delta}$ lymphoma cells. Analysis of cell cycle by BrdU staining showed no difference in cell cycle distribution between miR17~92$^{fl/fl}$ and miR17~92$^{\Delta/\Delta}$ cells (Fig. 2B), while levels of active caspases were consistently higher in the miR17~92$^{\Delta/\Delta}$ cells, as measured by the FMK-VAD caspase specific inhibitor staining (Fig. 2C). These results suggest that miR17~92 expression enhances survival of the lymphoma cells by suppressing apoptotic mechanisms. This hypothesis was further confirmed by means of the TUNEL assay (Fig. 2D). Taken together these results demonstrate that miR17~92 cluster expression is necessary for the survival of the Eμ-Myc lymphoma cells.

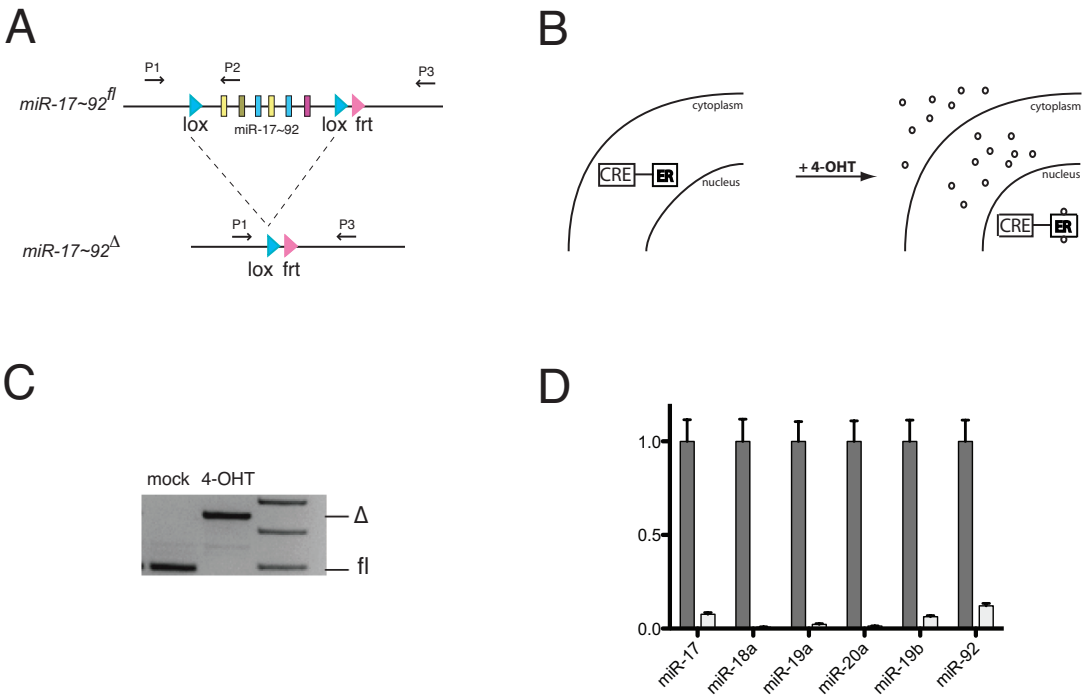

Fig. 1 CRE-ER-mediated miR-17-92 deletion. A) Schematic of the conditional miR-17~92 KO allele. Arrows represent the primers used to detect the floxed and the deleted (Δ) allele. **B)** Schematic of the CRE-ER^{T2} system **C)** PCR on genomic DNA extracted from Eμ-Myc; miR-17~92$^{fl/fl}$; Cre-ER lymphoma cells mock treated or after four days of 4-OHT treatment. **D)** Quantitative RT-PCR analysis of the expression of miR-17~92 in lymphoma cells before (gray bars) and after (white bars) 4-OHT treatment. Each component of miR-17~92 was detected independently and the results normalized relative to the expression observed in mock-treated cells. Each experiment was performed in quadruplicate, Error bar = Standard Deviation (SD).

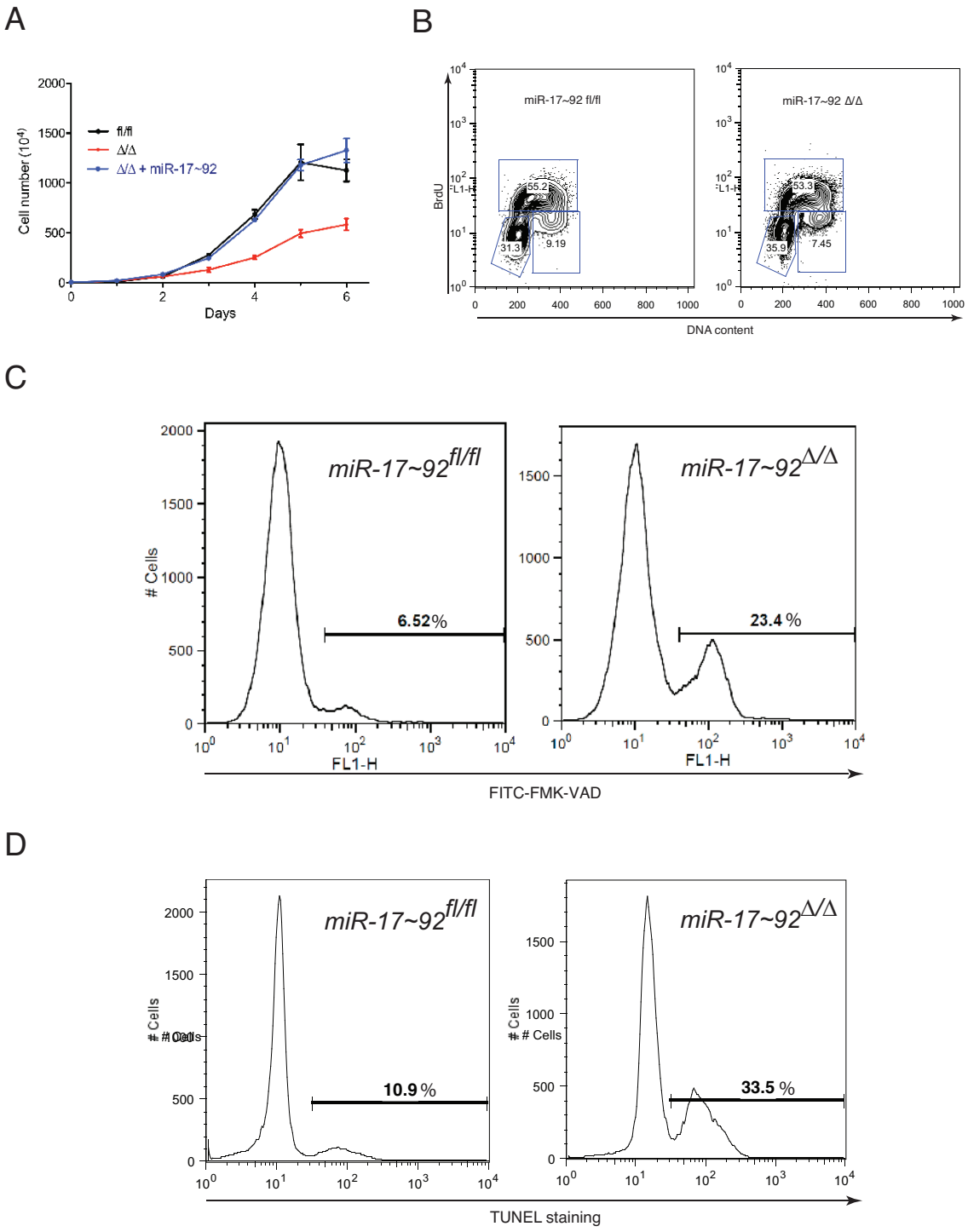

Fig. 2 miR-17~92 suppresses cell death in Eμ-Myc lymphomas. A) Growth curves of miR-17~92$^{fl/fl}$ (black line) miR-17~92$^{\Delta/\Delta}$ (red line) and miR-17~92$^{\Delta/\Delta}$ cells infected with a retrovirus expressing the entire miR-17~92 cluster (blue line). Error bars=SD of three technical replicates. The plot is representative of three independent experiments. **B)** BrdU incorporation in miR-17~92$^{fl/fl}$ and miR-17~92$^{\Delta/\Delta}$ lymphoma cells. Cells were incubated with BrdU for one hour. Incorporated BrdU was detected with a FITC-conjugated anti-BrdU antibody. DNA content was measured by propidium iodide staining. **C)** Caspase activity in exponentially growing miR-17~92$^{fl/fl}$ and miR-17~92$^{\Delta/\Delta}$ lymphoma cells as detected by flow cytometry using FITC-conjugated VAD-FMK. The percent of VAD-FMK+ cells is shown. **D)** TUNEL assay to detect spontaneous apoptosis in miR-17~92$^{fl/fl}$ and miR-17~92$^{\Delta/\Delta}$ isogenic lymphoma cells.

Genetic dissection of the miR17~92 cluster: Role of miR-19

Based on these preliminary results we next decided to genetically dissect the miR17~92 cluster by determining the relative role of its individual components in mediating the oncogenic properties. To this purpose we generated a series of mutant alleles each carrying a single miRNA or lacking a whole seed family (Fig. 3A). In addition we generated a construct lacking all miRNAs except miR-19a and miR-19b (Fig. 3A). The wild type and the mutants alleles were cloned into the MSCV-Puro-IRES-GFP vector, a retroviral vector encoding the green fluorescent protein (GFP) and the puromycin resistance gene (Fig. 3B). Considering that the deletion of even a single miRNA from the cluster inevitably alters the structure of the primary trancript (pri-miRNAs) and could negatively affect the processing or expression of the remaining miRNAs, we first transduced the miR-17~92$^{\Delta/\Delta}$ cells and verified the correct expression of the miRNAs for each construct (Fig. 3C, data not shown).
To determine the ability of each construct to suppress the increased cell death observed in the miR-17~92$^{\Delta/\Delta}$ cells we transduced those cells by titrating the virus to achieve an infection efficiency of 5-30%. We reasoned that if reintroduction of the wild-type or mutant alleles is sufficient to rescue the phenotype observed upon removal of the cluster, then the fraction of GFP+ cells should increase over time (Fig. 4A). We monitored cells for up to 8 days from the time of the infection. As expected, reintroduction of the full-length miR-17~92 cluster determined a strong increase in the fraction of GFP+ cells at day 8 from the infection (Fig. 4B). When ectopically overexpressed, the miR-106a~363 paralog cluster, but not the miR-106b~25 cluster, also determined an increase of the fraction of GFP+ cells over time (Fig.4B, C). Because the miR-106b~25 cluster lacks two of the four seed families, miR-18 and miR-19, we hypothesized that those miRNAs might have a prominent role in the context of Eμ -Myc driven B-cell lymphomas. In fact, when we reintroduced each miRNA individually we noticed that re-expressing miR-19b was sufficient to phenocopy the miR-17~92 full-length cluster reintroduction while none of the other miRNAs (mir-17, 18, 19a, 20, 92) seemed to have an effect (Fig. 4B). This model was confirmed by the observation that the rescuing ability of the miR-17~92 cluster was completely lost only upon deletion of the miR-19 seed family (Fig. 5A, B). Moreover re-expressing the miR-19 seed family only (miR-19a and miR-19b) could largely recapitulate the effect seen when reintroducing the whole cluster (Fig. 5A, B). Interestingly, the rescuing ability of the miR-19 family alone was slightly lower than the full cluster thus suggesting the existence of a certain degree of cooperativity among the different seed families in this context. Importantly, we observed a reduction in the number of apoptotic cells following reintroduction of miR-19a and miR-19b in these cells (Fig. 5C).

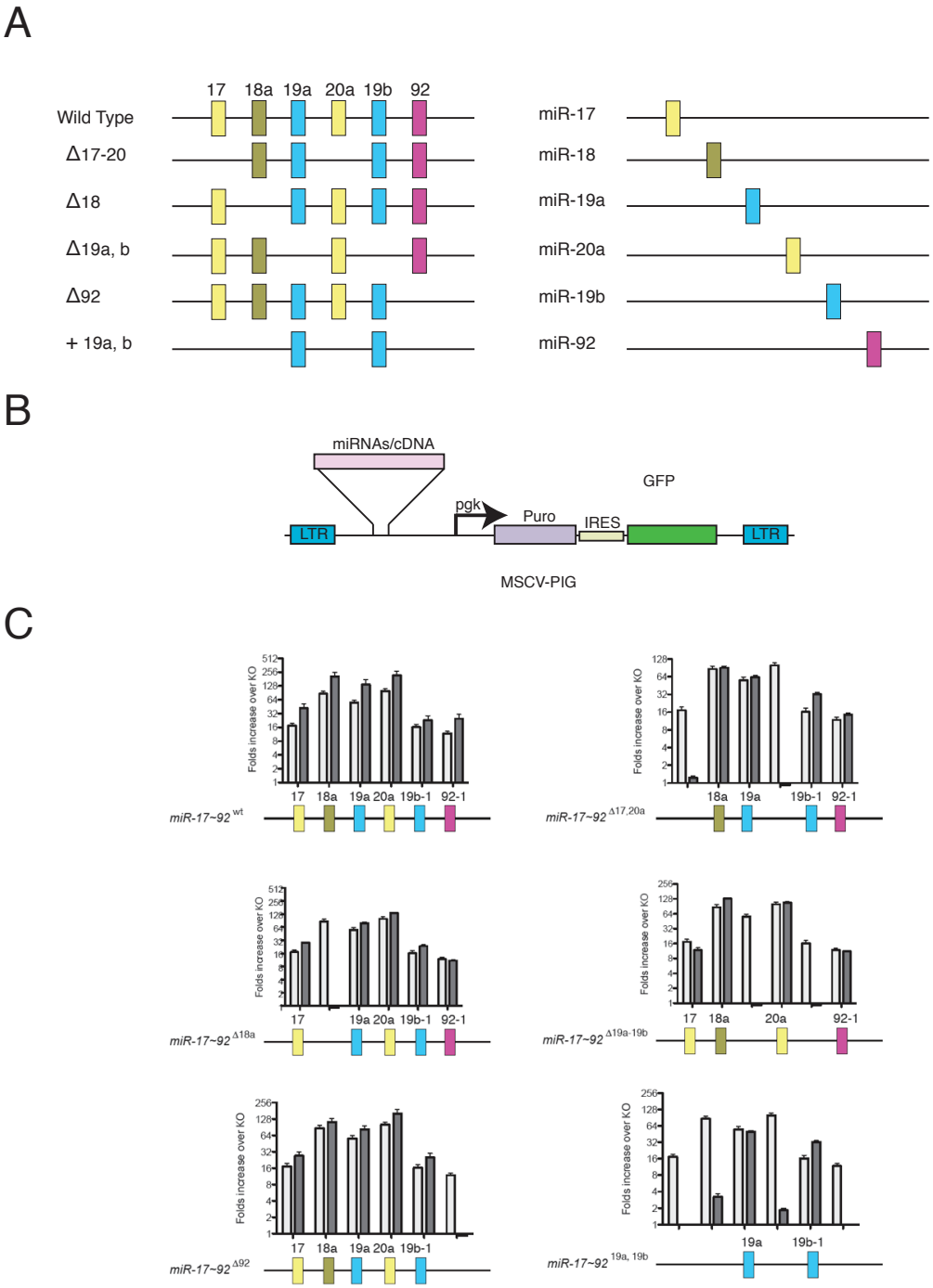

Fig. 3 Validation of retroviral constructs. A) Schematic of the miR-17~92 derivatives cloned into MSCV-PIG. **B)** the MSCV-Puro-IRES-GFP vector. **C)** Plots showing the relative expression of each member of the miR-17~92 in cells transduced with the indicated retroviral constructs. miR-17~92$^{\Delta/\Delta}$ lymphoma cells were transduced with the indicated retroviruses and treated with Puromycin (2μg/ml) for four days to eliminate uninfected cells. After selection, total RNA was extracted and analysed by quantitative RT-PCR to determine the relative expression of each member of the miR-17~92 cluster using Taqman probes from Applied Biosystem. Internal normalization was to sno-146 (four replicates per sample, error bar = 1 SD). Expression of each miRNA is plotted as fold increase relative to cells transduced with the empty vector (gray bars). For comparison, in each graph we have included the expression levels of the endogenous miRNAs as detected in miR-17~92$^{fl/fl}$ cells (white bars).

A

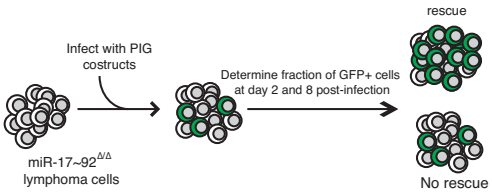

C

Construct name	miRNAs encoded	Rescue
Empty vector	-	-
miR-17~92	17, 18a, 19a, 20a, 19b, 92	+++
miR-106a~363	106a,18b, 20b,19b-2,92-2, 363	++
miR-106b~25	106b, 93, 25	-
miR-17	17	-
miR-18	18a	-
miR-20	20a	-
miR-19a	19a	-
miR-19b	19b	++
miR-92	92	-

B

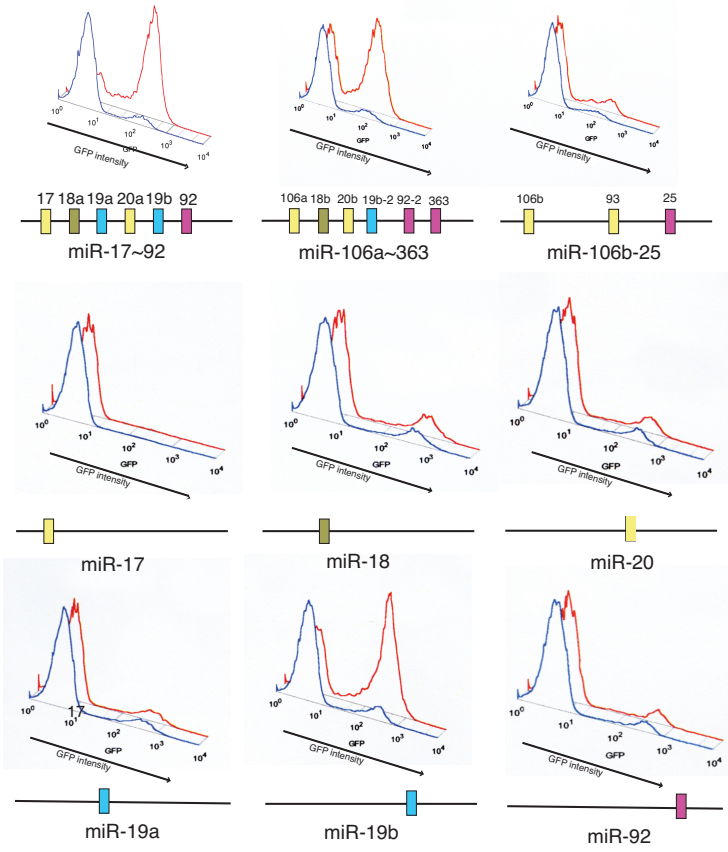

Fig. 4 miR-19b is the critical oncogenic miRNA in the Eμ –Myc model. A) Schematic of the experimental design. **B)** Histogram overlays of miR-17~92$^{\Delta/\Delta}$ cells transduced with PIG retroviruses expressing the indicated miR-17~92 derivatives. The cells were assayed by flow cytometry to detect GFP expression at day 2 (blue plot) and day 8 (red plot) post-infection. A schematic of the miR-17~92 derivative used is shown under each overlay. **C)** Table summarizing the results of the experiments shown in panel B.

A

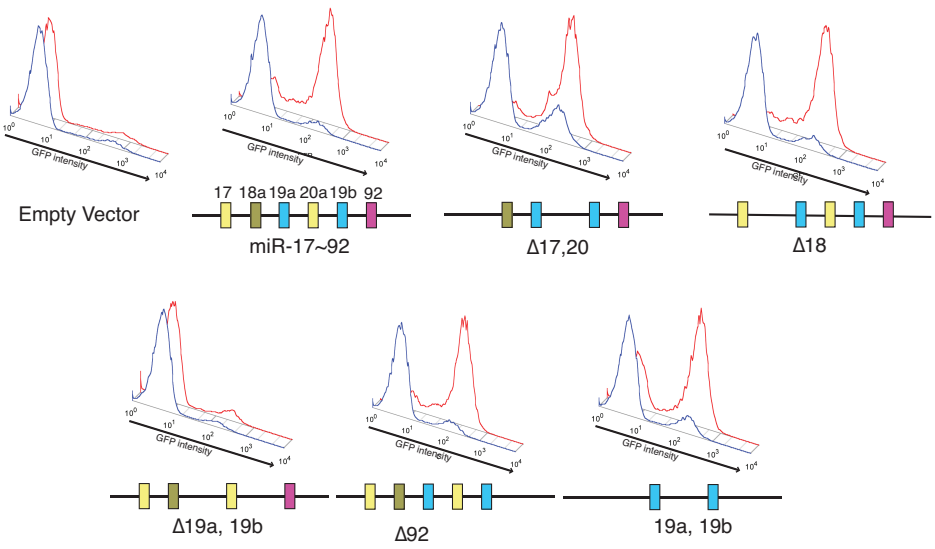

B

Construct name	miRNAs encoded	Rescue
Empty vector	-	-
miR-17~92 **wild type**	17, 18a, 19a, 20a, 19b, 92	+++
miR-17~92 **Δ17, 20**	19a, 19b, 92	+++
miR-17~92 **Δ18**	17, 19a, 20a, 19b, 92	+++
miR-17~92 **Δ19a, 19b**	17, 18a, 20a, 92	-
miR-17~92 **Δ 92**	17, 18a, 19a, 20a, 19b	+++
miR-17~92 **19a, 19b**	19a,19b	++

C

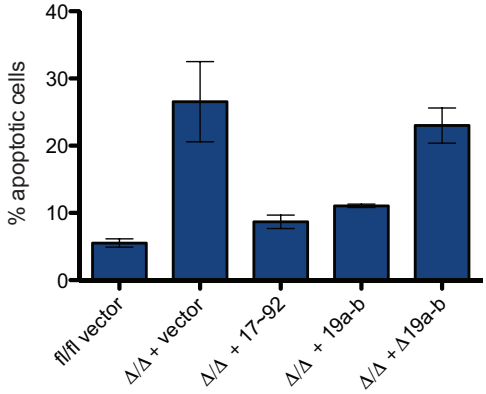

Fig. 5 MiR-19a and miR-19b mediate the pro-survival and oncogenic functions of *miR-17~92* in Eμ-Myc B-cell lymphomas. A) Histogram overlays of miR-17~92$^{\Delta/\Delta}$ cells transduced with PIG retroviruses expressing the indicated miR-17~92 derivatives. The cells were assayed by flow cytometry to detect GFP expression at day 2 (blue plot) and day 8 (red plot) post-infection. A schematic of the miR-17~92 derivative used is shown under each overlay. **B)** Table summarizing the results of the experiments shown in panel B. **C)** Caspase activity in miR-17~92$^{fl/fl}$ and miR-17~92$^{\Delta/\Delta}$ cells transduced with the indicated PIG constructs. Error bar = 1 SD deviation.

Deletion of mir-19 affects tumorigenicity in vivo

To determine whether miR-19 is required for the tumorigenicity of the Eμ-Myc B-lymphomas cells in vivo we injected a cohort of nude athymic mice with miR-17~92$^{fl/fl}$ and miR-17~92$^{\Delta/\Delta}$ lymphoma cells. While miR17~92$^{fl/fl}$ cells invariably formed lymphomas that lead to death within 2–3 weeks, the miR-17~92$^{\Delta/\Delta}$ cells produced lymphomas with a significantly ($P < 0.0001$) longer latency (Fig. 6A). The tumorigenicity of the miR-17~92$^{\Delta/\Delta}$ cells was fully restored by reintroduction of the full cluster ($P<0.0001$) and, to a lower extent, by re-expression of miR-19a and miR-19b (Fig.6A, B). Moreover a construct lacking miR-19a and miR-19b did not have any effect on the latency ($P=0.9816$) (Fig.6A, B). Therefore we confirmed that miR-19 profoundly influences the tumorigenicity of the miR-17~92$^{\Delta/\Delta}$ lymphoma cells. As seen in the in vitro rescue experiment re-expression of the whole cluster ad a stronger effect than reintroduction of miR-19a and miR-19b only.

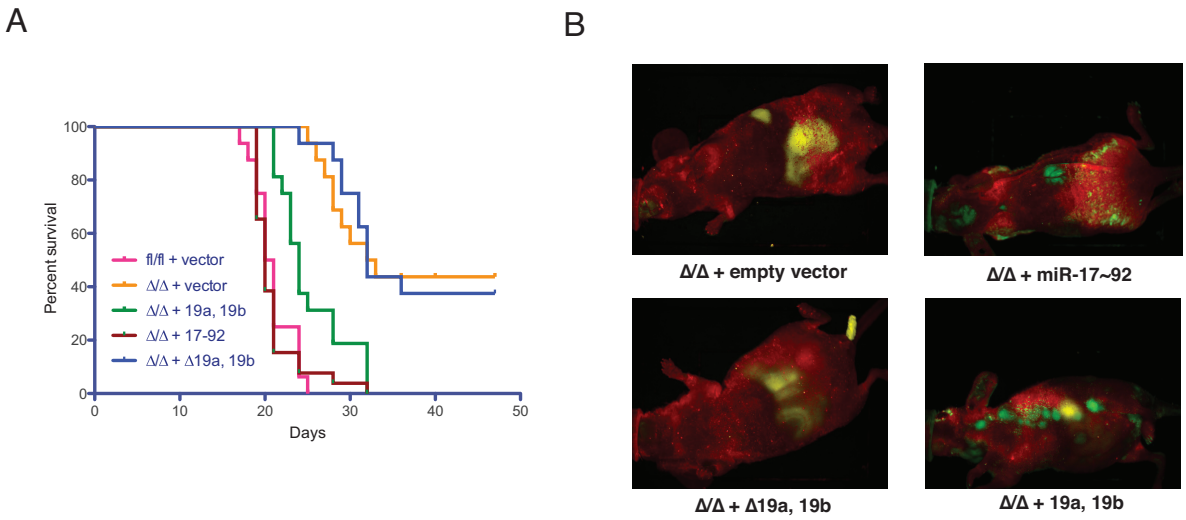

Fig. 6 miR-19 oncogenic role in vivo. A) Survival analysis of mice injected with of miR-17~92$^{fl/fl}$ and miR-17~92$^{\Delta/\Delta}$ lymphoma cells transduced with the indicated PIG constructs. N = 16 mice for each construct, over three independent experiments. **B)** In vivo GFP imaging showing GFP positive tumors derived from injected cells.

Identification of miR-19 targets in B-cell lymphomas

The results showed so far confirm a prominent oncogenic role for the miR-19 seed family in the context of Eμ-Myc driven B-cell lymphomas. We next sought to identify the critical targets of mir-19 by combining bioinformatic tools with gene expression analysis data. Algorithm-based miRNA prediction tools such as miRANDA, TargetScan, Pictar identify hundreds of possible targets, but many of them are likely to be false positive or irrelevant targets. A number of recent reports have shown that mRNA destabilization is the primary mechanism through which miRNAs act on their targets, therefore gene expression profiling would allow us to identify the majority of true relevant miR-17~92 targets in our model [5]. We compared the gene expression profile of the miR-17~92$^{fl/fl}$ and miR-17~92$^{\Delta/\Delta}$ cell lines. To gain additional information, we also profiled miR17~92$^{\Delta/\Delta}$ cells transduced with constructs expressing miR-17~92 wild type or miR-19a, b only (Fig. 7A). Deletion of miR-17~92 led to preferential upregulation of genes whose 3' untranslated regions (UTRs) contain binding sites for the miRNAs of the cluster (Fig. 7B, P-value<2.22e-16 Kolmogorov and Smirnov test). Accordingly, ectopic expression of miR-17~92 in miR-17~92$^{\Delta/\Delta}$ cells led to the preferential down-regulation of miR-17~92 targets (Fig. 7C left panel, P-value < 2.22e-16 KS test). Finally, reintroduction of miR-19a and miR-19b only selectively affected mRNAs carrying binding sites for these two miRNAs (P-value = 6.35e-15), but not genes with binding sites for the other members of the miR-17~92 cluster (Fig.7C, right panel).

A total of 568 genes were identified whose expression was upregulated (log2 expression change >0.20) by removal of the endogenous miR-17~92 locus and downregulated by the reintroduction of the full miR-17~92 cluster or miR-19a, b only (Fig. 7D). Among them 95 genes contained at least one mir-19 binding site in their 3'UTR and were chosen for further analysis (Tab. 1). In an effort to identify those targets directly linked to the phenotype observed the list of genes was further narrowed down to 46 genes (Fig. 8B, Tab.1). We reasoned that if miR-19 promotes survival by repressing the expression of one or more of these genes, their knockdown by RNAi should at least partially phenocopy miR-19 reintroduction. To test this hypothesis we designed three shRNA for each of the 46 genes and cloned them into the MLP vector (Fig. 8A), a retroviral vector expressing GFP. The experimental design was similar to that described in Fig. 4A. Briefly each construct was individually transduced into the miR-17~92$^{\Delta/\Delta}$ lymphoma cells and the viral preparations were titrated to achieve an infection efficiency of 5-30%. The fraction of GFP+ cells was measured at 2 and 11 days after the infection. As shown in Fig. 8C, for the majority of shRNAs the number of GFP+ cells did not change over time or was slightly lower at day 11 indicating that the expression of that shRNAs did not provide any growth advantage or was detrimental, respectively. However, for some of shRNAs we observed a significant increase in the fraction of GFP+ cells at day 11 suggesting that they were positively affecting the growth of the tumor cells. Among them, two of the three shRNAs against PTEN had the stronger effect, largely phenocopying the ectopic expression of miR-19a/b (Fig. 8C). Moreover a number of other shRNAs had a more modest but still significant effect. In particular all three shRNAs directed against Sbf2 and two out of three directed against Bcl7a and Rnf44 scored positive suggesting that these genes might contribute to the pro-survival functions of miR-19.

A

Lymphoma line	Sample name	Genotype endogenous miR-17~92	miRNAs Added back
AV4182	fl/fl	flox/flox	none (empty vector)
AV4182 (after 4-OHT)	Δ/Δ	Δ/Δ	none (empty vector)
AV4182 (after 4-OHT)	Δ/Δ + 17~92	Δ/Δ	miR-17~92
AV4182 (after 4-OHT)	Δ/Δ + 19a,b	Δ/Δ	miR-19a and miR-19b

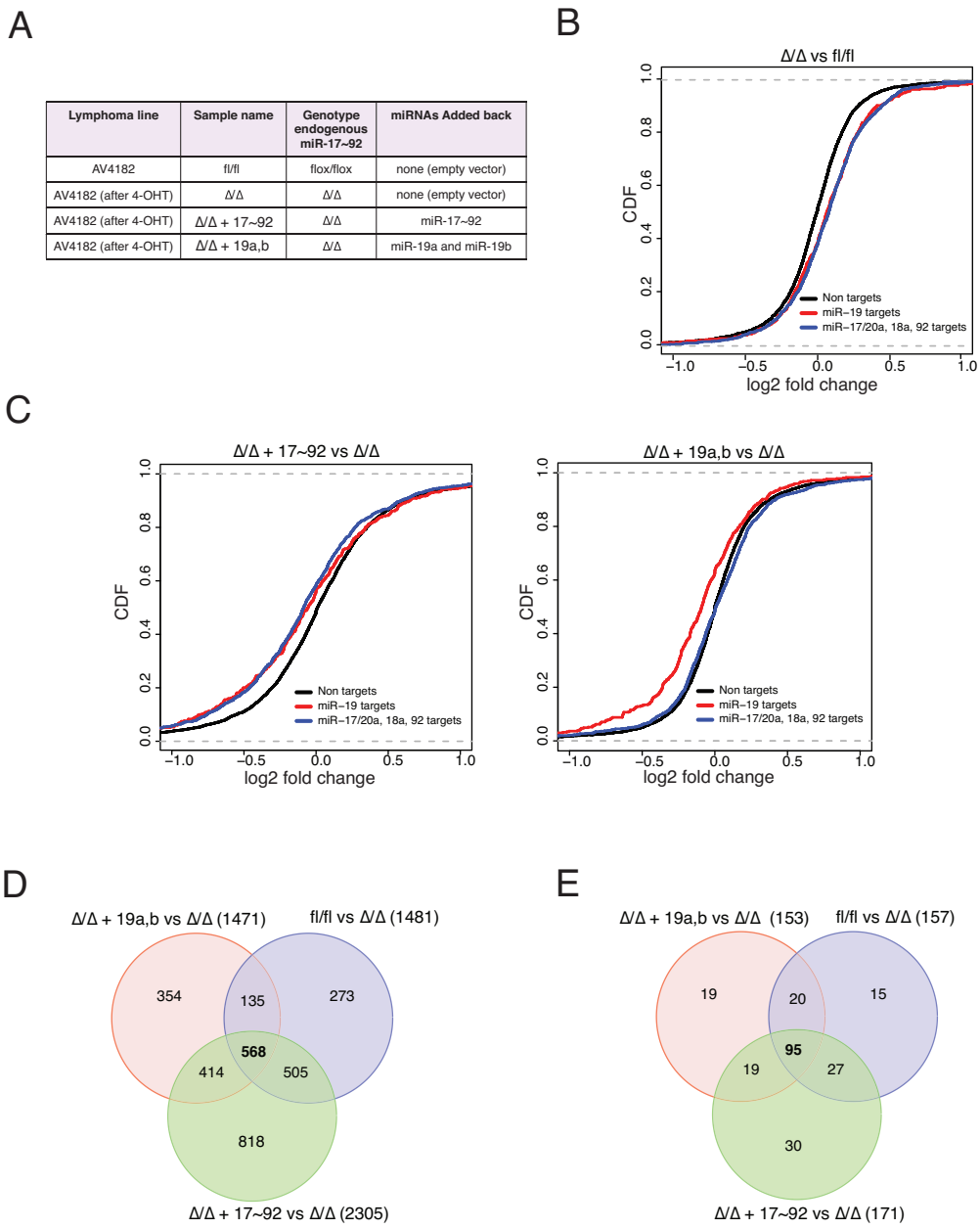

Fig. 7 Gene expression profiling identifies miR-19 targets in Eμ-Myc lymphoma cells. A) Description of the various lymphoma cells generated for the gene expression analysis experiments. **B)** Differences in mRNA levels between miR-17~92$^{fl/fl}$ and miR17~92$^{\Delta/\Delta}$ lymphoma cells transduced with empty PIG vector were monitored with microarrays. Cumulative distribution functions (CDF) plots are shown for: mRNAs that do not contain miR-17~92 seed matches in their 3'UTRs (black line), mRNAs containing one or more seed matches for miR-19 in their 3'UTR (red line) and for mRNAs containing one or more seed matches for either miR-17, miR-20a, miR-18a or miR-92 (blue line). In the absence of endogenous miR-17~92 expression, a statistically significant upregulation (p-value<2.22e-16, KS-test) is observed for the predicted miR-17~92 targets relative to the background gene population. **C)** CDF plots of the changes in mRNA expression levels between miR17~92$^{\Delta/\Delta}$ + PIG-miR-17~92 and miR17~92$^{\Delta/\Delta}$ lymphoma cells (left panel) and between miR17~92$^{\Delta/\Delta}$ + PIG-miR-19a, b and miR17~92$^{\Delta/\Delta}$ lymphoma cells (right panel). Figure legend is as in panel B. A significant downregulation is observed for mRNA with predicted miR-17~92 targets (left panel) and for genes with only miR-19 in the case of PIG-miR-19a,b and miR17~92$^{\Delta/\Delta}$ (right panel). **D)** Venn diagram summarizing the overlap in gene expression changes observed between the various transduction experiments. **E)** As in panel D), but the analysis was limited to mRNAs whose 3'-UTR contains at least one predicted binding site for miR-19 (according to TargetScan 5).

	Δ/Δ+19 vs Δ/Δ		fl/fl vs Δ/Δ		Δ/Δ+17~92 vs Δ/Δ			predicted miR-19 sites (Targetscan 5.1)	
GENE SYMBOL	Fold Change (log2)	(adj. p value)	Fold Change (log2)	(adj. p value)	Fold Change (log2)	(adj. p value)	*Refseq*	*conserved*	*poorly conserved*
Abhd10	-0.945585	0	-0.510971	1.40E-05	-0.960787	0	NM_172511	1	0
Adss	-0.788548	0	-0.530647	9.00E-06	-1.0889	0	NM_007422	1	0
Aff1	-0.316819	3.30E-05	-0.210856	0.000457	-0.259142	2.90E-05	NM_001080798 /// NM_133919	1	0
Akap1	-0.391012	0.000778	-0.324241	0.002765	-0.352087	0.000564	NM_001042541 /// NM_009648	1	0
Apaf1	-0.332099	0.018329	-0.219618	0.015958	-0.469226	8.50E-05	NM_001042558 /// NM_009684	1	0
Arfgef1	-0.582405	1.70E-05	-0.221628	0.004648	-0.716172	1.00E-06	NM_001102430 /// XM_001473166 /// XM_975420	1	0
Asna1	-1.01891	3.00E-06	-0.579796	0.000119	-0.667606	9.00E-06	NM_019652	1	0
Atg16l1	-0.394261	0.000255	-0.27322	0.002462	-1.26189	0	NM_029846	1	1
Bcas3	-1.11395	0.001095	-1.02447	0.002257	-1.31721	0.000153	NM_138681	1	0
Bcl7a	-0.828489	0.000645	-0.360794	0.042122	-0.360794	0.023846	NM_029850	1	0
Brwd1	-0.925747	0.000528	-0.505951	0.014347	-1.12079	5.80E-05	NM_001103179 /// NM_145125 /// NM_176928	1	0
Btf3l4	-1.00313	0	-0.568229	1.90E-05	-0.841379	0	NM_027453	1	0
Cc2d1a	-0.41953	0.00241	-0.983705	3.40E-05	-2.18916	0	NM_145970	1	0
Ccm2	-0.920819	0	-0.869641	2.00E-06	-0.984723	0	NM_146014	1	0
Clock	-0.845546	0.000811	-1.00608	0.00045	-1.05138	8.00E-05	NM_007715	1	0
Cnot6	-0.348227	1.20E-05	-0.269643	8.00E-05	-0.419142	1.00E-06	NM_212484	2	0
Cnot6l	-0.378275	0.000391	-0.463202	0.000505	-0.958214	1.00E-06	NM_144910 /// NM_178854	1	0
Cnot7	-0.288397	0.000762	-0.332077	0.000505	-0.500304	9.00E-06	NM_011135	1	0
Cs	-0.362272	4.50E-05	-0.301502	0.000191	-0.643382	0	NM_026444	1	0
Cenk1g1	-0.377891	0.008941	-0.226375	0.077903	-0.727359	8.90E-05	NM_173185	1	1
Ddx3x	-0.423046	3.90E-05	-0.310166	0.000331	-0.522545	3.00E-06	NM_010028	2	0
Eea1	-0.360744	0.014521	-0.709428	0.000607	-0.466133	0.001931	NM_001001932	1	1
Elovl5	-0.636816	3.00E-06	-0.211186	0.001608	-0.343798	2.90E-05	NM_134255	1	0
Epn2	-0.422472	0.000913	-0.332737	0.004113	-0.558761	6.10E-05	NM_010148	1	1
G3bp2	-0.646111	2.00E-06	-0.394669	4.80E-05	-0.581214	1.00E-06	0794 /// NM_001080795 /// NM_001080796 /// NM_001080797 /// N	1	1
Gigyf2	-0.400983	0.004413	-0.237369	0.04992	-1.07816	5.00E-06	NM_001110212 /// NM_146112 /// XM_001475127	1	0
Grk6	-0.219783	0.0022	-0.348181	0.000269	-0.369335	3.70E-05	NM_001038018 /// NM_001112711 /// NM_011938	1	0
Hbp1	-1.1085	4.00E-06	-0.731394	6.40E-05	-0.854379	4.00E-06	NM_153198 /// NM_177993	2	0
Hdlbp	-0.431304	0.001206	-0.226281	0.203307	-0.428208	8.00E-06	NM_133808	1	0
Hipk1	-0.37086	0.002583	-0.371681	0.003258	-0.304454	0.003583	NM_010432	1	0
Id2	-1.89846	0.011595	-1.98856	0.010824	-3.09813	0.000349	NM_010496	1	0
Impdh1	-0.393629	0.000456	-0.379751	0.000776	-0.469998	5.20E-05	NM_011829	2	0
Ireb2	-0.376369	3.30E-05	-0.216803	0.000982	-0.519989	1.00E-06	NM_022655	1	0
Itpkb	-0.216431	0.12789	-0.225201	0.119486	-0.482111	0.002508	NM_001081175	1	0
Ivns1abp	-0.933776	1.40E-05	-0.404372	0.002039	-0.438087	3.70E-05	NM_001039511 /// NM_001039512 /// NM_054102	1	0
Kif1b	-0.301373	0.001903	-1.00712	5.00E-06	-2.29247	0	NM_008441 /// NM_207682	1	0
Klhdc5	-0.379993	0.019328	-0.775383	0.000692	-0.554559	0.001372	NM_001081237	1	3
Klhl20	-0.880302	0.00044	-0.487471	0.01168	-1.30197	1.30E-05	NM_001039482	2	1
Kpna3	-0.39224	4.00E-06	-0.299641	3.20E-05	-0.526989	0	NM_008466	1	0
Kpna6	-1.28911	1.00E-06	-0.805089	2.70E-05	-0.695877	1.00E-05	NM_008468	2	0
Lin9	-0.819609	0.001282	-0.558608	0.010928	-1.34726	2.30E-05	NM_001103182 /// NM_175186	1	0
Ligl2 /// LOC100047332	-0.525739	0.084155	-0.525739	0.088724	-0.619351	0.030096	NM_145438 /// XR_033868	1	0
LOC100044703 /// March2	-2.08339	0.000124	-1.18801	0.003377	-1.6253	0.000172	NM_145486 /// XR_030915	1	1
LOC100047915 /// Memo1	-0.214203	0.006117	-0.206095	0.00883	-0.390141	0.115396	NM_133771 /// XM_001479122	1	0
LOC677213 /// Uhmk1	-0.78869	1.90E-05	-0.478768	0.000455	-1.00735	1.00E-06	NM_010633 /// XM_001001408	1	0
Lrrc16a	-3.96132	0	-0.266596	0.139844	-1.45789	1.10E-05	NM_026825	1	0
Luzp1	-0.416762	0.703943	-0.410254	0.711707	-5.23336	0.000134	NM_024452	1	0
Mphosph9	-0.693423	5.50E-05	-0.751726	5.70E-05	-1.01988	2.00E-06	NM_001081323	2	0
Mrpl17	-0.302937	4.80E-05	-0.366971	2.70E-05	-0.308838	1.10E-05	NM_025301	1	0
Mylip	-0.425625	0.000127	-1.19595	1.00E-06	-1.27282	0	NM_153789 /// NM_181043	1	0
Nbeal2	-0.917561	0.005059	-0.607256	0.036302	-0.727898	0.008408	XM_911187 /// XM_977572	1	0
Nrbp1	-1.06468	3.00E-06	-1.23034	3.00E-06	-1.50281	0	NM_147201	1	0
Pdik1l	-0.310175	0.07945	-0.432131	0.025175	-0.722209	1.70E-05	NM_146156	1	0
Pknox1	-0.678475	7.00E-06	-0.927782	3.00E-06	-1.11125	0	NM_016670	1	0
Polr3d	-0.534661	0.00016	-0.596968	0.000129	-0.578283	2.90E-05	NM_025945	1	0
Ppp1r15b	-0.720361	0.00265	-0.224743	0.23214	-0.945143	0	NM_133819	1	0
Prc1	-0.531908	1.80E-05	-0.656194	1.10E-05	-0.762907	1.00E-06	NM_145150	1	0
Psap	-0.35069	0.000951	-0.330573	0.001765	-0.504631	3.70E-05	NM_011179	1	0
Pten	-0.247117	0.002467	-0.323515	0.000788	-0.62696	1.00E-06	NM_008960	2	0
Ptk2b	-0.383817	0.101902	-0.243341	0.30037	-0.98303	0.000685	NM_172498	1	0
Rab21	-0.55152	2.10E-05	-0.39599	0.000217	-0.74429	1.00E-06	NM_024454	1	0
Rab2b	-0.872005	0.000778	-0.242881	0.059139	-0.955124	0.000168	NM_172601	1	0
Raf1	-0.323161	0.00079	-0.219672	0.007436	-0.391843	9.00E-05	NM_029780	1	0
Rapgef6	-0.383903	0.001017	-0.34388	0.002405	-0.770514	5.00E-06	NM_175258	1	0
Reep3	-0.461504	0.003265	-0.663993	0.000644	-0.471987	0.001302	NM_178606	1	0
Rhebl1	-0.920708	2.00E-06	-0.636447	3.00E-05	-0.951223	1.00E-06	NM_026967	1	0
Rnf11	-2.74748	1.00E-06	-1.60232	8.00E-06	-2.09095	1.00E-06	NM_013876	1	0
Rnf111	-0.386686	0.004924	-0.393618	0.005524	-0.590877	0.00018	NM_033604	1	0
Rnf167	-0.970857	2.00E-06	-0.515601	0.000122	-0.773101	2.00E-06	NM_027445 /// XM_001471737	1	0
Rnf44	-0.569936	6.70E-05	-0.396033	0.000726	-0.490355	4.80E-05	NM_134064	1	0
Sbf2	-0.704564	4.60E-05	-0.352467	0.002674	-0.693244	1.30E-05	XM_001477215 /// XM_001478567	1	0
Sdc1	-2.38769	1.60E-05	-0.987545	0.002887	-0.698718	0.006933	NM_011519	1	0
Sec22b	-0.534173	5.50E-05	-0.335016	0.001034	-0.549603	1.20E-05	NM_011342	1	0
Sgk1	-0.903681	2.80E-05	-0.876704	5.30E-05	-1.45557	1.00E-06	NM_011361	1	0
Sin3b	-0.596809	0.00789	-0.306751	0.115591	-0.4829	0.011946	NM_001113248 /// NM_009188	1	0
Slc11a2	-1.00648	0.000282	-0.544537	0.02455	-0.760413	0.002144	NM_008732	1	0
Slc9a1	-0.298962	0.064325	-0.675083	0.001988	-1.0362	4.20E-05	NM_016981	1	1
Smoc1	-5.81147	0	-0.25057	0.216805	-6.55082	0	NM_022316	1	1
Snx17	-0.431608	0.000682	-0.260003	0.011424	-0.400008	0.000407	NM_153680	1	0
Spryd3	-1.08837	1.00E-06	-1.04676	2.00E-06	-1.65601	0	NM_001033277	1	0
St8sia4	-0.630003	1.00E-06	-0.255409	0.000342	-0.637969	0	NM_009183	1	0
Stk35	-0.456695	0.012665	-0.27123	0.009404	-0.282802	0.057105	NM_001038514 /// NM_183262	1	1
Suz12	-0.561164	4.00E-06	-0.280736	0.000342	-0.60882	1.00E-06	NM_199196	1	1
Tbk1	-0.257656	7.20E-05	-0.439693	8.00E-06	-0.88559	0	NM_019786	1	0
Tgif1	-0.652019	0.000286	-0.919113	6.50E-05	-0.832961	1.90E-05	NM_009372	1	0
Tnip1	-0.364596	0.020244	-0.36798	0.021592	-0.645539	0.000452	NM_021327	1	0
Tnpo2	-0.843061	0.000197	-0.269129	0.058035	-0.415346	0.004342	NM_001122843 /// NM_145390	1	0
Tnrc6a	-0.24573	0.004625	-0.32399	0.001441	-0.643239	6.00E-06	NM_144925	1	0
Tor1b	-0.719815	2.00E-06	-0.809602	2.00E-06	-1.30517	0	NM_133673	2	0
Usp8	-0.446311	3.60E-05	-0.281848	0.000642	-0.29965	0.000109	NM_019729	1	0
Vps37a	-1.09408	2.00E-05	-0.638268	0.001663	-0.777138	4.30E-05	NM_033560	1	0
Vps4b	-0.433199	2.60E-05	-0.32874	0.000189	-1.06854	0	NM_009190	1	0
Wdr45l	-0.637551	1.10E-05	-0.25104	0.002569	-0.278694	0.000449	NM_025793	1	0
Wwp1	-0.494092	0.012115	-0.426337	0.025876	-0.510665	0.017188	NM_177327	1	0
Zmynd11	-1.16165	7.00E-06	-0.406848	0.000702	-0.48495	5.90E-05	NM_144516	3	0

Tab. 1 This table includes the 95 genes from the interesection of the Venn diagram shown in figure 7E. Each gene contains at least one conserved miR-19 binding site in its 3'-UTR according to TargetScan 5.1 (Column I) and shows a log2 fold change<-0.2 in each of the three comparisons (columns B, D and F). The adjusted p-value is also shown (columns C, E and G). In red are indicated the genes that were selected for the in vitro RNAi screen and functional validation.

A

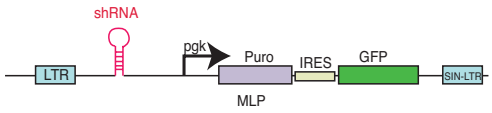

B

REFSEQ	Gene symbol
NM_026825	Lrrc16a
NM_145486	March2
NM_011519	Sdc1
NM_144516	Zmynd11
NM_011361	Sgk1
NM_147201	Nrbp1
NM_027453	Btf3l4
NM_013876	Rnf11
NM_001033277	Spryd3
NM_027445	Rnf167
NM_001103182	Lin9
NM_007715	Clock
NM_026967	Rhebl1
NM_133673	Tor1b
NM_029850	**Bcl7a**
NM_001039482	Klhl20
NM_033560	Vps37a
XM_911187	Nbeal2
XM_001477215	**Sbf2**
NM_025793	Wdr45l
NM_001102430	Arfgef1
NM_001080798	Aff1
NM_134064	**Rnf44**

REFSEQ	Gene symbol
NM_009372	Tgif1
NM_001081323	Mphosph9
NM_212484	Cnot6
NM_016670	Pknox1
NM_024454	Rab21
NM_001103179	Brwd1
NM_010496	Id2
NM_010432	Hipk1
NM_001113248	Sin3b
NM_145150	Prc1
NM_010028	Ddx3x
NM_178606	Reep3
NM_199196	Suz12
NM_175258	Rapgef6
NM_001042541	Akap1
NM_033604	Rnf111
NM_011135	Cnot7
NM_173185	Csnk1g1
NM_008960	**Pten**
NM_001038018	Grk6
NM_144910	Cnot6l
NM_001042558	Apaf1
NM_153198	Hbp1

C

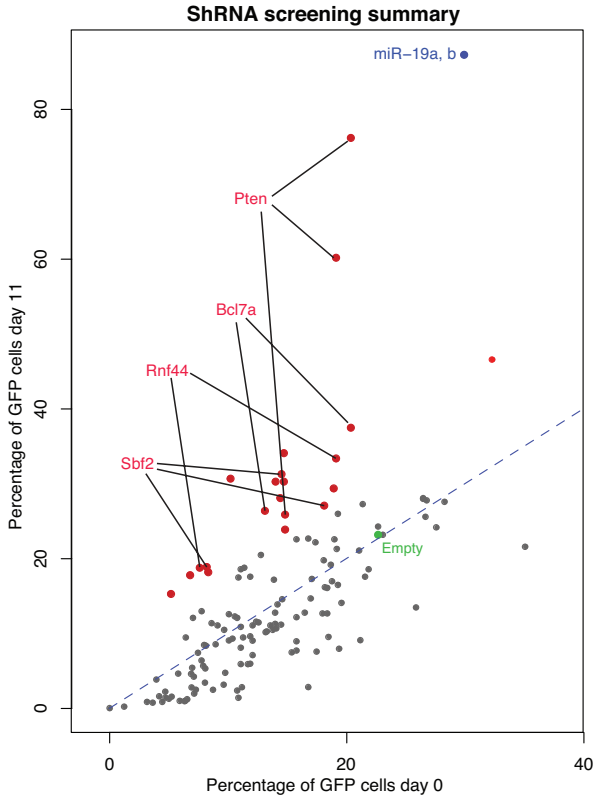

Fig. 8 An in vitro RNAi screen to identify functionally relevant miR-19 targets. A) The MLP retroviral vector **B)** List of 46 miR-19 genes assayed in the in vitro shRNA screen. Genes for whom at least two distinct shRNAs scored positive in the assay are shown in bold. **C)** Scatter plot summarizing the result of the screen. Each dot represents an individual shRNA construct where the x-axis is the percentage of GFP cells at the beginning of the experiment (two days after infection) and the y-axis is the percentage of GFP cells eleven days later. The green dot identifies the empty-vector control. shRNAs that scored positive in the screen are highlighted in red and labeled. Dots corresponding to genes for which at least 2 out of three shRNAs provided significant growth advantage are labeled. PIG-miR-19a/b was included in the screen as positive control and for comparison (blue dot).

PTEN is a direct miR-19 target

PTEN is one of the most frequently mutated tumor suppressor genes in human cancers, it is an haploinsufficient tumor suppressor gene and monoallelic mutations at this locus are observed in >50% of sporadic tumors [77]. In mice loss of a single allele dramatically increase incidence of a variety of tumors, including T-cell lymphomas, as well as tumors of endometrium, liver, prostate, gastrointestinal tract, and thyroid [83]. PTEN negatively regulates cell proliferation by inhibiting the PI3K/AKT pathway. Specifically, PTEN is a phospholipid phosphatase that antagonizes the phosphatidylinositol-3-kinase (PI3K) pathway by hydrolyzing the 3-phosphate on phosphatidylinositol 3,4,5-trisphosphate (PIP_3), a second messenger that promotes cell growth and survival, to generate phosphatidylinositol 4,5-bisphosphate (PIP_2) [77]. In conclusion, a number of experimental observations indicate that even a minor impairment in PTEN function can lead to the development of cancer, suggesting that modest modulation of its levels by miRNAs may have important functional consequences.
The PTEN 3'UTR contains two conserved miR-19 binding sites (Fig. 9A) and it has previously been shown to be a direct miR-19 target [17, 21, 65]. Here we first confirmed that miR-19 directly acts on the PTEN 3'UTR by performing a luciferase reporter assay in both HeLa cells and miR-17~92$^{+/+}$ and miR-17~92$^{\Delta/\Delta}$ primary mouse embryo fibroblasts (Fig. 9B). Both western blot (Fig. 9C) and immunohistochemistry (Fig. 9D) confirmed a consistent upregulation of PTEN upon removal of the miR-17~92 cluster. Importantly reintroduction of the full-length cluster or miR-19a, b only, but not of miR-17~92$^{\Delta 19a, b}$, was sufficient to restore normal PTEN expression levels (Fig. 9D, E). In addition, analogous to miR-19 reintroduction, PTEN knockdown also determined a reduction in the number of apoptotic cells to the levels observed in the miR-17~92$^{fl/fl}$ cells (Fig. 9E).

PTEN knockdown affects tumorigenicity in vivo

Finally we examined whether PTEN knockdown could phenocopy miR-19 reintroduction *in vivo*. To this purpose we injected a cohort of nude mice with miR-17~92$^{\Delta/\Delta}$; sh-PTEN lymphoma cells. As shown in Fig. 10, mice injected with miR-17~92$^{\Delta/\Delta}$; sh-PTEN lymphoma cells develop aggressive lymphomas with a latency similar to that observed in mice injected with miR-17~92$^{\Delta/\Delta}$ cells ectopically expressing miR-19a/b. Again the survival was slightly longer compared to control mice injected with miR17~92$^{fl/fl}$ cells (P=0.0002), suggesting the existence of additional targets and/or cooperative mechanisms possibly involving the other members of the cluster.

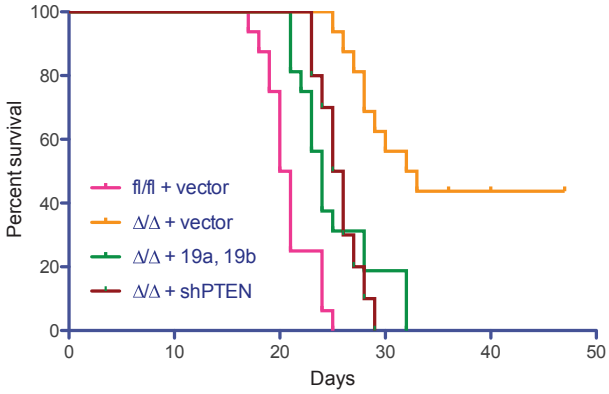

Fig. 10 PTEN knock-down phenocopy miR-19b reintroduction in vivo. Kaplan-Meier survival curve of mice injected with miR-17~92$^{\Delta/\Delta}$ lymphoma cells transduced with retroviruses expressing shRNAs against PTEN. N = 10 (5 mice for shPTEN-1 and 5 mice for shPTEN-2). For comparison, the survival curves of mice injected with miR-17~92$^{fl/fl}$, miR-17~92$^{\Delta/\Delta}$ and miR17~92$^{\Delta/\Delta}$ + miR-19a, b from figure 6A are also included.

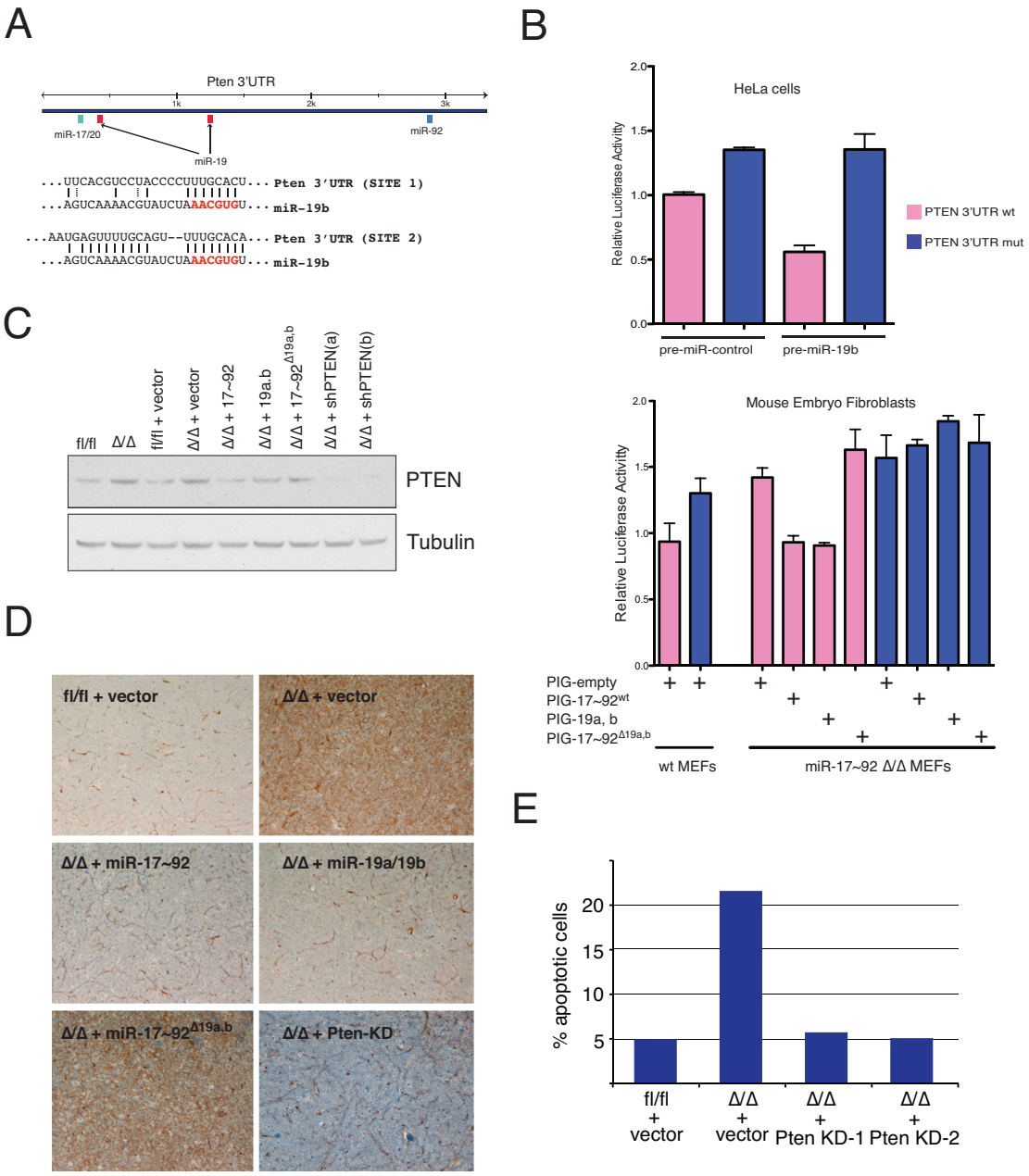

Fig. 9 Pten is a functionally relevant miR-19 target in B cell lymphomas. A) Schematic representation of the Pten 3'UTR with the location of the predicted binding sites for members of the miR-17~92 cluster. Sequence alignments between miR-19b and its two predicted binding sites are also shown. **B**) Luciferase reporter assays on Hela cells and MEFs transfected with a reporter plasmid expressing the firefly luciferase cDNA fused to a fragment of the PTEN 3'UTR containing the two putative miR-19 sites (pink bars) or carrying mutations in both sites (blue bars). Hela Cells were cotransfected with either a pre-miR-control or with pre-miR-19b. MEFs were cotransfected with the indicated PIG constructs. For internal normalization, each transfection included 20 ng of a plasmid encoding for the Renilla luciferase. Cells were assayed 48 hrs later. For comparison the ratio renilla/firefly luciferase measured in cells transfected with the wild-type 3'UTR was set to 1. Error bar is the standard deviation of triplicates. **C)** PTEN Western blot on whole cell lysates of B-lymphoma cells transduced with the indicated PIG constructs. For comparison, lysates from miR-17~92$^{\Delta/\Delta}$ cell expressing the two PTEN shRNAs that scored positive in the in vitro screen were also assayed (lanes 8 and 9). **D)** PTEN immunohistochemistry on lymphoma sections obtained from mice injected with miR-17~92$^{fl/fl}$ and miR-17~92$^{\Delta/\Delta}$ B-lymphoma cells transduced with the indicated miR-17~92 derivatives (objective = 20X). Brown staining indicates PTEN signal. Slides were processed by automated immunostaining and the images collected under identical acquisition conditions. **E)** Knockdown of Pten suppresses apoptosis in miR-17~92$^{\Delta/\Delta}$ cells. Apoptosis was measured by detecting caspase activity in miR-17~92 $^{fl/fl}$ and miR-17~92$^{\Delta/\Delta}$ cells transduced with the indicated retroviruses.

The oncogenic potential of miR-19b resides in the seed sequence

The results shown above strongly support the idea that one miRNA of the cluster, miR-19b, is of a particular relevance in the context of Myc driven B-cell lymphomas. The mature miRNA sequence is made of two structural components: the seed region (nt. 2-8) through which the miRNA interacts with their targets and the non-seed region, extending from nt. 9 to ~23. The non-seed region frequently participates to the target recognition process by providing additional 3' pairing regions [1, 84]. Interestingly, mature miRNAs sequences are highly evolutionary conserved suggesting that both the seed and non-seed region are somehow essential and both contribute to create a perfectly functional miRNA [1]. To experimentally determine the relative importance of the seed and non-seed regions of miR-19b, we next asked whether substituting the non-seed region affects the ability of miR-19b to enhance survival of the tumor cells. In our growth competition experiment (Fig. 4B) miR-20a, another member of the miR-17~92 cluster, was shown to have very little or no effect on the growth of tumor cells. Therefore, we decided to generate two new chimeric constructs, named miR-19b:20 and miR-20:19b, by exchanging the miR-19b non-seed sequence (nt. 9-21) with that of miR-20 (Fig. 11A). We cloned the two chimeric constructs into the MSCV-Puro-IRES-GFP vector and verified that they were correctly being expressed by northern blot (Fig. 11B). This is an essential control as modifying the structure of the pri-miRNA could in principle alter the processing events that lead to the production of the mature miRNA. By using the same experimental approach shown in Fig. 4B and 5B, we reasoned that if the non-seed region is required for the miRNA to exert its biological function then the two chimeric constructs should provide little or no growth advantage to the cells. Following transduction cells were monitored over the course of ten days for increase in the GFP+ fraction of cells. Surprisingly, the miR-19b:20 chimeras could fully recapitulate the effect seen when re-expressing miR-19b in the miR17~92$^{\Delta/\Delta}$ lymphoma cells (Fig. 11C bottom left panel). Accordingly, the miR-20:19b chimeras, equally to miR-20, was not able to rescue the growth defect (Fig. 11C, bottom right panel). Based on these experiments we conclude that the oncogenic properties of miR-19b are mainly mediated by the seed sequence.

Mutations in the seed sequence affect miR-19b function

To further investigate the role of the miR-19b seed sequence in suppressing cell-death, we performed a systematic mutational analysis. We introduced single point mutations in the seed sequence of miR-19b starting from position 2 to position 8, substituting each base with its complementary one and cloned the resulting constructs into the MSCV-Puro-IRES-GFP vector (Fig. 12A). We repeated the growth rescue experiment by infecting the miR17~92$^{\Delta/\Delta}$ lymphoma cells with our miR-19b wild-type and mutant constructs and checked for an increase in the GFP+ fraction of cells over the course of ten days. As expected, none of the seed mutants was able to rescue the growth of the B-lymphoma cells to the same extent of the wild-type miR-19b (Fig. 12B). However a moderate effect was observed for mutations in position 5 and 8 of the miR-19b seed sequence possibly reflecting a partial loss of binding specificity or affinity towards targets. In conclusion, the experiment described so far showed that the seed sequence is the critical determinant of miR-19b oncogenicity. Furthermore, analysis of the gene expression profiles is required to determine whether loss of PTEN repression can fully explain the observed phenotype.

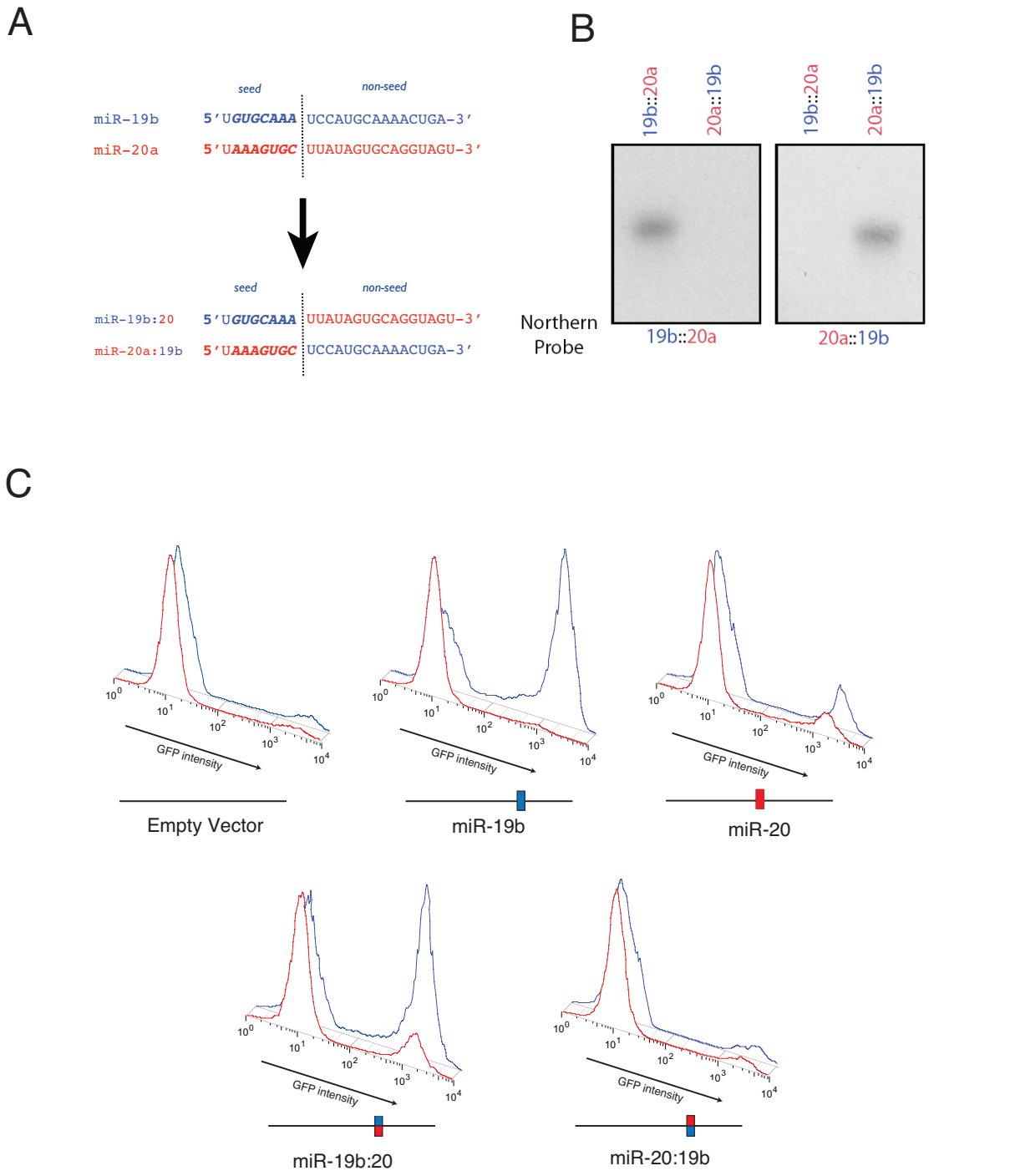

Fig. 11 The oncogenic properties of miR-19b are specified by the seed sequence. A) Schematic representation of the two chimeric constructs obtained by swapping the miR-19b and miR-20 non-seed sequences. **B)** Northern blot on 15 ug of total RNA from the mir-17-92$^{\Delta/\Delta}$ cells transduced with the chimeric constructs. **C)** Histogram overlays of miR-17~92$^{\Delta/\Delta}$ cells transduced with PIG retroviruses expressing either the wild type miR-19b/miR-20 or the chimeric miRNAs. The cells were assayed by flow cytometry to detect GFP expression at day 2 (red plot) and day 10 (blue plot) post-infection. A schematic of the miR-17~92 derivative used is shown under each overlay.

A

miR-19b	5′-U**GUGCAAA**UCCAUGCAAAACUGA-3′
miR-19b-mut2	5′-U**C**U**GCAAA**UCCAUGCAAAACUGA-3′
miR-19b-mut3	5′-UG**A**G**CAAA**UCCAUGCAAAACUGA-3′
miR-19b-mut4	5′-UGU**C**C**AAA**UCCAUGCAAAACUGA-3′
miR-19b-mut5	5′-UGUG**G**AAAUCCAUGCAAAACUGA-3′
miR-19b-mut6	5′-UGUGC**T**AAUCCAUGCAAAACUGA-3′
miR-19b-mut7	5′-UGUGCA**T**AUCCAUGCAAAACUGA-3′
miR-19b-mut8	5′-UGUGCAA**T**UCCAUGCAAAACUGA-3′

B

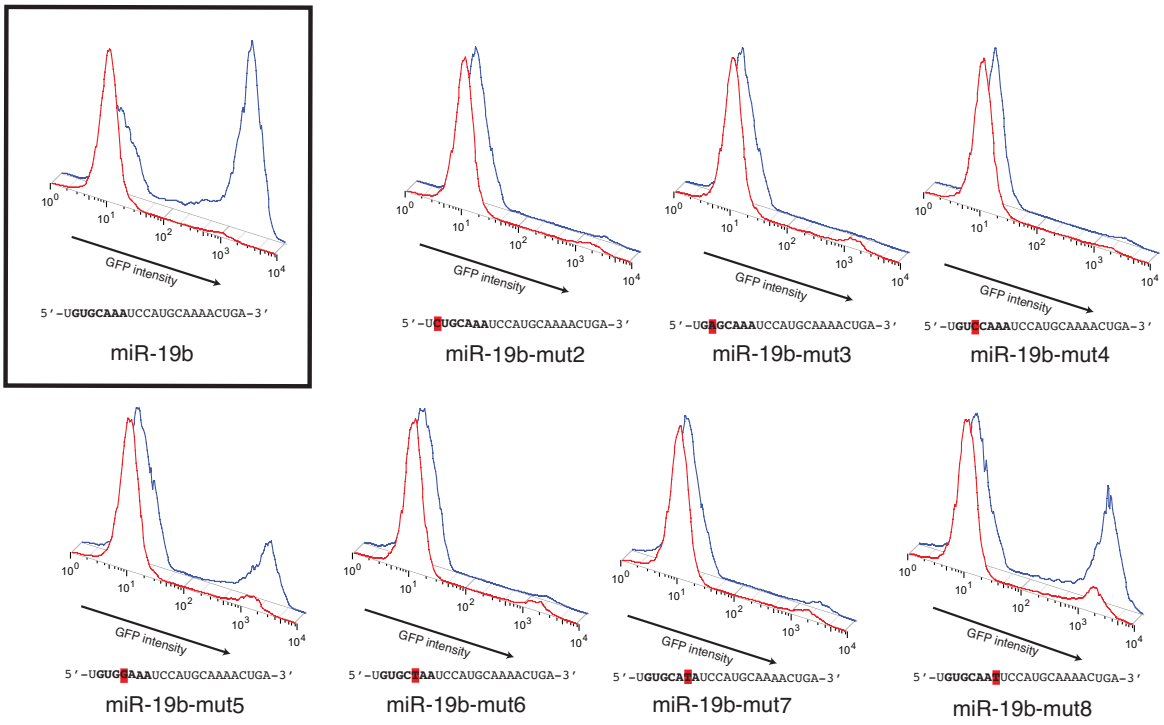

Fig. 12 Mutations in the seed sequence impair miR-19b function. A) Schematic of the miR-19b seed mutant allele series. The seed sequence is shown in bold, the mutated base is highlighted in red. B) Histogram overlays of miR17~92$^{\Delta/\Delta}$ cells transduced with PIG retroviruses expressing the indicated miR-19b derivatives. The cells were assayed by flow cytometry to detect GFP expression at day 2 (red plot) and day 10 (blue plot) post-infection. A schematic of the miR-19b derivative used is shown under each overlay**.** The wild-type miR-19b allele was included for comparison.

Results – Part II

Effects of miR-20b on VEGF expression

In our preliminary study we investigated the role of the miR-17 family in regulating the angiogenic factor VEGF. Oxygen deficiency is proven to stimulate VEGF production leading to increased angiogenesis in tumors [85, 86]. Tumors-induced blood vessel growth is essential for cancer progression as it sustains tumor expansion and allow cells to escape from the primary tumors through the blood stream and metastasize [48]. Since miR-20b, a member of the miR-17 family, has been suggested to act as a negative regulator of VEGF in nasopharyngeal carcinoma epithelioid (CNE) cells [50], we set out to study the effects of this miRNA on VEGF expression in breast cancer cells under hypoxia. VEGF intracellular protein levels were reduced in pre-miR-20b transfected cells by 2.5-fold related to untransfected cells (Fig. 13A). Stimulation with $CoCl_2$, an hypoxia-mimetic agent for 4 or 24 h increased intracellular VEGF protein levels by 2.9- and 2.7-fold, respectively (Fig. 13A). However, transfection of MCF-7 cells with pre-miR-20b, reduced a 4 h $CoCl_2$-induced stimulation of VEGF protein by 3.3-fold (Fig. 13A). In cells treated with $CoCl_2$ for 24 h, pre-miR-20b inhibited VEGF intracellular protein levels by 2.7-fold (Fig. 13A). The effects of miR-20b on the secreted VEGF protein mirrored the above findings. As expected, $CoCl_2$ treatment for 4 and 24 h induced extracellular VEGF protein by 60% and 105%, respectively (Fig. 13B). Consistent with previous results, transfection with pre-miR-20b inhibited 4 and 24 h $CoCl_2$-mediated induction of extracellular VEGF by 30% and 25%, respectively, relative to negative control , while basal level of secreted VEGF were reduced by 32% (Fig. 13B). In further validate the impact of miR-20b on VEGF expression, we used a synthetic oligonucleotide (anti-miRs) designed to target the mature forms of miR-20b and thereby inhibit their expression. Following miR-20b silencing, intracellular VEGF proteins levels increased by 1.5-fold (Fig. 13C), while the amount of secreted VEGF were elevated by 20% (Fig. 13D). Taken togheter these results suggest that VEGF is, indeed, a true miR-17~92 target in human breast cancer.

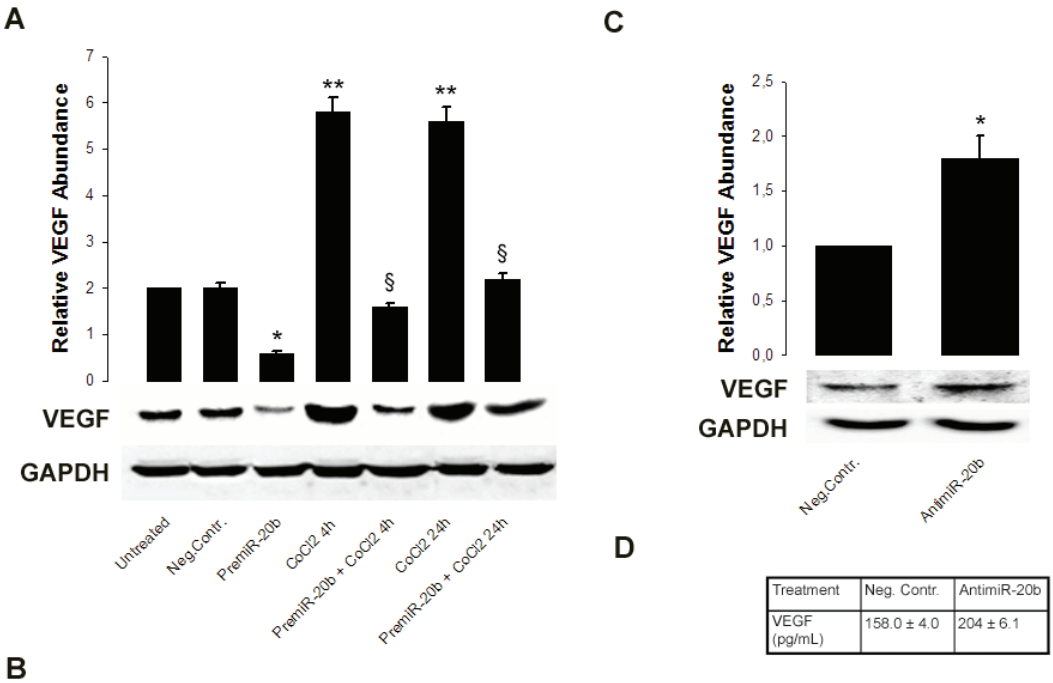

Treatment	Neg. Contr.	AntimiR-20b
VEGF (pg/mL)	158.0 ± 4.0	204 ± 6.1

B

Treatment	Untreated	Neg. Contr.	PremiR-20b	CoCl2 4h	PremiR-20b + CoCl2 4h	CoCl2 24h	PremiR-20b + CoCl2 24h
VEGF (pg/mL)	193.0 ± 12.0	186.0 ± 6.8	124.1 ± 7.0	298.6 ± 8.7	216.2 ± 6.5	402.4 ± 25.3	294.0 ± 12.2

Fig. 13 VEGF protein levels are decreased by transfection with pre-miR-20b and increased by miR-20b silencing. A) The abundance of VEGF total protein was determined by WB in 120 µg of total proteins, as decribed in Materials and Methods Section. The graph represents the increase of VEGF protein levels relative to untrasfected cells±SD; columns, mean; bars, SD. *P < 0.05, control versus pre-miR-20b; **P < 0.05, control versus $CoCl_2$; §P < 0.05, CoCl2 versus miR-20b+CoCl2. **B)** The secreted protein levels were determined by ELISA. A total of 7*10^5 MCF-7 cells were treated as described Materials and Methods Section. The concentrations represent pg of VEGF/ml of conditioned medium from 4*10^5 cells. **C)** The abundance of VEGF proteins was studied by WB in 120 µg of total proteins in MCF-7 cells transfected with synthetic oligonucleotides targeting miR-20b (anti-miR-20b) or with negative control anti-miR molecules, as described in Materials and Methods Section. The graph represents the increase of VEGF protein levels relative to negative control+SD; columns, mean; bars, SD. * P < 0.05 control versus anti-miR-20b. **D)** The concentration of secreted VEGF was measured by ELISA in cells transfected with anti-miR20b or with negative control anti-miR. The concentrations represent pg of VEGF per ml of conditioned medium from 4*10^5 cells.

Defective angiogenesis in the miR-17~92 family knockout embryos

VEGF levels are tightly regulated during embryo development [45]. In particular, a 2-3 fold VEGF overexpression, following removal of the entire 3'UTR from the messenger RNA, has been shown to impairs embryo development at early stages (13.5-14.5) due to cardiovascular defects [43]. Despite they can often complete development and die at birth, ~60% of the miR-17~92 single knockout embryos and ~80% of the double knockout embryos (DKO, miR-17~92$^{\Delta/\Delta}$; miR-106a~363$^{\Delta/\Delta}$) prematurely die around E14.5 showing a phenotype similar to that described by *Miquerol et al.* in 2000. As threshold levels of VEGF are extremely important during embryonic development we hypothesized that the deregulation of the VEGF signaling pathway is, at least partially, responsible for the early embryonic lethality observed in those embryos and that combinatory deletion of the miR-17~92 and miR-106a~363 cluster could in fact facilitate crossing this threshold. As shown in Fig. 14A no obvious phenotype is seen in the miR-17~92$^{\Delta/\Delta}$; miR-106a~363$^{\Delta/y}$ (DKO) embryos until E11.5 except for a slight reduction in body size compared to wild type embryos. Transversal sections throughout the embryonic heart at ~E12.5 reveal the presence of a ventricular septal defect and a thinner compact layer of the myocardium (Fig. 14B). By day 13.5 the embryos become edematous with extensive hemorrhagic areas, features strictly linked to heart failure and defective blood circulation. Embryos invariably die around E14.5 (Fig. 14A). As VEGF signaling is also known to control vascular development during embryogenesis [44], we sought to visualize the embryonic vascular pattern by means of the CD-31 staining (PECAM), a surface molecule highly expressed in both embryonic and adult endothelial cells (Fig. 14C). By comparing the gross appearance of the WT and DKO embryos at E12.5 we observed a clear loss of structural organization in the vasculature of the latter. A closer look revealed defects in the intersomitic vessels formation (Fig. 14D, E). The intersomitic blood vessels appeared to be discontinuous in the mutants particularly in the caudal region (Fig. 14E). This is in contrast to the organized intersomitic blood vessels observed in a control littermate (Fig. 14D). Moreover they failed to correctly fuse along the medial surface of the somites to form the vertebral arteries (Fig. 14C, D and Fig. 14F, G). Finally we noticed a consistent increase in vessels density and number of branching points in the vasculature of the head (Fig. 14H, I).

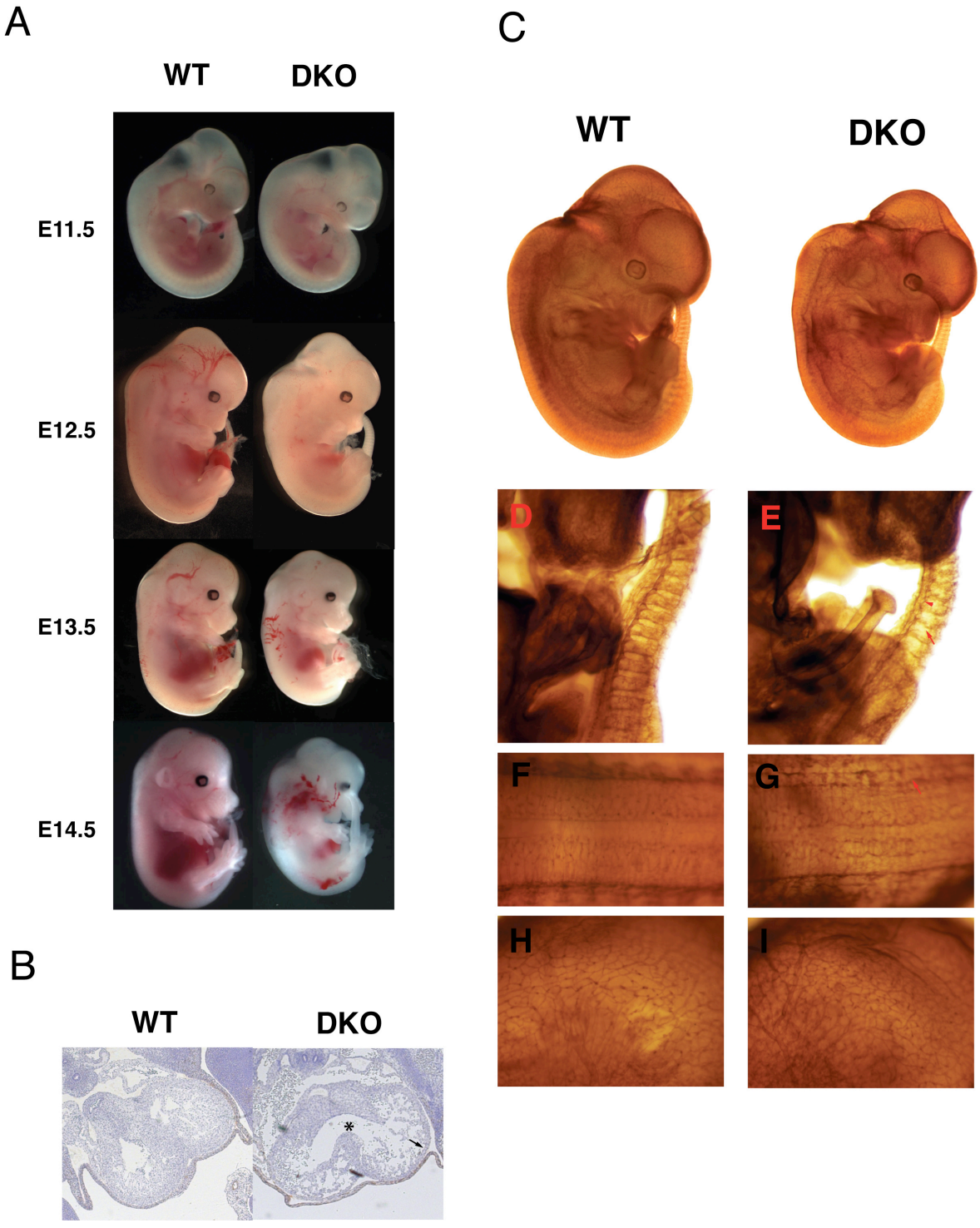

Fig. 14 Defective heart development and angiogenesis in the miR-17 family of miRNAs Knockout mice. **A)** miR-17~92$^{+/+}$;miR-106a~363$^{+/y}$ and miR-17~92$^{\Delta/\Delta}$; miR-106a~363$^{\Delta/y}$ (DKO) embryos at various developmental stages. **B)** Hematoxylin staining of transversal sections of WT and DKO hearts at E12.5. The asterisk indicates the ventricular septal defect; the arrow indicates the thinner compact layer of the ventricular wall. **C)** CD-31 (PECAM) whole mount immunostaining of WT and DKO E12.5 embryos. **D, E)** High magnification images of the tail region of WT and DKO E12.5 embryos. Arrow indicates the intersomitic vessels; arrowhead indicates the posterior region of vertebral artery. **F, G)** High magnification images of the dorsal thoracic spine region of WT and DKO E12.5 embryos. Arrow indicates the vertebral artery. **H, I)** High magnification images of the right lateral head region of WT and DKO E12.5 embryos.

VEGF levels are increased in the miR-17~92 KO embryos

Next we verified whether miR-17~92 deletion led to derepression of VEGF expression in the knockout embryos. Several primary mouse embryo fibroblast (MEF) cell lines were derived from miR-17~92$^{+/+}$, miR-17~92$^{\Delta/+}$, miR-17~92$^{\Delta/\Delta}$ embryos at E13.5. Single Knockout embryos with a more severe phenotype were selected, as judged by the presence of edemas and hemorrhages in the body. No obvious difference was observed in the growth kinetics of the various MEF cell lines when cultured in vitro (data not shown). Levels of secreted VEGF were then measured through an enzyme-linked immunosorbent assay (ELISA) specifically recognizing the 164aa. isoform of VEGF. As shown in Fig. 15A, under normoxic conditions levels of VEGF were ~3 and ~7 fold higher in the miR-17~92$^{\Delta/\Delta}$ MEFs compared to the miR-17~92$^{\Delta/+}$ and miR-17~92$^{+/+}$ MEFs, respectively. Moreover we cultured the cells under mild hypoxic condition (5% O2) that closely resembles physiological oxygen levels found in embryos [87]. VEGF secretion was correctly induced and ~2 fold higher in the miR-17~92$^{-/-}$ MEFs compare to the miR-17~92$^{+/+}$ cells (Fig. 15A). Consistent with the ELISA results, we observed a ~2 fold increase in the levels of VEGF mRNA in the miR-17~92$^{\Delta/\Delta}$ compared to the miR-17~92$^{+/+}$ under both normoxic and mild hypoxic conditions (Fig. 15B). These findings prompted us to investigate whether VEGF was also upregulated in vivo. Indeed, the levels of VEGF mRNA in the embryo limb, a region known to be highly vascularized and actively proliferating at this stage (E13.5), were 40% higher in the knockout embryos compared to the wild-type ones (Fig. 15C). Finally we measured the levels of cytoplasmic VEGF in whole organ lysates from E13.5 embryos. VEGF was slightly higher in the head of the knockout embryos (1.3 fold) and strongly induced in the liver (4 fold) and lungs (9 fold) compared to miR-17~92$^{+/+}$ embryos (Fig. 15D). Noteworthy, the embryonic lung and liver are two of the highest vascularized organs. Thus we concluded that miR-17~92 knockout embryos have increased levels of the pro-angiogenic factor VEGF and this upregulation could be responsible for the cardiovascular and angiogenetic defects described earlier in this manuscript.

VEGF is not a direct miR-17~92 target

In order to determine whether VEGF upregulation is a direct consequence of the absence of the miR-17~92 cluster we transduced a miR-17~92$^{\Delta/\Delta}$ MEF cell line with the full length miR-17~92 cluster or a series of mutant alleles lacking respectively the miR-17, 19 and 92 miRNA family or expressing the miR-19 family only. We first verified that these constructs were correctly expressing the desired miRNAs by Real-time PCR (data not shown) and then measured the levels of secreted VEGF upon reintroduction of the different constructs. We found that, both in normoxia and at 5%O_2, secreted VEGF levels were slightly decreased by restoration of the miR-17~92 full-length cluster expression but not by a construct lacking the miR-17 family (Fig. 16A). Nevertheless VEGF levels were still consistently higher than those observed in miR-17~92$^{+/+}$ MEFs (Fig. 16A) indicating that, in MEFs, miR-17~92 absence is only partially responsible for the upregulation of VEGF. Targetscan [88] analysis identified a conserved miR-17 binding site in the mouse VEGF 3'UTR (position 161-167). A 314 bp region comprising the miR-17 binding site was cloned downstream of the firefly luciferase gene into the psiCHECK-2 vector. The miR-17~92$^{\Delta/\Delta}$ MEFs were transfected with the resulting VEGF3'UTR-psiCHECK-2 vector together with a single miRNA of the cluster (miR-17, 18, 20, 19b and 92). The luciferase reporter assay confirmed that VEGF is not a direct miR-17~92 target as none of the miRNAs, including miR-17 and miR-20, were able to modulate firefly luciferase expression (Fig. 16B).
In conclusion the miR-17 family does not directly target VEGF in mouse. VEGF upregulation might be instead a consequence of the oxygen deficiency caused by a defective fetal blood circulation.

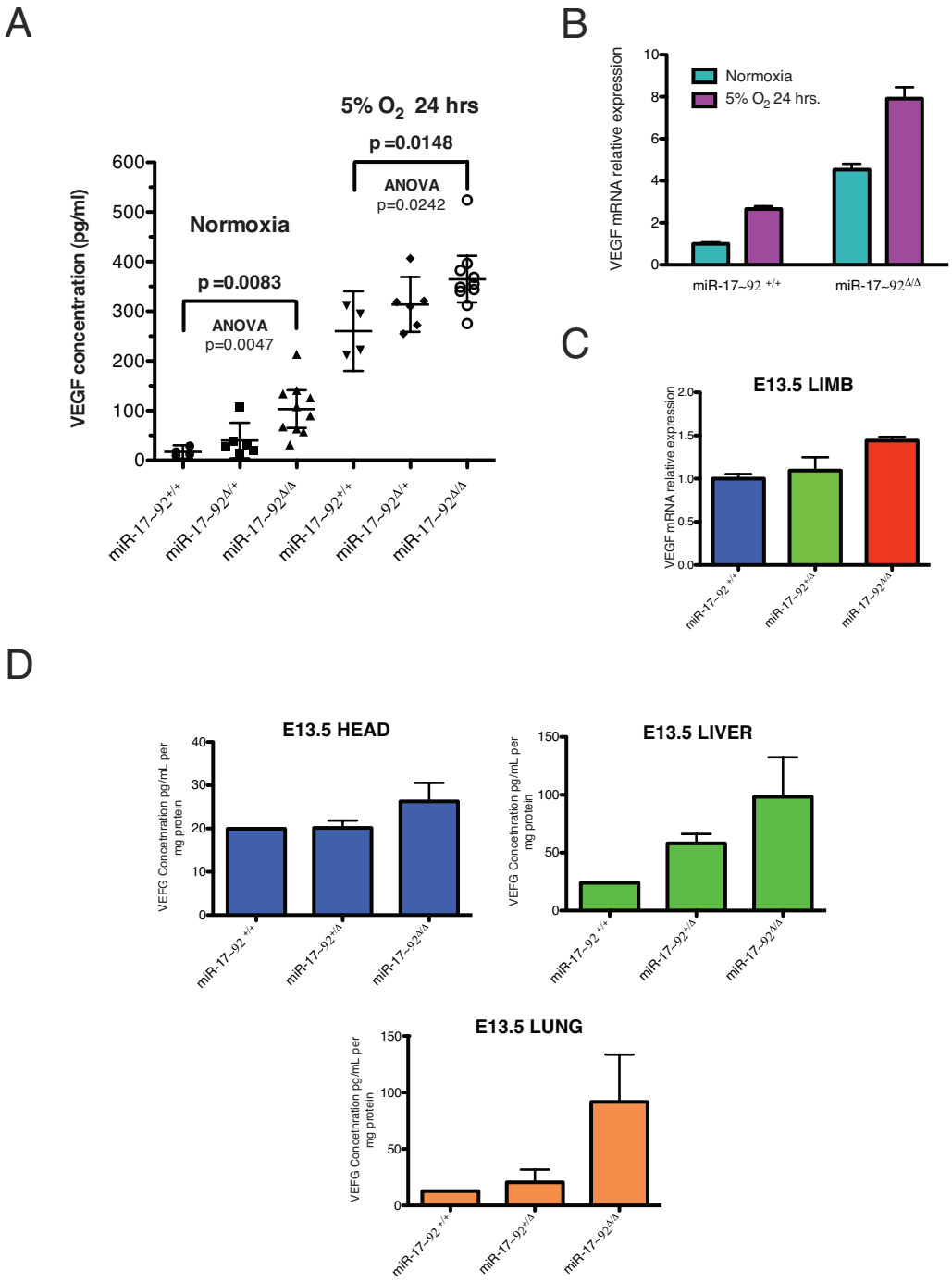

Fig. 15 VEGF is upregulated in the absence of miR-17~92. **A)** Secreted VEGF levels in miR-17~92$^{+/+}$, miR-17~92$^{\Delta/+}$ and miR-17~92$^{\Delta/\Delta}$ of primary MEFs as determined by ELISA. Each dot of the scatter plot represents a different cell line. Error bar= 95% C.I. p< 0.01 for comparison between WT and KO MEFs in normoxia; p<0.05 for comparison between WT and KO MEFs under 5%O_2 . p=0.0047 and p=0.0242 under normoxia and 5%O_2 respectively for multiple group comparison with the one-way ANOVA test. **B)** Relative expression levels of the VEGF mRNA were measured by Real-time in miR-17~92$^{+/+}$ and miR-17~92$^{\Delta/\Delta}$ embryos under normoxic and hypoxic (5% O_2) conditions. For comparison VEGF mRNA levels in WT MEFs under normoxia were set to 1. Columns, mean. Bars=SD. P<0.01 for comparison between miR-17~92 WT and KO cells. C) Relative VEGF mRNA expression levels in miR-17-92 WT and KO E13.5 embryos. RNA was extracted from the right posterior limb. Expression levels in the WT embryos were set to 1. Columns, mean; bars=SD. P=<0.01 for comparison between WT and KO embryos. C) Cytosolic VEGF levels in the head, lungs and liver whole organ lysates from miR-17~92$^{+/+}$, miR-17~92$^{\Delta/+}$ and miR-17~92$^{\Delta/\Delta}$ E13.5 embryos measured by ELISA. Columns, VEGF mean concentration (pg/mL) per mg of protein; bars=SD. P<0.05 for comparison between +/+ and -/- embryos.

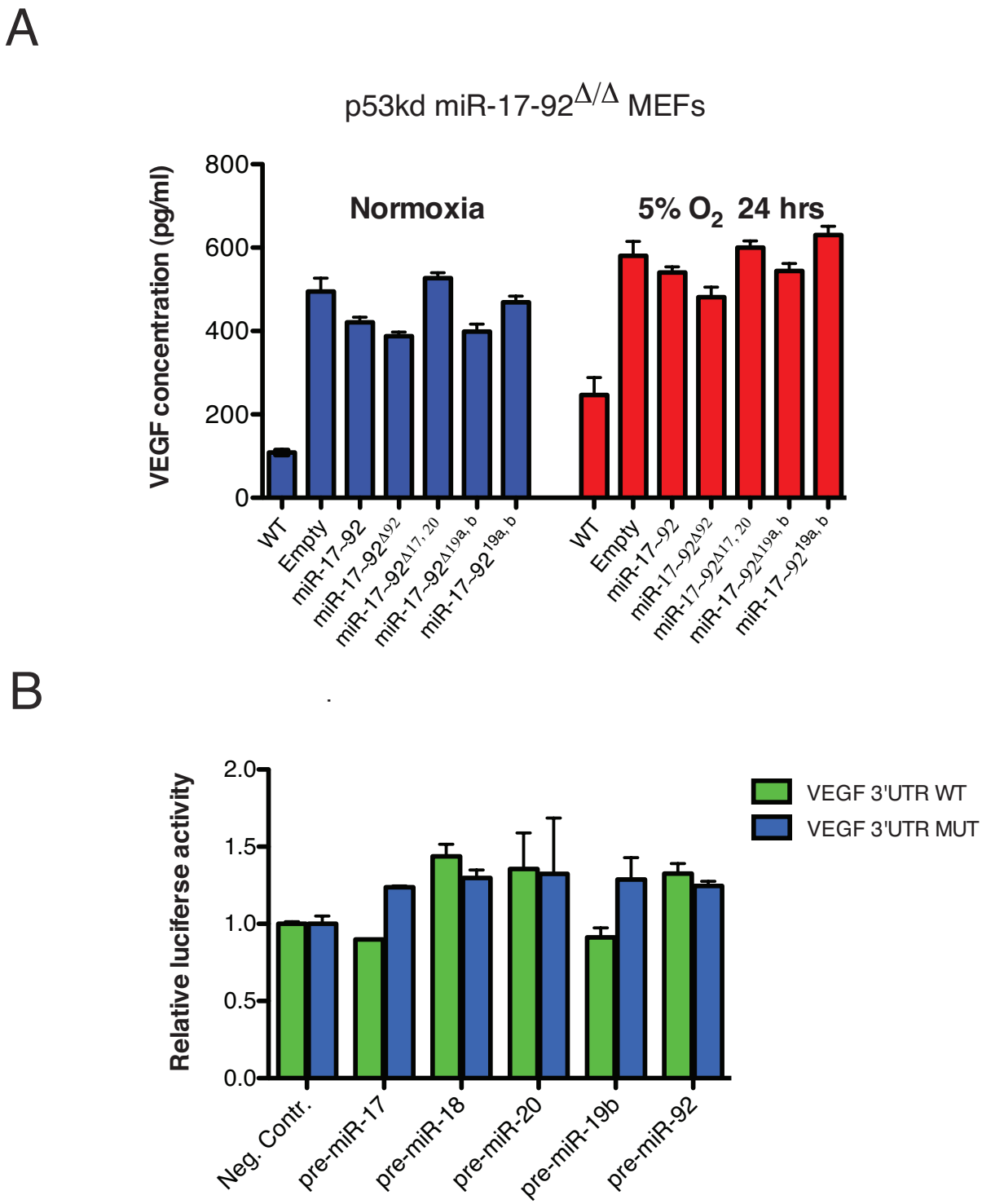

Fig. 16 miR-17-92 does not target VEGF. A) Secreted VEGF levels, upon reintroduction of different PIG constructs in miR-17~92$^{\Delta/\Delta}$; p53-kd immortalized MEFs, were measured by ELISA**.** Columns, mean; Error Bars, SD **B)** Luciferase reporter assays on miR-17~92$^{\Delta/\Delta}$; p53-kd MEFs transfected with a reporter plasmid expressing the firefly luciferase cDNA fused to a 314bp fragment of the VEGF 3'UTR containing a putative miR-17 binding site (green bars) or carrying a mutation (blue bars) and a Renilla firefly luciferase gene for internal normalization. Cells were cotransfected with a pre-miR-control or with the pre-miR-17, 18, 20, 19b and 92. For comparison the ratio Firefly/Renilla luciferase measured in WT MEFs transfected with the wild-type 3'UTR was set to 1. No significant difference was observed.

Discussion and Conclusions

PART I

In this study we identified miR-19 as the key mediator of the oncogenic properties of the miR-17~92 cluster in the context of Myc-driven B-cell transformation. Consistent with initial studies by *He et al.* we confirmed that miR-17~92 cooperates with c-Myc in accelerating lymphomagenesis. Over-activation of the c-Myc pathway is known to elicit a strong proliferative effect but also to sensitize cells to apoptosis [76]. Although mir-17~92 has been shown to promote cell proliferation in other cellular contexts [23, 24], removal of the mir-17~92 cluster did not affect cell proliferation in the Eμ-Myc model. c-Myc driven activation of the cluster rather protected the tumor cells from apoptosis, as removal of the cluster caused a strong increase in the number of cells undergoing programmed cell death. By genetically dissecting the various components of the cluster we showed that only members of the mir-19 family can suppress apoptosis.

The tumor suppressor PTEN was identified as the critical miR-19 target. PTEN is a haploinsufficient tumor suppressor gene, giving that lost of even a single allele promotes malignant transformation [77]. Functionally PTEN is a lipid phosphatase that negatively regulates the pro-survival PI3K/AKT signaling pathway [78]. It has previously been identified as a target of mir-17-92 in cell culture-based experiments [17, 21] but how individual mir-17-92 components contribute to repress PTEN and, more importantly, whether the downregulation of PTEN by mir-17~92 has any functional impact on cell survival in a tumorigenic setting was yet to be proven. Here we provide strong evidences that PTEN is a direct mir-19 target and that knockdown of PTEN can phenocopy miR-19 expression, restoring the tumorigenicity of the miR-17-92 deleted Eμ-Myc lymphoma cells. A recent report also confirmed our findings and extended them to Notch1-induced T-cell leukemias showing that the importance of miR-17~92 is not confined to the B-cell compartment nor is necessary linked to the c-Myc induced activation of the cluster [89].

It is well established that miRNA are able to regulate several targets at the same time, affecting different pathways or multiple nodes on the same pathway [1]. Moreover clusterization of miRNAs likely evolved to coordinate miRNA tuning of the cell transcriptome thus eliciting a more complex response. In this scenario the stronger oncogenic potential of the full-length miR17~92 cluster, compared to the miR-19 family alone, can be partially explained by assuming that the other members of the cluster are actively cooperating with miR-19 by enhancing repression of their common targets (e.g. PTEN) or downregulating additional targets. Moreover, since only 46 out of 95 genes found upregulated following miR-19 deletion were functionally validated, additional relevant targets might come out from an extended analysis of the gene expression analysis data.

A systematic mutational analysis demonstrated that the oncogenic potential of miR-19b is entirely dependent on the seed sequence. A possible explanation is that disrupting the seed sequence completely or partially affects miR-19b ability to interact with its targets. In fact, even a partial loss of affinity towards a target's binding site could lower the repressive effect and abrogate miR-19b anti-apoptotic activity. Despite evolutionary conserved, the non-seed sequence seemed to have a minor role in the target recognition process. Perhaps the non-seed primary function is to drive the processing of the miRNA precursor or the correct assembly of the mature miRNA into the RISC complex. Analysis of the gene expression profile, for each mutant we have generated, will allow us to determine whether loss of PTEN repression can fully explain miR-19b loss of activity and possibly identify additional important miR-19b targets. Moreover, in order to confirm that the observed difference in oncogenic effects reflects a true functional difference rather than a difference in the expression levels, we need to verify whether the mutants are correctly processed and expressed at levels comparable to that of the wild type miR-19b. Finally we will also test, *in vivo*, the oncogenicity of the mutants.

In conclusion, the findings described in this manuscript provide a solid explanation for the functional cooperation of miR-17~92 and c-Myc. They further demonstrates that miR-17~92 is required for tumorigenesis and its oncogenic potential is completely dependent on miR-19b. To our knowledge, we are among the first to show that mutations in the mature sequence of an oncogenic miRNA have an impact on the growth of cancer cells. Finally, our results have important implications for the development of novel anti-cancer therapies based on miRNA inhibitor as targeting miR-19b might be an effective treatment against apoptosis-resistant tumors.

PART II

In this study we shed light on the molecular mechanisms and the factors involved in miR-17~92 regulation of angiogenesis. In our preliminary work, we observed a miR-20b dependent regulation of the pro-angiogenic factor VEGF in an *in vitro* model of breast cancer. Deregulation of the VEGF signaling pathway in solid tumors has a strong impact on tumor progression as it stimulates the growth of blood vessels to provide nutrients and oxygen to the tumor cells [48]. In accordance with our findings, members of the miR-17 family have been reported to target VEGF in tumors [50, 51]. VEGF is a master regulator of cardiovascular development and deregulation of developmental pathways is commonly associated with cancer. When we looked at mouse cardiovascular development, we indeed found that embryos lacking miR-17~92 alone or together with its paralog miR-106a~363, have a defective heart and a profoundly altered vascular pattern. VEGF was found to be upregulated, but it was not directly regulated by miR-17~92. VEGF increase in embryos could be indirectly caused by the absence of miR-17~92. Indeed, cardiac defects might be responsible for an insufficient blood circulation that causes tissues to become hypoxic and ultimately leads to the activation of a VEGF-mediated angiogenic response. Another possible explanation is that the interaction between miR-17~92 and VEGF is restricted to a particular cell-type (e.g. endothelial cells) or is context-dependent.

Our data support the idea that miR-17~92 negatively regulates angiogenesis. Accordingly, a recent report showed that individual miR-17~92 members have anti-angiogenic properties [70]. However, further analyses are required in order to identify the critical targets affecting vascular development. In recent years, some reports have attributed to this cluster of miRNAs a proangiogenic role in tumors [69]. It is possible that in a tumorigenic context miR-17~92 function is altered, as a consequence of multiple deregulated or constitutively activated oncogenic pathways.

In the last few years researchers have focused their attention on the development of anti-angiogenic drugs for the treatment of solid tumors. Understanding the physiologic role of miR-17~92 in controlling angiogenesis will be of great help in developing new anti-cancer therapies based on miRNA mimics or inhibitors.

Acknowledgments

The work described in this thesis was done in collaboration with Ping Mu and Hoon-chi Han. I would like to thank all my lab mates, in Italy and in the USA, for their help and support during these three years. A special thank goes to my mentor, Prof. Antonio Russo, who gave me the opportunity to do part of my Ph.D. in one of the best cancer research center in the world, The Memorial Sloan Kettering of New York. I'm also immensely grateful to Dr. Andrea Ventura, the best boss I could ever met, who hosted me in his lab as a visiting student for 2 years. Finally I would like to thank my family, friends, my girlfriend and all the people who helped me achieving this goal.

References

1. Bartel, D.P. MicroRNAs: target recognition and regulatory functions. *Cell* **136**, 215-33 (2009).

2. Wang, Y., Sheng, G., Juranek, S., Tuschl, T. & Patel, D.J. Structure of the guide-strand-containing argonaute silencing complex. *Nature* **456**, 209-13 (2008).

3. Hock, J. & Meister, G. The Argonaute protein family. *Genome Biol* **9**, 210 (2008).

4. Ambros, V. The functions of animal microRNAs. *Nature* **431**, 350-5 (2004).

5. Guo, H., Ingolia, N.T., Weissman, J.S. & Bartel, D.P. Mammalian microRNAs predominantly act to decrease target mRNA levels. *Nature* **466**, 835-40 (2010).

6. Megraw, M., Sethupathy, P., Corda, B. & Hatzigeorgiou, A.G. miRGen: a database for the study of animal microRNA genomic organization and function. *Nucleic Acids Res* **35**, D149-55 (2007).

7. Altuvia, Y., Landgraf, P., Lithwick, G., Elefant, N., Pfeffer, S., Aravin, A., Brownstein, M.J., Tuschl, T. & Margalit, H. Clustering and conservation patterns of human microRNAs. *Nucleic Acids Res* **33**, 2697-706 (2005).

8. Baskerville, S. & Bartel, D.P. Microarray profiling of microRNAs reveals frequent coexpression with neighboring miRNAs and host genes. *RNA* **11**, 241-7 (2005).

9. Lewis, M.A. & Steel, K.P. MicroRNAs in mouse development and disease. *Semin Cell Dev Biol* **21**, 774-80 (2010).

10. Sevignani, C., Calin, G.A., Nnadi, S.C., Shimizu, M., Davuluri, R.V., Hyslop, T., Demant, P., Croce, C.M. & Siracusa, L.D. MicroRNA genes are frequently located near mouse cancer susceptibility loci. *Proc Natl Acad Sci U S A* **104**, 8017-22 (2007).

11. Calin, G.A. & Croce, C.M. MicroRNA signatures in human cancers. *Nat Rev Cancer* **6**, 857-66 (2006).

12. Ventura, A. & Jacks, T. MicroRNAs and cancer: short RNAs go a long way. *Cell* **136**, 586-91 (2009).

13. Ota, A., Tagawa, H., Karnan, S., Tsuzuki, S., Karpas, A., Kira, S., Yoshida, Y. & Seto, M. Identification and characterization of a novel gene, C13orf25, as a target for 13q31-q32 amplification in malignant lymphoma. *Cancer Res* **64**, 3087-95 (2004).

14. Olive, V., Jiang, I. & He, L. mir-17-92, a cluster of miRNAs in the midst of the cancer network. *Int J Biochem Cell Biol* **42**, 1348-54 (2010).

15. Mu, P., Han, Y.C., Betel, D., Yao, E., Squatrito, M., Ogrodowski, P., de Stanchina, E., D'Andrea, A., Sander, C. & Ventura, A. Genetic dissection of the miR-17~92 cluster of microRNAs in Myc-induced B-cell lymphomas. *Genes Dev* **23**, 2806-11 (2009).

16. Olive, V., Bennett, M.J., Walker, J.C., Ma, C., Jiang, I., Cordon-Cardo, C., Li, Q.J., Lowe, S.W., Hannon, G.J. & He, L. miR-19 is a key oncogenic component of mir-17-92. *Genes Dev* **23**, 2839-49 (2009).

17. Lewis, B.P., Shih, I.H., Jones-Rhoades, M.W., Bartel, D.P. & Burge, C.B. Prediction of mammalian microRNA targets. *Cell* **115**, 787-98 (2003).

18. Ventura, A., Young, A.G., Winslow, M.M., Lintault, L., Meissner, A., Erkeland, S.J., Newman, J., Bronson, R.T., Crowley, D., Stone, J.R. *et al.* Targeted deletion reveals essential and overlapping functions of the miR-17 through 92 family of miRNA clusters. *Cell* **132**, 875-86 (2008).

19. Koralov, S.B., Muljo, S.A., Galler, G.R., Krek, A., Chakraborty, T., Kanellopoulou, C., Jensen, K., Cobb, B.S., Merkenschlager, M., Rajewsky, N. *et al.* Dicer ablation affects antibody diversity and cell survival in the B lymphocyte lineage. *Cell* **132**, 860-74 (2008).

20. Petrocca, F., Visone, R., Onelli, M.R., Shah, M.H., Nicoloso, M.S., de Martino, I., Iliopoulos, D., Pilozzi, E., Liu, C.G., Negrini, M. *et al.* E2F1-regulated microRNAs impair TGFbeta-dependent cell-cycle arrest and apoptosis in gastric cancer. *Cancer Cell* **13**, 272-86 (2008).

21. Xiao, C., Srinivasan, L., Calado, D.P., Patterson, H.C., Zhang, B., Wang, J., Henderson, J.M., Kutok, J.L. & Rajewsky, K. Lymphoproliferative disease and autoimmunity in mice with increased miR-17-92 expression in lymphocytes. *Nat Immunol* **9**, 405-14 (2008).

22. Woods, K., Thomson, J.M. & Hammond, S.M. Direct regulation of an oncogenic micro-RNA cluster by E2F transcription factors. *J Biol Chem* **282**, 2130-4 (2007).

23. Ivanovska, I., Ball, A.S., Diaz, R.L., Magnus, J.F., Kibukawa, M., Schelter, J.M., Kobayashi, S.V., Lim, L., Burchard, J., Jackson, A.L. *et al.* MicroRNAs in the miR-106b family regulate p21/CDKN1A and promote cell cycle progression. *Mol Cell Biol* **28**, 2167-74 (2008).

24. O'Donnell, K.A., Wentzel, E.A., Zeller, K.I., Dang, C.V. & Mendell, J.T. c-Myc-regulated microRNAs modulate E2F1 expression. *Nature* **435**, 839-43 (2005).

25. Sylvestre, Y., De Guire, V., Querido, E., Mukhopadhyay, U.K., Bourdeau, V., Major, F., Ferbeyre, G. & Chartrand, P. An E2F/miR-20a autoregulatory feedback loop. *J Biol Chem* **282**, 2135-43 (2007).

26. Tanzer, A. & Stadler, P.F. Molecular evolution of a microRNA cluster. *J Mol Biol* **339**, 327-35 (2004).

27. Brosh, R., Shalgi, R., Liran, A., Landan, G., Korotayev, K., Nguyen, G.H., Enerly, E., Johnsen, H., Buganim, Y., Solomon, H. *et al.* p53-Repressed miRNAs are involved with E2F in a feed-forward loop promoting proliferation. *Mol Syst Biol* **4**, 229 (2008).

28. Uren, A.G., Kool, J., Matentzoglu, K., de Ridder, J., Mattison, J., van Uitert, M., Lagcher, W., Sie, D., Tanger, E., Cox, T. *et al.* Large-scale mutagenesis in p19(ARF)- and p53-deficient mice identifies cancer genes and their collaborative networks. *Cell* **133**, 727-41 (2008).

29. Landais, S., Landry, S., Legault, P. & Rassart, E. Oncogenic potential of the miR-106-363 cluster and its implication in human T-cell leukemia. *Cancer Res* **67**, 5699-707 (2007).

30. Mendell, J.T. miRiad roles for the miR-17-92 cluster in development and disease. *Cell* **133**, 217-22 (2008).

31. Park, C.Y., Choi, Y.S. & McManus, M.T. Analysis of microRNA knockouts in mice. *Hum Mol Genet* **19**, R169-75 (2010).

32. Bernstein, E., Kim, S.Y., Carmell, M.A., Murchison, E.P., Alcorn, H., Li, M.Z., Mills, A.A., Elledge, S.J., Anderson, K.V. & Hannon, G.J. Dicer is essential for mouse development. *Nat Genet* **35**, 215-7 (2003).

33. Wang, Y., Medvid, R., Melton, C., Jaenisch, R. & Blelloch, R. DGCR8 is essential for microRNA biogenesis and silencing of embryonic stem cell self-renewal. *Nat Genet* **39**, 380-5 (2007).

34. Fukuda, T., Yamagata, K., Fujiyama, S., Matsumoto, T., Koshida, I., Yoshimura, K., Mihara, M., Naitou, M., Endoh, H., Nakamura, T. *et al.* DEAD-box RNA helicase subunits of the Drosha complex are required for processing of rRNA and a subset of microRNAs. *Nat Cell Biol* **9**, 604-11 (2007).

35. Morita, S., Horii, T., Kimura, M., Goto, Y., Ochiya, T. & Hatada, I. One Argonaute family member, Eif2c2 (Ago2), is essential for development and appears not to be involved in DNA methylation. *Genomics* **89**, 687-96 (2007).

36. Thai, T.H., Calado, D.P., Casola, S., Ansel, K.M., Xiao, C., Xue, Y., Murphy, A., Frendewey, D., Valenzuela, D., Kutok, J.L. *et al.* Regulation of the germinal center response by microRNA-155. *Science* **316**, 604-8 (2007).

37. Rodriguez, A., Vigorito, E., Clare, S., Warren, M.V., Couttet, P., Soond, D.R., van Dongen, S., Grocock, R.J., Das, P.P., Miska, E.A. *et al.* Requirement of bic/microRNA-155 for normal immune function. *Science* **316**, 608-11 (2007).

38. Dorsett, Y., McBride, K.M., Jankovic, M., Gazumyan, A., Thai, T.H., Robbiani, D.F., Di Virgilio, M., Reina San-Martin, B., Heidkamp, G., Schwickert, T.A. *et al.* MicroRNA-155 suppresses activation-induced cytidine deaminase-mediated Myc-Igh translocation. *Immunity* **28**, 630-8 (2008).

39. Teng, G., Hakimpour, P., Landgraf, P., Rice, A., Tuschl, T., Casellas, R. & Papavasiliou, F.N. MicroRNA-155 is a negative regulator of activation-induced cytidine deaminase. *Immunity* **28**, 621-9 (2008).

40. Wang, S. & Olson, E.N. AngiomiRs--key regulators of angiogenesis. *Curr Opin Genet Dev* **19**, 205-11 (2009).

41. Fish, J.E., Santoro, M.M., Morton, S.U., Yu, S., Yeh, R.F., Wythe, J.D., Ivey, K.N., Bruneau, B.G., Stainier, D.Y. & Srivastava, D. miR-126 regulates angiogenic signaling and vascular integrity. *Dev Cell* **15**, 272-84 (2008).

42. Wang, S., Aurora, A.B., Johnson, B.A., Qi, X., McAnally, J., Hill, J.A., Richardson, J.A., Bassel-Duby, R. & Olson, E.N. The endothelial-specific microRNA miR-126 governs vascular integrity and angiogenesis. *Dev Cell* **15**, 261-71 (2008).

43. Miquerol, L., Langille, B.L. & Nagy, A. Embryonic development is disrupted by modest increases in vascular endothelial growth factor gene expression. *Development* **127**, 3941-6 (2000).

44. Coultas, L., Chawengsaksophak, K. & Rossant, J. Endothelial cells and VEGF in vascular development. *Nature* **438**, 937-45 (2005).

45. Ferrara, N., Carver-Moore, K., Chen, H., Dowd, M., Lu, L., O'Shea, K.S., Powell-Braxton, L., Hillan, K.J. & Moore, M.W. Heterozygous embryonic lethality induced by targeted inactivation of the VEGF gene. *Nature* **380**, 439-42 (1996).

46. Carmeliet, P., Ferreira, V., Breier, G., Pollefeyt, S., Kieckens, L., Gertsenstein, M., Fahrig, M., Vandenhoeck, A., Harpal, K., Eberhardt, C. *et al.* Abnormal blood vessel development and lethality in embryos lacking a single VEGF allele. *Nature* **380**, 435-9 (1996).

47. Shalaby, F., Rossant, J., Yamaguchi, T.P., Gertsenstein, M., Wu, X.F., Breitman, M.L. & Schuh, A.C. Failure of blood-island formation and vasculogenesis in Flk-1-deficient mice. *Nature* **376**, 62-6 (1995).

48. Ferrara, N. & Kerbel, R.S. Angiogenesis as a therapeutic target. *Nature* **438**, 967-74 (2005).

49. Cascio, S., D'Andrea, A., Ferla, R., Surmacz, E., Gulotta, E., Amodeo, V., Bazan, V., Gebbia, N. & Russo, A. miR-20b modulates VEGF expression by targeting HIF-1 alpha and STAT3 in MCF-7 breast cancer cells. *J Cell Physiol* **224**, 242-9 (2010).

50. Hua, Z., Lv, Q., Ye, W., Wong, C.K., Cai, G., Gu, D., Ji, Y., Zhao, C., Wang, J., Yang, B.B. *et al.* MiRNA-directed regulation of VEGF and other angiogenic factors under hypoxia. *PLoS One* **1**, e116 (2006).

51. Lei, Z., Li, B., Yang, Z., Fang, H., Zhang, G.M., Feng, Z.H. & Huang, B. Regulation of HIF-1alpha and VEGF by miR-20b tunes tumor cells to adapt to the alteration of oxygen concentration. *PLoS One* **4**, e7629 (2009).

52. Croce, C.M. Causes and consequences of microRNA dysregulation in cancer. *Nat Rev Genet* **10**, 704-14 (2009).

53. Calin, G.A., Dumitru, C.D., Shimizu, M., Bichi, R., Zupo, S., Noch, E., Aldler, H., Rattan, S., Keating, M., Rai, K. *et al.* Frequent deletions and down-regulation of micro- RNA genes miR15 and miR16 at 13q14 in chronic lymphocytic leukemia. *Proc Natl Acad Sci U S A* **99**, 15524-9 (2002).

54. Cimmino, A., Calin, G.A., Fabbri, M., Iorio, M.V., Ferracin, M., Shimizu, M., Wojcik, S.E., Aqeilan, R.I., Zupo, S., Dono, M. *et al.* miR-15 and miR-16 induce apoptosis by targeting BCL2. *Proc Natl Acad Sci U S A* **102**, 13944-9 (2005).

55. Klein, U., Lia, M., Crespo, M., Siegel, R., Shen, Q., Mo, T., Ambesi-Impiombato, A., Califano, A., Migliazza, A., Bhagat, G. *et al.* The DLEU2/miR-15a/16-1 cluster controls B cell proliferation and its deletion leads to chronic lymphocytic leukemia. *Cancer Cell* **17**, 28-40 (2010).

56. Costinean, S., Zanesi, N., Pekarsky, Y., Tili, E., Volinia, S., Heerema, N. & Croce, C.M. Pre-B cell proliferation and lymphoblastic leukemia/high-grade lymphoma in E(mu)-miR155 transgenic mice. *Proc Natl Acad Sci U S A* **103**, 7024-9 (2006).

57. Krichevsky, A.M. & Gabriely, G. miR-21: a small multi-faceted RNA. *J Cell Mol Med* **13**, 39-53 (2009).

58. Medina, P.P., Nolde, M. & Slack, F.J. OncomiR addiction in an in vivo model of microRNA-21-induced pre-B-cell lymphoma. *Nature* **467**, 86-90 (2010).

59. He, L., Thomson, J.M., Hemann, M.T., Hernando-Monge, E., Mu, D., Goodson, S., Powers, S., Cordon-Cardo, C., Lowe, S.W., Hannon, G.J. *et al.* A microRNA polycistron as a potential human oncogene. *Nature* **435**, 828-33 (2005).

60. Tagawa, H., Karube, K., Tsuzuki, S., Ohshima, K. & Seto, M. Synergistic action of the microRNA-17 polycistron and Myc in aggressive cancer development. *Cancer Sci* **98**, 1482-90 (2007).

61. Navarro, A., Bea, S., Fernandez, V., Prieto, M., Salaverria, I., Jares, P., Hartmann, E., Mozos, A., Lopez-Guillermo, A., Villamor, N. *et al.* MicroRNA expression, chromosomal alterations, and immunoglobulin variable heavy chain hypermutations in Mantle cell lymphomas. *Cancer Res* **69**, 7071-8 (2009).

62. Inomata, M., Tagawa, H., Guo, Y.M., Kameoka, Y., Takahashi, N. & Sawada, K. MicroRNA-17-92 down-regulates expression of distinct targets in different B-cell lymphoma subtypes. *Blood* **113**, 396-402 (2009).

63. Volinia, S., Calin, G.A., Liu, C.G., Ambs, S., Cimmino, A., Petrocca, F., Visone, R., Iorio, M., Roldo, C., Ferracin, M. *et al.* A microRNA expression signature of human solid tumors defines cancer gene targets. *Proc Natl Acad Sci U S A* **103**, 2257-61 (2006).

64. Hayashita, Y., Osada, H., Tatematsu, Y., Yamada, H., Yanagisawa, K., Tomida, S., Yatabe, Y., Kawahara, K., Sekido, Y. & Takahashi, T. A polycistronic microRNA cluster, miR-17-92, is overexpressed in human lung cancers and enhances cell proliferation. *Cancer Res* **65**, 9628-32 (2005).

65. Takakura, S., Mitsutake, N., Nakashima, M., Namba, H., Saenko, V.A., Rogounovitch, T.I., Nakazawa, Y., Hayashi, T., Ohtsuru, A. & Yamashita, S. Oncogenic role of miR-17-92 cluster in anaplastic thyroid cancer cells. *Cancer Sci* **99**, 1147-54 (2008).

66. Matsubara, H., Takeuchi, T., Nishikawa, E., Yanagisawa, K., Hayashita, Y., Ebi, H., Yamada, H., Suzuki, M., Nagino, M., Nimura, Y. *et al.* Apoptosis induction by antisense oligonucleotides against miR-17-5p and miR-20a in lung cancers overexpressing miR-17-92. *Oncogene* **26**, 6099-105 (2007).

67. Northcott, P.A., Fernandez, L.A., Hagan, J.P., Ellison, D.W., Grajkowska, W., Gillespie, Y., Grundy, R., Van Meter, T., Rutka, J.T., Croce, C.M. *et al.* The miR-17/92 polycistron is up-regulated in sonic hedgehog-driven medulloblastomas and induced by N-myc in sonic hedgehog-treated cerebellar neural precursors. *Cancer Res* **69**, 3249-55 (2009).

68. Schulte, J.H., Horn, S., Otto, T., Samans, B., Heukamp, L.C., Eilers, U.C., Krause, M., Astrahantseff, K., Klein-Hitpass, L., Buettner, R. *et al.* MYCN regulates oncogenic MicroRNAs in neuroblastoma. *Int J Cancer* **122**, 699-704 (2008).

69. Dews, M., Homayouni, A., Yu, D., Murphy, D., Sevignani, C., Wentzel, E., Furth, E.E., Lee, W.M., Enders, G.H., Mendell, J.T. *et al.* Augmentation of tumor angiogenesis by a Myc-activated microRNA cluster. *Nat Genet* **38**, 1060-5 (2006).

70. Doebele, C., Bonauer, A., Fischer, A., Scholz, A., Reiss, Y., Urbich, C., Hofmann, W.K., Zeiher, A.M. & Dimmeler, S. Members of the microRNA-17-92 cluster exhibit a cell-intrinsic antiangiogenic function in endothelial cells. *Blood* **115**, 4944-50 (2010).

71. Kuhnert, F. & Kuo, C.J. miR-17-92 angiogenesis micromanagement. *Blood* **115**, 4631-3 (2010).

72. Kuppers, R. Mechanisms of B-cell lymphoma pathogenesis. *Nat Rev Cancer* **5**, 251-62 (2005).

73. Goossens, T., Klein, U. & Kuppers, R. Frequent occurrence of deletions and duplications during somatic hypermutation: implications for oncogene translocations and heavy chain disease. *Proc Natl Acad Sci U S A* **95**, 2463-8 (1998).

74. Kuppers, R. & Dalla-Favera, R. Mechanisms of chromosomal translocations in B cell lymphomas. *Oncogene* **20**, 5580-94 (2001).

75. Vennstrom, B., Sheiness, D., Zabielski, J. & Bishop, J.M. Isolation and characterization of c-myc, a cellular homolog of the oncogene (v-myc) of avian myelocytomatosis virus strain 29. *J Virol* **42**, 773-9 (1982).

76. Pelengaris, S., Khan, M. & Evan, G. c-MYC: more than just a matter of life and death. *Nat Rev Cancer* **2**, 764-76 (2002).

77. Salmena, L., Carracedo, A. & Pandolfi, P.P. Tenets of PTEN tumor suppression. *Cell* **133**, 403-14 (2008).

78. Igney, F.H. & Krammer, P.H. Death and anti-death: tumour resistance to apoptosis. *Nat Rev Cancer* **2**, 277-88 (2002).

79. Adams, J.M., Harris, A.W., Pinkert, C.A., Corcoran, L.M., Alexander, W.S., Cory, S., Palmiter, R.D. & Brinster, R.L. The c-myc oncogene driven by immunoglobulin enhancers induces lymphoid malignancy in transgenic mice. *Nature* **318**, 533-8 (1985).

80. Hwang, H.W., Wentzel, E.A. & Mendell, J.T. A hexanucleotide element directs microRNA nuclear import. *Science* **315**, 97-100 (2007).

81. Ventura, A., Kirsch, D.G., McLaughlin, M.E., Tuveson, D.A., Grimm, J., Lintault, L., Newman, J., Reczek, E.E., Weissleder, R. & Jacks, T. Restoration of p53 function leads to tumour regression in vivo. *Nature* **445**, 661-5 (2007).

82. Schmidt-Supprian, M. & Rajewsky, K. Vagaries of conditional gene targeting. *Nat Immunol* **8**, 665-8 (2007).

83. Di Cristofano, A., Pesce, B., Cordon-Cardo, C. & Pandolfi, P.P. Pten is essential for embryonic development and tumour suppression. *Nat Genet* **19**, 348-55 (1998).

84. Brennecke, J., Stark, A., Russell, R.B. & Cohen, S.M. Principles of microRNA-target recognition. *PLoS Biol* **3**, e85 (2005).

85. Hicklin, D.J. & Ellis, L.M. Role of the vascular endothelial growth factor pathway in tumor growth and angiogenesis. *J Clin Oncol* **23**, 1011-27 (2005).

86. Forsythe, J.A., Jiang, B.H., Iyer, N.V., Agani, F., Leung, S.W., Koos, R.D. & Semenza, G.L. Activation of vascular endothelial growth factor gene transcription by hypoxia-inducible factor 1. *Mol Cell Biol* **16**, 4604-13 (1996).

87. Simon, M.C. & Keith, B. The role of oxygen availability in embryonic development and stem cell function. *Nat Rev Mol Cell Biol* **9**, 285-96 (2008).

88. Grimson, A., Farh, K.K., Johnston, W.K., Garrett-Engele, P., Lim, L.P. & Bartel, D.P. MicroRNA targeting specificity in mammals: determinants beyond seed pairing. *Mol Cell* **27**, 91-105 (2007).

89. Mavrakis, K.J., Wolfe, A.L., Oricchio, E., Palomero, T., de Keersmaecker, K., McJunkin, K., Zuber, J., James, T., Khan, A.A., Leslie, C.S. *et al.* Genome-wide RNA-mediated interference screen identifies miR-19 targets in Notch-induced T-cell acute lymphoblastic leukaemia. *Nat Cell Biol* **12**, 372-9 (2010).

LAST THREE YEARS PHD CURRICULUM VITAE

ALECO D'ANDREA

Date of birth: March 18 1983
Place of birth: Palermo (PA), Italy
Nationality: Italy

PROFESSIONAL CAREER

- From June 2009 graduate research assistant - , Memorial Sloan Kettering Cancer Center, Department of cancer biology and genetics, New York USA
- From January 2008 to December 2010 - **Research Ph.D. course "Oncopatologia Cellulare e Molecolare clinica"** (XXII cycle) - Oncology Department of Policlinico, University of Palermo, Italy.
- December 2008 - **Qualified as a practicing biologist**.
- Academic year 2007/2008 and 2008/2009. **Biotechnologies applied at the diagnosis and therapy of the solid tumors** (Prof. A. Russo) – Teaching assistant
- Academic year 2007/2008 and 2008/2009. **Oncological Markers in Molecular Oncology** (Prof. A. Russo) – Teaching assistant
- From January 2005 to October 2007 - **Molecular and cellular biology Master's Degree (MD)** 110/110 summa cum laude – University of Palermo, Italy.
- From October 2001 to July 2005 - **Biological sciences Bachelor's Degree (BS)** 110/110 summa cum laude – University of Palermo, Italy.
- From 1996 to 2001 - **High school diploma**, vote 100/100 - "B.Croce" scientific high school – Palermo, Italy.

PROFESSIONAL SOCIETIES MEMBERSHIP

December 2008: **Qualified Biologist,** Ordine Nazionale dei Biologi, Roma (Italy).

SCIENTIFIC ACTIVITIES

January 2008 – May 2009: Graduate student, Molecular Genetic and Oncology Unit - University of Palermo. Research in the following projects: "***miR-20b Modulates VEGF Expression by Targeting HIF-1a and STAT3 in MCF-7 Breast Cancer Cells***", "***Expression of angiogenic regulators, VEGF and leptin, is regulated by the EGF/PI-3K/STAT3 pathway in colorectal cancer cells***". Tutor: Viviana Bazan.

June 2009 - December 2010: Visiting student, Memorial Sloan Kettering Cancer Center - New York. Involved in the project ***"Genetic dissection of the miR-17-92 cluster of miRNAs in cancer and development"***, Mentor Prof. Andrea Ventura.

ORAL PRESENTATIONS

-

MEETINGS

February 15-20, 2010: **Stem Cell differentiation and dedifferentiation.** Keystone, Colorado, USA.

BOOKS, PAPERS AND ABSTRACTS PUBLISHED DURING THE PHD COURSE

Papers

Cascio S, **D'Andrea A**, Ferla R, Surmacz E, Gulotta E, Amodeo V, Bazan V, Gebbia N, Russo A. **miR-20b Modulates VEGF Expression by Targeting HIF-1a and STAT3 in MCF-7 Breast Cancer Cells**. J Cell Physiol. 2010 Jul;224(1):242-9.

Mu P, Han YC, Betel D, Yao E, Squatrito M, Ogrodowski P, de Stanchina E, **D'Andrea A,** Sander C, Ventura A. **Genetic dissection of the miR-17~92 cluster of microRNAs in Myc -induced B-cell lymphomas.** Genes Dev. 2009 Dec 15;23(24):2806-11

Cascio S, Ferla R, **D'Andrea A**, Gerbino A, Bazan V, Surmacz E and Russo A. **Expression of angiogenic regulators, VEGF and leptin, is regulated by the EGF/PI-3K/STAT3 pathway in colorectal cancer cells.** J Cell Physiol. 2009 Oct;221(1):189-94.

Abstracts

1. Mu P, Han YC, Betel D, Yao E, Squatrito M, Ogrodowski P, de Stanchina E, **D'Andrea A,** Sander C, Ventura A. **Genetic dissection of the miR-17~92 cluster of microRNAs in Myc-induced B-cell lymphomas.** (Geoffrey Beene Cancer Research Retreat, April 8-9 2010, Skytop, PA, USA)

2. Mu P, Han YC, Betel D, Yao E, Squatrito M, Ogrodowski P, de Stanchina E, **D'Andrea A,** Sander C, Ventura A. **Genetic dissection of the miR-17~92 cluster of microRNAs in Myc-induced B-cell lymphomas.** (RNA Silencing: Mechanism, Biology and Application. January 14 - 19, 2010. Keystone, Colorado, USA)

3. Fanale D., Corsini L. R., **D'Andrea A**., Terrasi M., La Paglia L., Amodeo V., Bronte G., Rizzo S., Bazan V., Calvo E. L., Iovanna J. L., Russo A. **Analysis of germline gene copy number variation in patients with sporadic pancreatic adenocarcinoma.** XXVII National Conference of the Italian society of cytometry (GIC) - Centro Congressi Fiera, October 14-17, 2009 – Ferrara, Italy.

4. Amodeo V., Insalaco L., Terrasi M., **D'Andrea A**., Fanale D., La Paglia L., Corsini L.R., Bazan V., Russo A. **Effect of EGF on VEGF expression in colon cancer cell lines.** XXVII National Conference of the Italian society of cytometry (GIC) - Centro Congressi Fiera, October 14-17, 2009 – Ferrara, Italy.

5. Corsini L.R., Fanale D., **D'Andrea A**., La Paglia L., Amodeo V., Terrasi M., Insalaco L., Perez M., Bazan V., Russo A. **EGF downregulates expression of CDC25A gene in Breast cancer cell lines**. XXVII National Conference of the Italian society of cytometry (GIC) - Centro Congressi Fiera, October 14-17, 2009 – Ferrara, Italy.

6. V. Amodeo, M. Terrasi, **A. D'Andrea**, L. Insalaco, D. Fanale, L. La Paglia, L.R. Corsini, M. Perez, M. Federico, G. Bronte ,S. Rizzo, S. Cimino, L. Bruno, V. Calò, V. Agnese, M. Messina, C.E. Symonds, F.P. Fiorentino, N. Grassi, G. Pantuso, M. Frazzetta, V. Bazan, A. Russo. **EGF**

Induces STAT3-Dependent VEGF Expression in HT-29 Colon Cancer Cells. Oncology 2009;77(suppl 1):132–162.

7. L. Bruno, V. Calò, V. Schirò, L. La Paglia, V. Agnese, D. Calcara, S. Cimino, D. Fanale, **A. D'Andrea**, L.R. Corsini, V. Amodeo, S. Rizzo, M. Terrasi, G. Bronte, D. Bruno, D. Piazza, E.S. Symonds, M. Federico, F.P. Fiorentino, N. Grassi, G. Pantuso, M. Frazzetta, V. Bazan, A. Russo. **BRCA 1 and BRCA2 Variants of Uncertain Clinical Significance and Their Implications for Genetic Counseling.** Oncology 2009;77(suppl 1):132–162.

8. V. Calò, L. Bruno, L. La Paglia, V. Schirò, V. Agnese, D. Calcara, S. Cimino, D. Fanale, **A. D'Andrea**, L.R. Corsini, V. Amodeo, S. Rizzo, M. Terrasi, G. Bronte, D. Bruno, D. Piazza, Fiorentino F.P., N. Grassi, G. Pantuso, M. Frazzetta, C.E. Symonds, M. Federico, V. Bazan, A. Russo. **BRCA1 and BRCA2 Germline Mutations in Sicilian Breast and/or Ovarian Cancer Families and Their Association with Familial Profiles**. Oncology 2009;77(suppl 1):132–162.

9. L.R. Corsini, D. Fanale, **A. D'Andrea**, L. La Paglia, D. Calcara, V. Amodeo, M. Terrasi, L. Insalaco, M. Perez, S. Cimino, L. Bruno, V. Calò, V. Agnese, V. Schirò, G. Bronte, S. Rizzo, M. Federico, C.E. Symonds, N. Grassi, G. Pantuso, M. Frazzetta, V. Bazan, A. Russo. **Downregulated Expression of Cdc25A Gene in MCF-7 Breast Cancer Cell**. Oncology 2009;77(suppl 1):132–162.

10. D. Fanale, L.R. Corsini, **A. D'Andrea**, M. Terrasi, L. La Paglia, V. Amodeo, G. Bronte, S. Rizzo, L. Insalaco, M. Perez, S. Cimino, L. Bruno, V. Calò, V. Agnese, C.E. Symonds, M. Federico, N. Grassi, G. Pantuso, M. Frazzetta, V. Bazan, E.L. Calvo, J.L. Iovanna, A. Russo. **Analysis of Germline Gene Copy Number Variants of Patients with Sporadic Pancreatic Adenocarcinoma Reveals Specific Variations.** Oncology 2009;77(suppl 1):132–162.

11. M. Terrasi, **A. D'Andrea**, V. Amodeo, L.R. Corsini, D. Fanale, L. Insalaco, L. La Paglia, M. Perez, M. Federico, C.E. Symonds, V. Bazan , E. Surmacz, A. Russo. **The Proximal Leptin Gene Promoter is Regulated by Ppara Agonist in MCF-7 and MDA-MB-231 Breast Cancer Cells**. Oncology 2009;77(suppl 1):132–162.

Appendix

ORIGINAL ARTICLE 242

Journal of Cellular Physiology

miR-20b Modulates VEGF Expression by Targeting HIF-1α and STAT3 in MCF-7 Breast Cancer Cells

SANDRA CASCIO,[1,2] ALECO D'ANDREA,[1] RITA FERLA,[1,3] EVA SURMACZ,[3] ELIANA GULOTTA,[1] VALERIA AMODEO,[1] VIVIANA BAZAN,[1,3] NICOLA GEBBIA,[1] AND ANTONIO RUSSO[1,3]*

[1] *Section of Medical Oncology, Department of Surgical and Oncological Sciences, Palermo University, Palermo, Italy*

[2] *Fondazione RiMED, Piazza Sett'Angeli, Palermo, Italy*

[3] *Sbarro Institute for Cancer Research and Molecular Medicine, Temple University, Philadelphia, Pennsylvania*

MicroRNAs (miRNAs) are small non-coding RNAs that regulate the expression of different genes, including genes involved in cancer progression. A functional link between hypoxia, a key feature of the tumor microenvironment, and miRNA expression has been documented. We investigated whether and how miR-20b can regulate the expression of vascular endothelial growth factor (VEGF) in MCF-7 breast cancer cells under normoxic and hypoxia-mimicking conditions ($CoCl_2$ exposure). Using immunoblotting, ELISA, and quantitative real-time PCR, we demonstrated that miR-20b decreased VEGF protein levels at 4 and 24 h following $CoCl_2$ treatment, and VEGF mRNA at 4 h of treatment. In addition, miR-20b reduced VEGF protein expression in untreated cells. Next, we investigated the molecular mechanism by which pre-miR-20b can affect VEGF transcription, focusing on hypoxia inducible factor 1 (HIF-1) and signal transducer and activator of transcription 3 (STAT3), transcriptional inducers of VEGF and putative targets of miR-20b. Downregulation of VEGF mRNA by miR-20b under a 4 h of $CoCl_2$ treatment was associated with reduced levels of nuclear HIF-1α subunit and STAT3. Chromatin immunoprecipitation (ChIP) assays revealed that HIF-1α, but not STAT3, was recruited to the VEGF promoter following the 4 h of $CoCl_2$ treatment. This effect was inhibited by transfection of cells with pre-miR-20b. In addition, using siRNA knockdown, we demonstrated that the presence of STAT3 is necessary for $CoCl_2$-mediated HIF-1α nuclear accumulation and recruitment on VEGF promoter. In summary, this report demonstrates, for the first time, that the VEGF expression in breast cancer cells is mediated by HIF-1 and STAT3 in a miR-20b-dependent manner.

J. Cell. Physiol. 224: 242–249, 2010.

MicroRNAs (miRNAs) are a group of non-coding regulatory RNAs, 20–25 nucleotides in length, which are known to regulate different cellular processes such as proliferation, differentiation, apoptosis, cell metabolism, angiogenesis (Bartel, 2004; Fabbri et al., 2008). miRNAs modulate gene expression either directly through translational repression, or by mRNA degradation, depending on partial or perfect complementarity to the 3′untranslated region of their targets (Bartel, 2004). In humans, it is estimated that 20–30% of all genes are targeted by miRNAs (Krek et al., 2005; Lewis et al., 2005). Several hundred miRNAs have been identified to date and each is thought to have hundreds of targets, accounting for the great complexity of their functions (Krek et al., 2005).

miRNAs expression profiles (miRNome) revealed specific miRNAs expression patterns in different cancers (Volinia et al., 2006). Recent evidences suggest that intratumoral hypoxia might be a master regulator of cancer-associated miNA expression (Kulshreshtha et al., 2007; Ivan et al., 2008). Under hypoxia, expression of a subset of miRNAs is transiently altered in colon and breast cancer cell lines (Kulshreshtha et al., 2007), possibly reflecting adaptive changes enabling survival of cancer cells by increased invasion and resistance to chemo- and radiotherapy (Blouw et al., 2003; Bertout et al., 2008).

Hypoxia inducible factor 1 (HIF-1) acts as a master regulator of the hypoxia response. HIF-1 is composed of alpha and beta subunits. In normoxia, HIF-1α is degraded by proteasomal pathways, while upon induction of hypoxia, HIF-1α is rapidly stabilized, dimerizes with HIF-1β subunit, translocates to the nucleus and binds specific consensus sequences—hypoxia response elements (HRE) within promoters of target genes (Iliopoulos et al., 1996; Ivan et al., 2001).

Vascular endothelial growth factor (VEGF) is the most prominent angiogenic factor promoting tumor progression and a recognized therapeutic target (Ferrara and Kerbel, 2005). VEGF promoter contains a potential HIF-1α binding site located at position −975 (Forsythe et al., 1996) and a signal transducer and activator of transcription 3 (STAT3) binding site at position −848 (Niu et al., 2002; Wei et al., 2003). It has been shown that upon induction of hypoxia, both factors bind respective regulatory sequences ensuring strong increase in VEGF transcription rate (Gray et al., 2005; Jung et al., 2005). Moreover, it has been recently demonstrated that STAT3 is involved in both hypoxia or growth signal induced HIF-1α stabilization (Xu et al., 2005; Jung et al., 2008).

Recently several miRNAs have been found to regulate angiogenic processes (Wang et al., 2008), including VEGF expression (Hua et al., 2006; Wu et al., 2009). miRNA-20b (miR-20b) belongs to the miRNA 106a-363 cluster, which

Sandra Cascio and Aleco D'Andrea contributed equally to this work.

*Correspondence to: Antonio Russo, Section of Medical Oncology, Department of Surgical and Oncological Sciences, Palermo University, via del Vespro 127, 90127 Palermo, Italy.
E-mail: lab-oncobiologia@usa.net

Received 13 November 2009; Accepted 1 February 2010

Published online in Wiley InterScience (www.interscience.wiley.com.), 15 March 2010.
DOI: 10.1002/jcp.22126

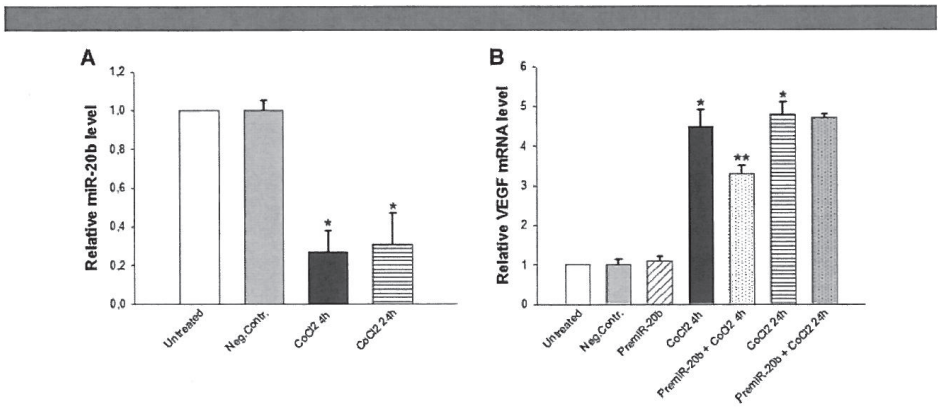

Fig. 1. MiR-20b is downregulated during hypoxia and regulates VEGF mRNA expression. The abundance of miR-20b (A) and VEGF mRNA (B) were studied with quantitative real-time PCR. MCF-7 cells were treated with $CoCl_2$ for 4 or 24 h, and/or transfected with pre-miR-20b for 48 h or left untreated. To normalize miR-20b and VEGF quantitative real-time PCR reactions, parallel reactions were run on each sample for RNU6B or Cyclophilin A, respectively. The graphs represent respectively the increase of miR-20b and VEGF mRNA relative to untreated ± SD; *Columns*, mean; *bars*, SD. $^{*}P < 0.05$, control versus $CoCl_2$; $^{**}P < 0.05$, $CoCl_2$ versus miR-20b + $CoCl_2$.

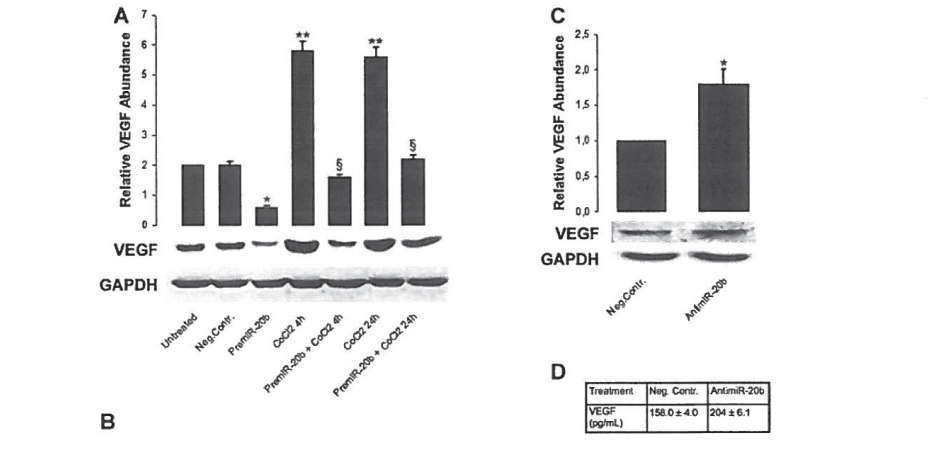

B

Treatment	Untreated	Neg. Contr.	PremiR-20b	CoCl2 4h	PremiR-20b + CoCl2 4h	CoCl2 24h	PremiR-20b + CoCl2 24h
VEGF (pg/mL)	193.0 ± 12.0	186.0 ± 6.8	124.1 ± 7.0	298.6 ± 8.7	216.2 ± 6.5	402.4 ± 25.3	294.0 ± 12.2

D

Treatment	Neg. Contr.	AntimiR-20b
VEGF (pg/mL)	158.0 ± 4.0	204 ± 6.1

Fig. 2. VEGF protein levels are decreased by transfection with pre-miR-20b and increased by miR-20b silencing. A: The abundance of VEGF total protein was determined by WB in 120 μg of total proteins, as decribed in Materials and Methods Section. The graph represents the increase of VEGF protein levels relative to untrasfected cells ± SD; *columns*, mean; *bars*, SD. $^{*}P < 0.05$, control versus pre-miR-20b; $^{**}P < 0.05$, control versus $CoCl_2$; §$P < 0.05$, $CoCl_2$ versus miR-20b + $CoCl_2$. B: The secreted protein levels were determined by ELISA. A total of 7×10^5 MCF-7 cells were treated as described Materials and Methods Section. The concentrations represent pg of VEGF/ml of conditioned medium from 4×10^5 cells. C: The abundance of VEGF proteins was studied by WB in 120 μg of total proteins in MCF-7 cells transfected with synthetic oligonucleotides targeting miR-20b (anti-miR-20b) or with negative control anti-miR molecules, as described in Materials and Methods Section. The graph represents the increase of VEGF protein levels relative to negative control ± SD; *columns*, mean; *bars*, SD. $^{*}P < 0.05$ control versus anti-miR-20b. D: The concentration of secreted VEGF was measured by ELISA in cells transfected with anti-miR20b or with negative control anti-miR. The concentrations represent pg VEGF/ml conditioned medium from 4×10^5 cells.

replaced with non-immune rabbit IgG. All experiments were repeated at least three times.

VEGF detection by ELISA

A total of 7×10^5 (pre-miR-20b transfections) or 4×10^5 (antimiR-20b and siSTAT3 transfections) MCF-7 cells were treated, as described before. VEGF protein was measured in conditioned medium using the Human Quantikine ELISA kit (R&D, Systems, Minneapolis, MN) with the lowest detection limit of 5 pg/ml, with intra-assay precision of <4.8% (or better than 2.5% and <4.8%) and inter-assay precision of <7.2% (or better than 4.7% and <7.2%). All points were done in triplicate, and the experiments were repeated three times. The range of curve standards was 0, 15.6, 31.2, 62.5, 125, 250, 500, 1,000 pg/ml; all VEGF concentrations in samples were within the range of curve standard. Linear regression analysis was performed to create the standard curve.

Statistical analysis

The correlations were studied by Student's *t*-test. *P*-values of <0.05 were considered statistically significant.

Results

Effects of miR-20b on VEGF expression under hypoxia-mimetic conditions

Since miR-20b has been suggested to act as a negative regulator of VEGF in nasopharyngeal carcinoma epithelioid (CNE) cells (Hua et al., 2006), we set out to study the effects of this miRNA on VEGF expression in breast cancer cells under hypoxia-mimetic conditions. First, we verified how treatment of cells with $CoCl_2$, a hypoxia-mimetic agent, affects miR-20b and VEGF expression. We found that $CoCl_2$ downregulated miR-20b expression at 4 and 24 h by 3.3- and 3.0-fold, respectively, relative to untreated cells (Fig. 1A). The specific downregulation of miR-20b was verified by running parallel reactions for miR-20a detection, where no change in miR-20a level under $CoCl_2$ was observed (data not shown). In parallel, $CoCl_2$ treatment induced VEGF mRNA expression by 4.5-fold compared to untreated cells (Fig. 1B).

Next, we investigated the effects of miR-20b on VEGF protein expression in breast cancer cells. VEGF intracellular protein levels were reduced in pre-miR-20b transfected cells by 2.5-fold related to untransfected cells (Fig. 2A), while VEGF basal mRNA levels were not significantly affected (Fig. 1B). Stimulation with $CoCl_2$ for 4 or 24 h increased intracellular VEGF protein levels by 2.9- and 2.7-fold, respectively (Fig. 2A). However, transfection of MCF-7 cells with pre-miR-20b, reduced a 4 h $CoCl_2$-induced stimulation of VEGF protein by 3.3-fold (Fig. 2A) and VEGF mRNA levels by 1.2-fold (Fig. 1B). In cells treated with $CoCl_2$ for 24 h, pre-miR-20b inhibited VEGF intracellular protein levels by 2.7-fold (Fig. 2A), but VEGF mRNA expression was not affected (Fig. 1B).

The effects of miR-20b on the secreted VEGF protein mirrored the above findings. As expected, $CoCl_2$ treatment for 4 and 24 h induced extracellular VEGF protein by 60% and 105%, respectively (Fig. 2B). Consistent with previous results, transfection with pre-miR-20b inhibited 4 and 24 h $CoCl_2$-mediated induction of extracellular VEGF by 30% and 25%, respectively, relative to negative control (Fig. 2B), while basal level of secreted VEGF were reduced by 32%.

In further validate the impact of miR-20b on VEGF expression, we used a synthetic oligonucleotide (anti-miRs) designed to target the mature forms of miR-20b and thereby inhibit their expression. Following miR-20b silencing, intracellular VEGF proteins levels increased by 1.5-fold (Fig. 2C), while the amount of secreted VEGF were elevated by 20% (Fig. 2D).

MiR-20b downregulates HIF-1α and STAT3

Next, we investigated the molecular mechanism by which miR-20b can regulate VEGF mRNA expression under $CoCl_2$ treatment. We hypothesize that this miRNA could exert its activity by targeting both HIF-1α and STAT3.

Transfection of pre-miR-20b reduced 4 h $CoCl_2$-dependent HIF-1α cytosolic and nuclear accumulation by 1.5- and 1.8-fold (Fig. 3A). Next, we tested whether miR-20b could downregulate STAT3. Cytosolic levels of STAT3 are not significantly affected by pre-mir-20b transfection. STAT3 nuclear accumulation was strongly inhibited by miR-20b relative to $CoCl_2$-treated cells for 4 h (Fig. 3A). At 24 h $CoCl_2$ treatment, miR-20b did not modulate nuclear accumulation of HIF-1α and STAT3 proteins (Fig. 3B), despite it retains the ability to downregulate HIF-1α, but not STAT3, in the cytoplasm (Fig. 3B).

Changes in nuclear accumulation and cytoplasmic downregulation of HIF-1α and STAT3 were confirmed by immunofluorescence analysis, which revealed that HIF-1α levels were considerably reduced in both cytoplasm and

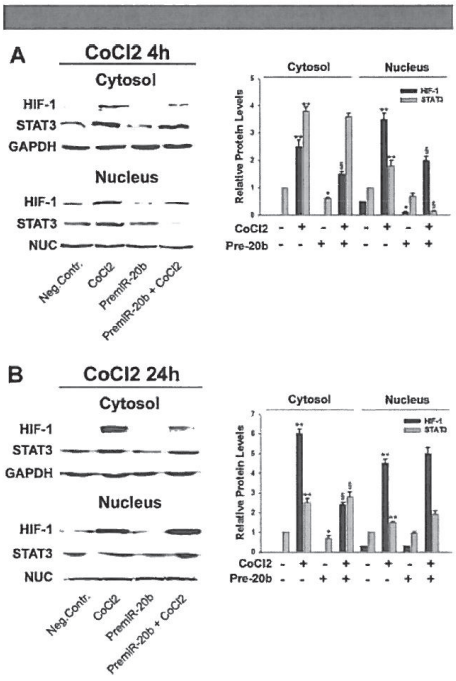

Fig. 3. MiR-20b modulates HIF-1α and STAT3 protein levels. The abundance of HIF-1α and STAT3 protein levels were studied by WB, as described in Materials and Methods Section. MCF-7 cells were treated with $CoCl_2$ for 4 (A) or 24 h (B), and/or transfected with pre-miR-20b for 48 h or left untreated. Protein loading was controlled by re-probing WB filters for the expression of a nuclear marker nucleolin (NUC) or cytosolic protein GAPDH. The graphs represent increase of HIF-1α and STAT3 levels relative to negative control ± SD. *Columns*, mean; *bars*, SD. *P < 0.05, control versus pre-miR-20b; **P < 0.05, control versus $CoCl_2$; §P < 0.05, $CoCl_2$ versus pre-miR-20b + $CoCl_2$.

nucleus of cells transfected with miR-20b and stimulated with 4 h $CoCl_2$ compared to the cells treated with $CoCl_2$ alone (Fig. 4A). Interestingly, as previously indicated by WB (Fig. 3A), miR-20b inhibited STAT3 nuclear accumulation rather than cytosolic. Moreover, immunofluorescence analysis shows that transfection with pre-miR-20b under normoxic conditions slightly downregulates both HIF-1α and STAT3 compared to negative control (Fig. 4A).

Finally, MCF-7 cells were transfected with the specific anti-miR-20b molecule or with anti-miR negative control. When the cells were transfected with anti-miR-20b, both cytoplasmic protein levels of HIF-1α and STAT3 were slightly increased, while the levels were increased by twofold and threefold, respectively, in the nucleus (Fig. 4B).

HIF-1 and STAT3 binding to VEGF promoter is modulated by miR-20b under $CoCl_2$ treatment

We hypothesized that miR-20b might be involved into the regulation of HIF-1α or STAT3 binding to VEGF regulatory sequences. Using ChIP assay, we found that the HIF-1α binding to VEGF promoter significantly decreased by fourfold in cells transfected with pre-miR-20b and treated with $CoCl_2$ for 4 h, compared to untreated cells (Fig. 4C). However, HIF-1α binding was no longer affected by miR-20b following 24 h $CoCl_2$ treatment (data not shown).

Next, we addressed STAT3 loading on VEGF promoter. We did not detect STAT3 binding to VEGF promoter after 4 h treatment with $CoCl_2$. Finally, RNA Polymerase II (RNAPII)

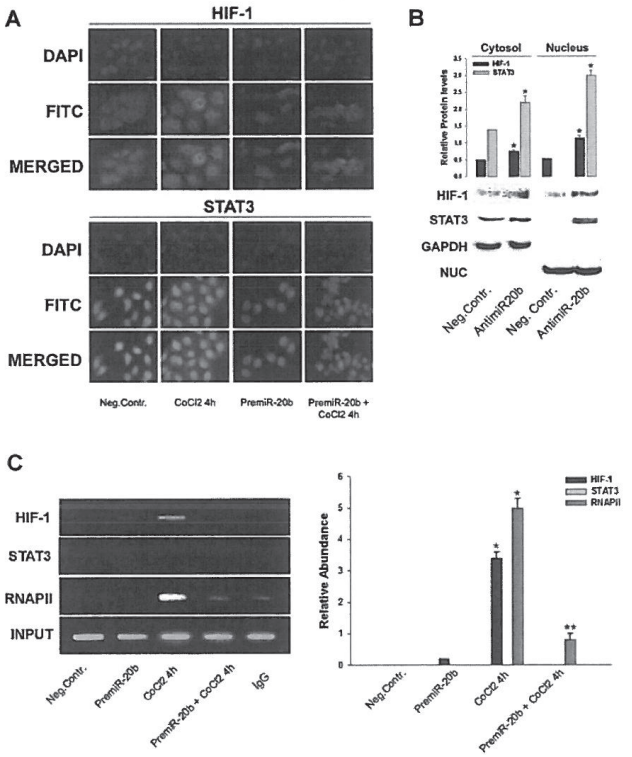

Fig. 4. miR-20b decreases HIF-1α and STAT3 nuclear accumulation and affects HIF recruitment on VEGF promoter. A: The expression of HIF-1α and STAT3 (green fluorescence) was assessed by immunostaining with specific Abs and fluorescence microscopy, as detailed in Materials and Methods Section. Cell nuclei were stained with DAPI (blue fluorescence). *Scale bar*, 10 μm. B: HIF-1α and STAT3 protein levels in anti-miR-20b or negative control transfected cells were studied by Western blotting. Protein loading and purity of fractions were controlled by re-probing WB filters for the expression of a cytoplasmic protein GAPDH and nucleolin (NUC). The graphs represent increase of HIF-1α and STAT3 levels relative to negative control ± SD. *columns*, mean; *bars*, SD. $^{*}P < 0.05$, control versus anti-miR-20b. C: miR-20b inhibits the recruitment of HIF-1 and RNAPII on VEGF promoter. ChIP experiments were performed as described in Materials and Methods Section. To test whether miR-20b could modulate the loading of HIF-1α, STAT3, and RNAPII transcription factors on the VEGF promoter. The graph represents relative abundance of HIF-1α, STAT3, or RNAPII on the VEGF promoter, relative to negative control ± SD; *columns*, mean; *bars*, SD. $^{*}P < 0.05$, control versus $CoCl_2$; $^{**}P < 0.05$, $CoCl_2$ versus miR-20b + $CoCl_2$.

binding to VEGF promoter was investigated to assess whether HIF-1α loading promotes assembly of a functional transcription complex. Similar to HIF-1α, RNAPII binds the VEGF promoter upon treatment with $CoCl_2$, while pre-miR20b transfection inhibits RNAPII binding in $CoCl_2$-treated cells by 3.5-fold (Fig. 4C).

$CoCl_2$-dependent modulation of VEGF by miR-20b requires STAT3

Finally, we investigated the role of STAT3 in miR-20b-modulated VEGF transcription. Specifically, we tested whether STAT3 could modulate loading of HIF-1α on the VEGF promoter, indirectly affecting VEGF transcriptional activation.

First, transcriptional regulation of VEGF by STAT3 was determined by targeting STAT3 with RNA-duplex interference. Targeting STAT3 did not significantly decrease basal levels of VEGF (Fig. 5A). However, siSTAT3 downregulated the 4 h $CoCl_2$-induced VEGF expression by 1.5-fold, relative to control. Following STAT3 silencing, VEGF protein levels were reduced by 20% relative to negative control, and by 80% in siSTAT3 plus $CoCl_2$, relative to $CoCl_2$ only treated cells (Fig. 5B). Negative (control) target RNA did not interfere with VEGF mRNA and protein expression (data not showed). ELISA assay confirmed a 20% decrease in secreted VEGF protein level in siSTAT3 cells, compared to negative control, and a 20% decrease in siSTAT3- and $CoCl_2$-treated cells, compared to $CoCl_2$-treated cells (Fig. 5B).

Immunoblot analysis revealed a significant decrease of 4 h $CoCl_2$-dependent HIF-1α nuclear accumulation under STAT3 silencing (Fig. 5C). Finally, we assessed whether STAT3 was able to regulate HIF-1 transcriptional activity. STAT3 silencing

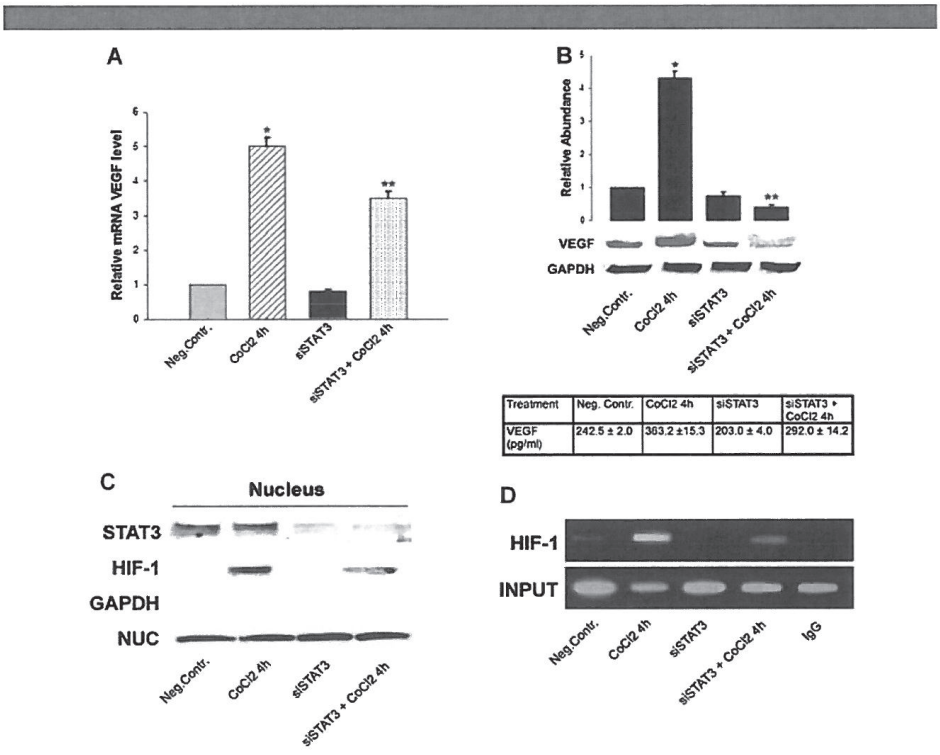

Treatment	Neg. Contr.	CoCl2 4h	siSTAT3	siSTAT3 + CoCl2 4h
VEGF (pg/ml)	242.5 ± 2.0	383.2 ±15.3	203.0 ± 4.0	292.0 ± 14.2

Fig. 5. Knockdown of STAT3 interferes with HIF-1 trascriptional activity and reduces VEGF expression. STAT3 knockdown was achieved using siRNA, as described in Material and Methods Section. MCF-7 cells were transfected with siSTAT3 for 48 h and/or treated with $CoCl_2$ for 4 h to mimic hypoxia or left untreated. Non-specific siRNA was used as a negative control. A: VEGF mRNA expression levels were determined by quantitative real-time PCR. The graphs represent increase in VEGF mRNA relative to negative control ± SD; *columns*, mean; *bars*, SD. $^{*}P < 0.05$, control versus $CoCl_2$; $^{**}P < 0.05$, $CoCl_2$ versus siSTAT3 + $CoCl_2$. B: The expression of VEGF protein was determined by WB in 80 μg of cytosolic proteins. GAPDH was used to normalize protein levels. Cells were transfected with STAT3 siRNA and/or treated for 4 h with $CoCl_2$ or left untreated. The graph represent increase in VEGF protein relative to negative control ± SD; *columns*, mean; *bars*, SD. $^{*}P < 0.05$, control versus $CoCl_2$; $^{**}P < 0.05$, control versus siSTAT3; §$P < 0.05$, $CoCl_2$ versus siSTAT3 + $CoCl_2$. The abundance of secreted VEGF (pg/ml) in conditioned medium was determined by ELISA, as described in Materials and Methods Section. A total of 4×10^5 cells were treated as described above. C: STAT3 silencing efficiency was confirmed by both quantitative real-time PCR (data not shown) and Western blot. The expression of HIF-1α and STAT3 proteins was analyzed in 50 μg of nuclear cell lysates. Nucleolin was used as nuclear loading control. D: In STAT3-knockdown MCF-7 cells, the modulation of HIF-1 binding on VEGF promoter was assessed by ChIP assay.

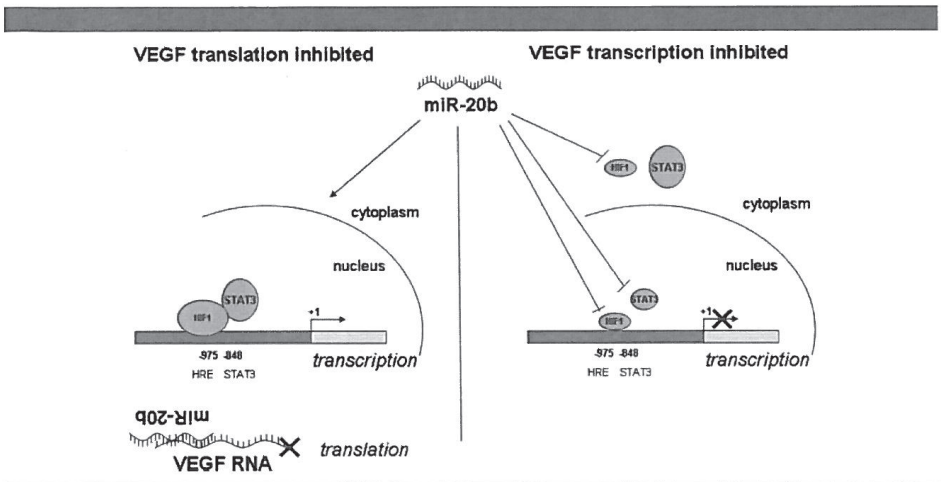

Fig. 6. Model of translational and transcriptional regulation of VEGF expression by miR-20b. (Left) pre-mir-20b transfection decreases VEGF protein levels. (Right) pre-mir-20b control VEGF transcription through HIF and STAT3 factors.

diminished HIF-1α recruitment to the VEGF promoter under $CoCl_2$ treatment, similar to that caused by miR-20b (Fig. 5D). In summary, these results indicate that STAT3 modulates HIF-1α binding to VEGF promoter at 4 h of hypoxia-mimetic treatment (Fig. 6).

Discussion

In the present study, we identified VEGF and its two main hypoxia-inducible transcriptional activators, HIF-1α and STAT3, as targets for miR-20b in MCF-7 breast cancer cells. One previous report identified miR-20b as a negative regulator of VEGF protein, and recently a reciprocal regulation of miR-20b and HIF-1 has been suggested in H22 cells (Hua et al., 2006; Lei et al., 2009). Here, we confirmed that VEGF is a direct target of miR-20b in breast cancer. First, we found that transfection with pre-miR-20b reduced the levels of both cytoplasmic and secreted VEGF protein under hypoxia-mimicking and normoxia conditions in MCF-7. On the other hand, transfection with synthetic anti-miR-20b increased cytoplasmic and secreted VEGF protein level significantly, even though the effect of miR-20b inhibition appears to be lower compared to pre-miR-20b activity. This is due to a decreased transfection efficiency.

In addition, we observed that transfection with pre-miR-20b decreased VEGF mRNA levels, suggesting that miR-20b can modulate VEGF transcription. According to our data, this effect is mediated by miR-20b-dependent inhibition of both HIF-1α and STAT3 nuclear accumulation under a 4 h $CoCl_2$ treatment. We hypothesize that this could be related to miR-20b-induced HIF-1α degradation in the cytoplasm and reduction of STAT3 nuclear translocation, perhaps via interference with its phosphorylation. Notably, miR-20b action on VEGF mRNA expression was noticeable only under a short $CoCl_2$ treatment (4 h), as prolonged $CoCl_2$ treatment (24 h) did not interfere with VEGF mRNA induction or nuclear accumulation of HIF-1α and STAT3. We hypothesize that miR-20b can directly target moderate amounts of HIF-1α in the cytoplasm (4 h $CoCl_2$), but is not able to compete with the enhanced accumulation of this protein under prolonged hypoxia-mimicking conditions (24 h $CoCl_2$; Bertout et al., 2008). Subsequent ChIP analyses revealed that miR-20b inhibited binding of HIF-1α on the VEGF promoter, which could explain the diminished VEGF mRNA transcription (Gray et al., 2005; Jung et al., 2005), we did not find STAT3 on VEGF promoter in MCF-7 cells at 4 h. Since it is known that transcription factors bind chromatin in an ordered and cyclical manner, which is dependent on cell type (Metivier, 2003; Cascio et al., 2007) we hypothesize that observed discrepancies could be related to cell-specific dynamics of STAT3 interactions the VEGF promoter.

Finally, our siRNA-mediated knockdown experiments indicated that VEGF expression can be controlled by STAT3 under hypoxia-mimicking conditions. Specifically, STAT3 downregulation inhibited HIF-1α nuclear accumulation and binding to the VEGF promoter in response to 4 h $CoCl_2$ treatment. This could be caused by reduced STAT3 interaction with HIF-1α, which normally increases HIF-1α stability by interfering with von Hippel–Lindau protein (pVHL) factor (Jung et al., 2008).

In summary, this report demonstrates for the first time that the VEGF expression in breast cancer cells is mediated by HIF-1α and STAT3 in a miR-20b-dependent manner. Our work also implies that angiogenesis of breast cancer can depend on the intricate circuit involving VEGF, STAT3, HIF-1α, and miR-20b, all of which can become novel targets in breast cancer treatment.

Literature Cited

Bartel DP. 2004. MicroRNAs: Genomics, biogenesis, mechanism, and function. Cell 116:281–297.
Bertout JA, Patel SA, Simon MC. 2008. The impact of O_2 availability on human cancer. Nat Rev Cancer 8:967–975.
Blouw B, Song H, Tihan T, Bosze J, Ferrara N, Gerber HP, Johnson RS, Bergers G. 2003. The hypoxic response of tumors is dependent on their microenvironment. Cancer Cell 4:133–146.
Cascio S, Bartella V, Garofalo C, Russo A, Giordano A, Surmacz E. 2007. Insulin-like growth factor 1 differentially regulates estrogen receptor-dependent transcription at estrogen response element and AP-1 sites in breast cancer cells. J Biol Chem 282:3498–3506.
Fabbri M, Croce CM, Calin GA. 2008. MicroRNAs. Cancer J 14:1–6.
Ferrara N, Kerbel RS. 2005. Angiogenesis as a therapeutic target. Nature 438:967–974.
Forsythe JA, Jiang BH, Iyer NV, et al. 1996. Activation of vascular endothelial growth factor gene transcription by hypoxia-inducible factor 1. Mol Cell Biol 16:4604–4613.

Foshay KM, Gallicano GI. 2009. miR-17 family miRNAs are expressed during early mammalian development and regulate stem cell differentiation. Dev Biol 326:431–443.
Gray MJ, Zhang J, Ellis LM, et al. 2005. HIF-1 alpha, STAT3, CBP/p300 and Ref-1/APE are components of a transcriptional complex that regulates Src-dependent hypoxia-induced expression of VEGF in pancreatic and prostate carcinomas. Oncogene 24:3110–3120.
Hayashita Y, Osada H, Tatematsu Y, et al. 2005. A polycistronic microRNA cluster, miR-17-92, is overexpressed in human lung cancers and enhances cell proliferation. Cancer Res 65:9628–9632.
Hua Z, Lv Q, Ye W, et al. 2006. MiRNA-directed regulation of VEGF and other angiogenic factors under hypoxia. PLoS ONE 1:e116.
Iliopoulos O, Levy AP, Jiang C, Kaelin WG, Jr., Goldberg MA. 1996. Negative regulation of hypoxia-inducible genes by the von Hippel–Lindau protein. Proc Natl Acad Sci USA 93:10595–10599.
Inomata M, Tagawa H, Guo YM, Kameoka Y, Takahashi N, Sawada K. 2009. MicroRNA-17-92 down-regulates expression of distinct targets in different B-cell lymphoma subtypes. Blood 113:396–402.
Ivan M, Kondo K, Yang H, et al. 2001. HIFalpha targeted for VHL-mediated destruction by proline hydroxylation: Implications for O_2 sensing. Science 292:464–468.
Ivan M, Harris AL, Martelli F, Kulshreshtha R. 2008. Hypoxia response and microRNAs: No longer two separate worlds. J Cell Mol Med 12:1426–1431.
Jung JE, Lee HG, Cho IH, et al. 2005. STAT3 is a potential modulator of HIF-1-mediated VEGF expression in human renal carcinoma cells. FASEB J 19:1296–1298.
Jung JE, Kim HS, Lee CS, et al. 2008. STAT3 inhibits the degradation of HIF-1alpha by pVHL-mediated ubiquitination. Exp Mol Med 40:479–485.
Krek A, Grun D, Poy MN, et al. 2005. Combinatorial microRNA target predictions. Nat Genet 37:495–500.
Kulshreshtha R, Ferracin M, Wojcik SE, et al. 2007. A microRNA signature of hypoxia. Mol Cell Biol 27:1859–1867.
Landais S, Landry S, Legault P, Rassart E. 2007. Oncogenic potential of the miR-106-363 cluster and its implication in human T-cell leukemia. Cancer Res 67:5699–5707.
Lei Z, Li B, Yang Z, Fang H, Zhang GM, Feng ZH. 2009. Huang regulation of HIF-1a and VEGF by miR-20b tunes tumor cells to adapt to the alteration of oxygen concentration. PLoS ONE 4:e7629.
Lewis BP, Burge CB, Bartel DP. 2005. Conserved seed pairing, often flanked by adenosines, indicates that thousands of human genes are microRNA targets. Cell 120:15–20.
Matsubara H, Takeuchi T, Nishikawa E, et al. 2007. Apoptosis induction by antisense oligonucleotides against miR-17-5p and miR-20a in lung cancers overexpressing miR-17-92. Oncogene 26:6099–6105.
Metivier H. 2003. A new model for the human alimentary tract: The work of a Committee 2 task group. Radiat Prot Dosimetry 105:43–48.
Niu GL, Wright KL, Huang M, et al. 2002. Constitutive Stat3 activity up-regulates VEGF expression and tumor angiogenesis. Oncogene 21:2000–2008.
Taguchi A, Yanagisawa K, Tanaka M, et al. 2008. Identification of hypoxia-inducible factor-1 alpha as a novel target for miR-17-92 microRNA cluster. Cancer Res 68:5540–5545.
Tanzer A, Stadler PF. 2004. Molecular evolution of a microRNA cluster. J Mol Biol 339:327–335.
Ventura A, Young AG, Winslow MM, et al. 2008. Targeted deletion reveals essential and overlapping functions of the miR-17 through 92 family of miRNA clusters. Cell 132:875–886.
Volinia S, Calin GA, Liu CG, et al. 2006. A microRNA expression signature of human solid tumors defines cancer gene targets. Proc Natl Acad Sci USA 103:2257–2261.
Wang S, Aurora AB, Johnson BA, et al. 2008. The endothelial-specific microRNA miR-126 governs vascular integrity and angiogenesis. Dev Cell 15:261–271.
Wei D, Le X, Zheng L, et al. 2003. Stat3 activation regulates the expression of vascular endothelial growth factor and human pancreatic cancer angiogenesis and metastasis. Oncogene 22:319–329.
Wu H, Zhu S, Mo YY. 2009. Suppression of cell growth and invasion by miR-205 in breast cancer. Cell Res 4:439–448.
Xu Q, Briggs J, Park S, et al. 2005. Targeting Stat3 blocks both HIF-1 and VEGF expression induced by multiple oncogenic growth signaling pathways. Oncogene 24:5552–5560.

RESEARCH COMMUNICATION

Genetic dissection of the *miR-17~92* cluster of microRNAs in Myc-induced B-cell lymphomas

Ping Mu,[1,5] Yoon-Chi Han,[1,5] Doron Betel,[2] Evelyn Yao,[1] Massimo Squatrito,[1] Paul Ogrodowski,[1] Elisa de Stanchina,[3] Aleco D'Andrea,[1,4] Chris Sander,[2] and Andrea Ventura[1,6]

[1]Cancer Biology and Genetics Program, Memorial Sloan Kettering Cancer Center, New York, New York 10021, USA; [2]Computational Biology Center, Memorial Sloan Kettering Cancer Center, New York, New York 10021, USA; [3]Department of Molecular Pharmacology and Chemistry, Memorial Sloan Kettering Cancer Center, New York, New York 10021, USA; [4]Department of Surgical and Oncological Sciences, Section of Medical Oncology, Università di Palermo, Palermo 90133, Italy

The *miR-17~92* cluster is frequently amplified or overexpressed in human cancers and has emerged as the prototypical oncogenic polycistron microRNA (miRNA). *miR-17~92* is a direct transcriptional target of c-Myc, and experiments in a mouse model of B-cell lymphomas have shown cooperation between these two oncogenes. However, both the molecular mechanism underlying this cooperation and the individual miRNAs that are responsible for it are unknown. By using a conditional knockout allele of *miR-17~92*, we show here that sustained expression of endogenous *miR-17~92* is required to suppress apoptosis in Myc-driven B-cell lymphomas. Furthermore, we show that among the six miRNAs that are encoded by *miR-17~92*, *miR-19a* and *miR-19b* are absolutely required and largely sufficient to recapitulate the oncogenic properties of the entire cluster. Finally, by combining computational target prediction, gene expression profiling, and an in vitro screening strategy, we identify a subset of *miR-19* targets that mediate its pro-survival activity.

Supplemental material is available at http://www.genesdev.org.

Received October 11, 2009; revised version accepted November 3, 2009.

The *miR-17~92* cluster encodes six distinct microRNAs (miRNAs) that are processed from a common primary transcript (Fig. 1A; for review, see Mendell 2008). A growing body of evidence points to an important role of this cluster of miRNAs in the pathogenesis of human cancers (for review, see Ventura and Jacks 2009). Overexpression of *miR-17~92* is observed in a large fraction of human cancers, including carcinomas of the breast, lung, and colon; medulloblastomas; neuroblastomas; and B-cell lymphomas (Hayashita et al. 2005; He et al. 2005; Tagawa and Seto 2005; Fontana et al. 2008; Uziel et al. 2009). In addition, a substantial fraction of diffuse large B-cell lymphomas harbors recurrent genomic amplification of the *miR-17~92* locus (Ota et al. 2004).

The evidence for a causal link between *miR-17~92* overexpression and tumorigenesis is strengthened by the observation that transgenic expression of this cluster in mice leads to a lymphoproliferative disorder (Xiao et al. 2008), while its genetic ablation impairs normal B-cell development (Ventura et al. 2008). In addition, ectopic expression of *miR-17~92* cooperates with the c-Myc oncogene in a mouse model of B-cell lymphomas (He et al. 2005). The functional interplay between *miR-17~92* and c-Myc is further underlined by the finding that c-Myc itself is a potent and direct transcriptional activator of *miR-17~92* (O'Donnell et al. 2005), thus suggesting that *miR-17~92* may contribute to the oncogenic properties of c-Myc.

The experiments presented in this study were designed to examine the role of the endogenous *miR-17~92* allele in Myc-driven lymphomas, and to determine the relative contribution of each of the six constituent miRNAs to the overall oncogenic potential of the cluster.

Our results show that, in the context of Myc-driven B-cell lymphomas, genetic ablation of the endogenous *miR-17~92* locus leads to a dramatic reduction of tumor cell growth in vitro and suppresses tumorigenicity in vivo, two effects that are largely the consequence of increased cell death. We also demonstrate that, among the six miRNAs encoded by the *miR-17~92* cluster, the members of the miR-19 family (*miR-19a* and *miR-19b*) are essential to mediate the oncogenic activity of the entire cluster, and that they do so at least in part by modulating the expression of the tumor suppressor gene *Pten* (phosphatase and tensin homologous).

Results and Discussion

Generation of miR-17~92$^{flox/flox}$;Eμ-Myc mice

To investigate the role of *miR-17~92* in Myc-induced cancers, we employed the *Eμ-Myc* mouse model of B-cell lymphomas (Adams et al. 1985). *Eμ-Myc* mice express a *c-Myc* transgene under the control of the B-cell-specific Eμ enhancer and develop B-cell lymphomas within 4–6 mo of age (Adams et al. 1985). *Eμ-Myc* mice were crossed to mice carrying a conditional *miR-17~92* knockout allele (*miR-17~92^{fl}*) (Fig. 1B; Ventura et al. 2008). To temporally control the deletion of the floxed *miR-17~92* allele, these mice were further crossed to mice carrying a 4-hydroxytamoxifen (4-OHT)-inducible Cre-recombinase estrogen receptor-T2 (*Cre-ER^{T2}*) knock-in allele targeted to the ubiquitously expressed *ROSA26* locus (*R26-Cre-ER^{T2}* mice, hereafter referred to as *Cre-ER*) (Ventura et al. 2007).

As expected, *Eμ-Myc; miR-17~92$^{fl/fl}$; Cre-ER* mice developed B-cell lymphomas with similar latency and phenotype as the parental *Eμ-Myc* strain (data not shown). From these mice, we derived two independent lymphoma lines (AV4174 and AV4182) that could be

[*Keywords*: microRNAs; Myc; *miR-17~92*; cancer; mouse]
[5]These authors contributed equally to this work.
[6]Corresponding author.
E-MAIL venturaa@mskcc.org; FAX (646) 422-0871.
Article is online at http://www.genesdev.org/cgi/doi/10.1101/gad.1872909.

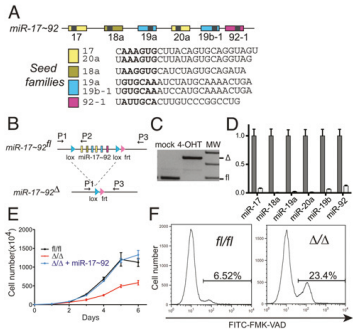

Figure 1. *miR-17~92* suppresses cell death in *Eμ-Myc* lymphomas. (*A*) Schematic representation of the *miR-17~92* cluster. Each miRNA is represented by a colored box and is color-coded based on the seed family to which it belongs. The sequence of each mature miRNA is also shown. (*B*) Schematic of the conditional *miR-17~92* knockout allele. Arrows represent the primers used to detect the floxed and the deleted (Δ) alleles. (*C*) PCR on genomic DNA extracted from *Eμ-Myc;miR-17~92*$^{fl/fl}$*;Cre-ER* lymphoma cells mock-treated or after 4 d of 4-OHT treatment. (*D*) Quantitative RT–PCR analysis of the expression of *miR-17~92* in lymphoma cells before (gray bars) and after (white bars) 4-OHT treatment. Each component of *miR-17~92* was detected independently, and the results were normalized relative to the expression observed in mock-treated cells. Each experiment was performed in quadruplicate. Error bar, standard deviation (SD). (*E*) Growth curves of *miR-17~92*$^{fl/fl}$ cells (black line), *miR-17~92*$^{\Delta/\Delta}$ cells (red line), and *miR-17~92*$^{\Delta/\Delta}$ cells infected with a retrovirus expressing the entire *miR-17~92* cluster (blue line). Error bars, SD of three replicates. The plot is representative of three independent experiments. (*F*) Caspase activity in exponentially growing *miR-17~92*$^{fl/fl}$ and *miR-17~92*$^{\Delta/\Delta}$ lymphoma cells as detected by flow cytometry using FITC-conjugated VAD-FMK. The percent of VAD-FMK$^+$ cells is shown.

propagated easily in culture and readily formed tumors when injected into immunocompromised mice. Both lymphoma lines exhibited similar behavior in vitro and in vivo. Unless otherwise specified, the experiments discussed here were performed using the AV4182 cell line.

To determine the efficiency of *miR-17~92* deletion, *miR-17~92*$^{fl/fl}$ lymphoma cells were treated with 250 nM 4-OHT. This treatment lead to the efficient deletion of both endogenous *miR-17~92* alleles (Fig. 1C), with concomitant loss of expression of the corresponding miRNAs (Fig. 1D).

We next examined the phenotypic consequences of deleting *miR-17~92* in B-lymphoma cells. Because sustained Cre expression has been reported to negatively affect the growth of *Eμ-Myc* lymphoma cells (Schmidt-Supprian and Rajewsky 2007), 4-OHT was administered for 4 d, after which the lymphoma cells were allowed to recover for a minimum of 4 d before being examined. As shown in Figure 1E, deletion of *miR-17~92* dramatically reduced the proliferation of *Eμ-Myc* lymphoma cells. Importantly, this phenotype was fully rescued by reintroduction of the entire *miR-17~92* cluster (Fig. 1E).

The different growth kinetics between the *miR-17~92*$^{fl/fl}$ and *miR-17~92*$^{\Delta/\Delta}$ lymphoma cells could be due to the latter displaying reduced proliferation, increased spontaneous cell death, or a combination of both. While cell cycle distribution and BrdU incorporation were similar between *miR-17~92*$^{fl/fl}$ and *miR-17~92*$^{\Delta/\Delta}$ cells (Supplemental Fig. 1A), the fraction of cells undergoing apoptosis, as determined by detecting caspase activation, was approximately fourfold higher in the absence of *miR-17~92* (Fig. 1F). Increased apoptosis was confirmed by measuring the DNA fragmentation using the TUNEL assay (Supplemental Fig. 1B). These results demonstrate that expression of the endogenous *miR-17~92* locus is required for the optimal survival of Myc-driven B-lymphoma cells. In addition, they are consistent with the finding by He et al. (2005) that ectopic expression of *miR-17~92* cooperates with c-Myc by reducing spontaneous apoptosis.

miR-19a *and* miR-19b *mediate the oncogenic properties of miR-17~92*

This observation provides a rationale and an opportunity to genetically dissect the functions of this cluster and to identify its relevant target mRNAs. The six miRNAs encoded by *miR-17~92* can be grouped into four "seed families," based on sequence identity at positions 2–7 (Fig. 1A): the miR-17 family (*miR-17* and *miR-20a*), the miR-18 family (*miR-18a*), the miR-19 family (*miR-19a* and *miR-19b-1*), and the miR-92 family (*miR-92-1*). miRNAs belonging to the same seed family are predicted to target highly overlapping sets of mRNAs, and thus are expected to exert similar biological functions (Bartel 2009). To examine the role of each seed family in the context of *Eμ-Myc* lymphomas, we generated a series of *miR-17~92* mutant alleles, each lacking expression of the miRNA(s) belonging to one of the four seed families (Supplemental Fig. 2A). The wild-type and the mutant alleles of *miR-17~92* were cloned into MSCV-Puro-IRES-GFP (PIG), a retroviral vector encoding the green fluorescent protein (GFP) and the Puromycin resistance gene, and the resulting constructs were transduced into *miR-17~92*$^{\Delta/\Delta}$ lymphoma cells. First, we verified that these constructs correctly expressed the desired miRNAs (Supplemental Fig. 2B). This was an essential control because deletion of even a single miRNA from the *miR-17~92* cluster could, in principle, negatively affect the processing and expression of the remaining ones, thus compromising our experimental approach.

To determine the ability of each construct to rescue the phenotype caused by *miR-17~92* deletion, we titrated the viral preparations to achieve an infection efficiency of 5%–30%, as judged by GFP expression. We reasoned that, if reintroduction of *miR-17~92* or one of its derivatives is sufficient to suppress the increased cell death observed in *miR-17~92*$^{\Delta/\Delta}$ cells, it will provide the infected cells with a growth advantage that will in turn be reflected by an increase in the fraction of GFP-positive cells over time (see schematic in Fig. 2A). As predicted, reintroduction of the full-length *miR-17~92* cluster resulted in a rapid increase of GFP$^+$ cells that quickly outcompeted the uninfected cells (Fig. 2B). Interestingly, among the four mutant constructs, only the one lacking the miR-19 seed family (Δ19a, 19b) failed to provide a growth advantage (Fig. 2B,C) and to suppress the increased apoptosis caused by deletion of *miR-17~92* (Fig. 2D), suggesting that this seed family is necessary for the oncogenic properties of the cluster. This was further confirmed by showing that reintroduction of *miR-19a* and *miR-19b* alone was largely sufficient to rescue the growth defect caused by deletion

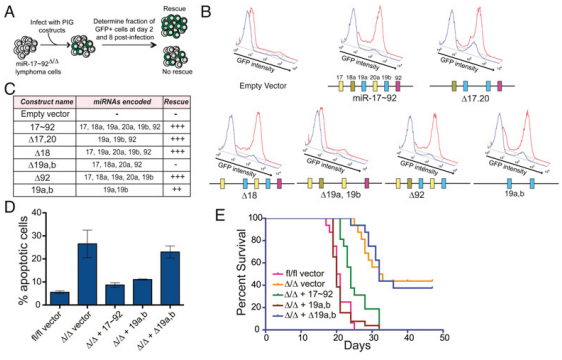

Figure 2. *miR-19a* and *miR-19b* mediate the prosurvival and oncogenic functions of *miR-17~92* in Eμ-Myc B-cell lymphomas. (*A*) Schematic of the experimental design. (*B*) Histogram overlays of *miR-17~92*$^{\Delta/\Delta}$ cells transduced with PIG retroviruses expressing the indicated *miR-17~92* derivatives. The cells were assayed by flow cytometry to detect GFP expression at day 2 (blue plot) and day 8 (red plot) post-infection. A schematic of the *miR-17~92* derivative used is shown *below* each overlay. (*C*) Table summarizing the results of the experiments shown in *B*. (*D*) Caspase activity in *miR-17~92*$^{fl/fl}$ and *miR-17~92*$^{\Delta/\Delta}$ cells transduced with the indicated PIG constructs. Error bar, 1 SD deviation. (*E*) Survival analysis of mice injected with *miR-17~92*$^{fl/fl}$ and *miR-17~92*$^{\Delta/\Delta}$ lymphoma cells transduced with the indicated PIG constructs. $N = 16$ mice for each construct, over three independent experiments.

of the entire *miR-17~92* cluster and to suppress apoptosis (Fig. 2B,D, *miR-19a,b* construct).

Deletion of miR-19 affects tumorigenicity in vivo

To determine whether the miR-19 seed family is required for the tumorigenicity of *Eμ-Myc*-driven B-cell lymphomas in vivo, we injected a cohort of nude mice with *miR-17~92*$^{fl/fl}$ and *miR-17~92*$^{\Delta/\Delta}$ lymphoma cells. While *miR-17~92*$^{fl/fl}$ cells invariably lead to the formation of lymphomas that lead to death within 2–3 wk, the *miR-17~92*$^{\Delta/\Delta}$ cells produced lymphomas with a significantly ($P < 0.0001$) longer latency (Fig. 2E). Tumorigenicity was fully restored by ectopic expression of the full-length *miR-17~92* cluster ($P < 0.0001$), but not by expression of the *miR-17~92* mutant lacking *miR-19a* and *miR-19b* ($P = 0.9816$) (Fig. 2E). Re-expression of *miR-19a* and *miR-19b* also largely rescued tumorigenicity, although it did so somewhat less efficiently than the full-length *miR-17~92* ($P = 0.0002$ for the comparison between Δ/Δ and Δ/Δ + miR-19a,b; $P = 0.0013$ for the comparison between fl/fl and Δ/Δ + miR-19a,b).

Identification of miR-19 targets in B-cell lymphomas

Having demonstrated a critical role of *miR-19a* and *miR-19b* in Myc-driven B-cell lymphomas, we next sought to identify their functionally relevant target mRNAs. miRNA target prediction algorithms (TargetScan, Miranda, and Pictar) (John et al. 2004; Krek et al. 2005; Grimson et al. 2007; Betel et al. 2008) identify several hundreds of potential targets of miR-19; however, only a fraction of these mRNAs will likely be functionally relevant in any particular cellular context. To identify the genes whose expression is effectively modulated by *miR-17~92* in B-cell lymphomas, we compared the gene expression profile of the AV4182 cell line before and after deletion of *miR-17~92* (fl/fl vs. Δ/Δ). We also included *miR-17~92*$^{\Delta/\Delta}$ lymphoma cells that had been transduced with either PIG-*miR-17~92*^{wt} or PIG-*miR-19a/19b* (Fig. 3A). In choosing this approach, we were supported by a number of recent reports showing that mRNA destabilization contributes to miRNA-mediated regulation of gene expression (Bagga et al. 2005; Lim et al. 2005; Baek et al. 2008; Selbach et al. 2008), which can be detected by conventional mRNA expression arrays. As predicted, deletion of *miR-17~92* led to the preferential up-regulation of genes whose 3′ untranslated regions (UTRs) contain seed matches for the miRNAs encoded by this cluster (P-value < 2.22e-16, KS test) (Fig. 3B; Supplemental Fig. 3). Accordingly, ectopic expression of *miR-17~92* in *miR-17~92*$^{\Delta/\Delta}$ cells led to the preferential down-regulation of *miR-17~92* targets (P-value < 2.22e-16, KS test) (Fig. 3C; Supplemental Fig. 3). Finally, reintroduction of a mutant version of the *miR-17~92* cluster expressing only *miR-19a* and *miR-19b* selectively affected mRNAs carrying binding sites for these two miRNAs (P-value = 6.35e-15), but not genes with binding sites for the other members of the *miR-17~92* cluster.

By comparing the four gene expression profiles, we identified a total of 568 genes whose expression was up-regulated (log2 expression change >0.20) by deletion of the endogenous *miR-17~29* locus (fl/fl vs. Δ/Δ comparison) and down-regulated by the reintroduction of the full-length *miR-17~92* cluster (*miR-17~92* vs. Δ/Δ) and of *miR-19a* and *miR-19b* only (*miR-19a/b* vs. Δ/Δ; log2 expression change <−0.20) (Fig. 3D). Ninety-five of them contained in their 3′UTR one or more conserved binding sites for miR-19, according to TargetScan 5.1 (Fig. 3E; Supplemental Table 1), and were analyzed further. Guided by our findings that miR-19 suppresses apoptosis in *Eμ-Myc* lymphoma cells, we inspected the list of 95 genes and selected a subset of 46 of them for functional validation (Fig. 4A; Supplemental Table 2). We reasoned that, if *miR-19* promotes survival by repressing the expression of one or more of these genes, this effect should be at least partially phenocopied by RNAi-mediated knockdown of the relevant targets. To test this hypothesis, for each of the 46 genes selected for validation we designed three shRNAs. The shRNAs were cloned into the MLP vector, a retroviral vector also expressing GFP, and each construct was individually transduced into *miR-17~92*$^{\Delta/\Delta}$ lymphoma cells. Analogous to the experiments described in Figure 2A, the viral preparations were titrated in order to achieve a transduction efficiency of 5%–30%, and the fraction of GFP$^+$ cells was measured 2 d after infection (day 0) and again 11 d later. The results of this experiment are summarized in Figure 4B. For the majority of shRNAs, the fraction of GFP$^+$-positive cells did not change over time or, for a small number of them, was lower at day 11 compared with day 0, indicating that expression of the shRNA did not provide any growth advantage to the infected cells or was detrimental, respectively (Fig. 4B; Supplemental Table 2). However, for a subset of shRNAs, we observed a significant increase in

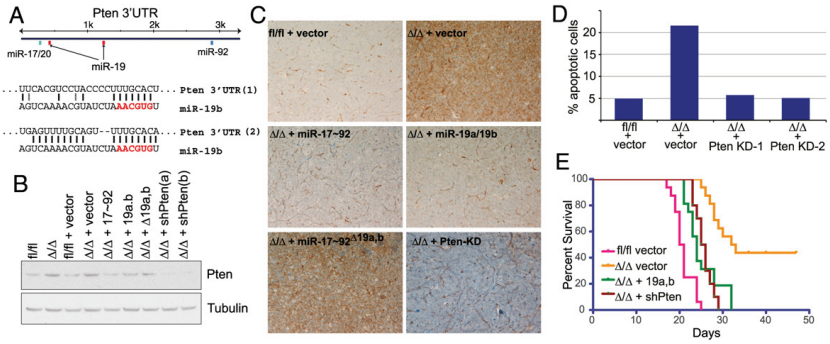

Figure 5. Pten is a functionally relevant *miR-19* target in B-cell lymphomas. (*A*) Schematic representation of the *Pten* 3′UTR with the location of the predicted binding sites for members of the *miR-17~92* cluster and sequence alignments between miR-19b and its two predicted binding sites. (*B*) Pten Western blot on lysates of B-lymphoma cells transduced with the indicated PIG constructs. (Lanes 8,9) For comparison, lysates from *miR-17~92*$^{\Delta/\Delta}$ cell expressing the two *Pten* shRNAs that scored positive in the in vitro screen were also assayed. (*C*) Pten immunohistochemistry on lymphoma sections obtained from mice injected with *miR-17~92*$^{fl/fl}$ and *miR-17~92*$^{\Delta/\Delta}$ B-lymphoma cells transduced with the indicated *miR-17~92* derivatives (objective, 20×). Brown staining indicates Pten signal. (*D*) Knockdown of Pten suppresses apoptosis in *miR-17~92*$^{\Delta/\Delta}$ cells. Apoptosis was measured by detecting caspase activity in *miR-17~92*$^{fl/fl}$ and *miR-17~92*$^{\Delta/\Delta}$ cells transduced with the indicated retroviruses. (*E*) Kaplan-Meier survival curve of mice injected with *miR-17~92*$^{\Delta/\Delta}$ lymphoma cells transduced with retroviruses expressing shRNAs against *Pten*. $N = 10$ (five mice for shPTEN-1 and five mice for shPTEN-2). For comparison, the survival curves of mice injected with *miR-17~92*$^{fl/fl}$, *miR-17~92*$^{\Delta/\Delta}$, and *miR-17~92*$^{\Delta/\Delta}$ + *miR-19a,b* from Figure 2C are included.

this case, survival was slightly longer compared with mice injected with *miR-17~92*$^{fl/fl}$ cells ($P = 0.0002$), indicating the existence of additional functionally relevant targets.

In summary, the results presented here provide a mechanistic explanation for the functional cooperation between c-Myc and *miR-17~92*, identify the miR-19 seed family as the primary oncogenic determinant of this cluster, and pave the way for the development of novel anti-cancer strategies based on the pharmacological inhibition of *miR-19* function.

Material and methods

Mouse husbandry

Animal studies and procedures were approved by the Memorial Sloan Kettering Cancer Center Institutional Animal Care and Use Committee. Mice were maintained in a mixed 129SvJae and C57/B6 background. The *Rosa26-Cre-ER*^{T2} and *miR-17~92*$^{fl/fl}$ mice have been described previously (Ventura et al. 2007, 2008). The *Eμ-Myc* mice were generated and described by Adams et al. (1985).

For the in vivo tumorigenicity studies, 4- to 8-wk-old athymic (nu/nu) mice were injected intravenously with 10^5 lymphoma cells and monitored daily. Mice were euthanized when moribund. Kaplan-Meier curves were plotted using PRISM software, and the log-rank Mantel-Cox test was used to determine statistical significance.

Antibodies and immunohistochemistry

Antibodies and experimental conditions for Western blotting and immunohistochemistry are described in the Supplemental Material.

Cell culture and retroviral transduction

The *Eμ-Myc;miR-17~92*$^{fl/fl}$*;Cre-ER*^{T2} lymphoma lines were cultured on a feeder of irradiated NIH-3T3 cells in a medium composed of 50% DMEM and 50% IMDM, supplemented with 10% fetal bovine serum.

To induce deletion of the *miR-17~92* cluster, cells were incubated for 4 d with 250 nM 4-OHT. During our initial set of experiments with 4-OHT-treated lymphoma cells, we noticed that, upon prolonged passages, the few cells that had escaped full *miR-17~92* deletion (*miR-17~92*$^{fl/fl}$ and *miR-17~92*$^{fl/\Delta}$) invariably outcompeted the *miR-17~92*$^{\Delta/\Delta}$ cells, eventually becoming the majority within a couple of weeks. To avoid this limitation and allow the execution of long-term in vivo experiments, 4 d after 4-OHT treatment, subclones were isolated by plating 10 cells per well into a 96-well plate using a MoFlo fluorescence-activated cell sorter. After expansion, clones composed solely of fully recombined cells were isolated and used for further manipulation.

Retroviruses were generated in Phoenix packaging cells. When required, transduced cells were selected by adding puromycin (2 μg/mL) to the culture medium for 4 d.

Plasmids and shRNA library

A 1.2-kb fragment encompassing the entire *miR-17~92* cluster was PCR-amplified from mouse genomic DNA and cloned into the MSCV-PIG retroviral vector (a gift from Mike Hemann, Massachusetts Institute of Technology). Deletion mutants were by site-directed PCR and verified by sequencing. Primers and sequences are available on request.

The shRNA library was cloned in the MLP retroviral vector (a gift from Michael Hemann, Massachusetts Institute of Technology). For each gene, three shRNA directed against the coding sequence were designed using the RNAi Central resource created by the laboratory of Greg Hannon (http://katahdin.cshl.org:9331/siRNA/RNAi.cgi?type=shRNA). Each construct was sequence-verified.

Apoptosis assays

Apoptosis was measured using the Caspase Detection Kit (Red-VAD-FMK or FITC-VAD-FMK, Calbiochem) and confirmed using the TUNEL assay (In Situ Cell Death Detection Kit, TMR red, Roche) following the manufacturer's instructions.

Gene expression analysis

Total RNA extracted from three technical replicates was hybridized to the Affymetrix 430 A2.0 gene chip, following the manufacturer's instruction. Gene expression was normalized using the GCRMA Bioconductor package, and log expression values were computed using the limma package. For genes with multiple probes, the probe with lowest adjusted *P*-value

was selected. Genes with a log expression change of <−0.2 in all three comparisons and with an adjusted *P*-value < 0.05 in at least one comparison were considered for subsequent overlap analysis.

miRNA target predictions

miRNA targets were predicted using miRanda (http://www.microrna.org) and TargetScan (http://www.targetscan.org). For the cumulative distribution function (CDF) plots, target sites were restricted to perfect seed complementarity between positions 2 and 7 of the miRNA. Empirical cumulative distributions were computed using R ecdf function for the set of predicted gene of the transduced miRNAs and for the genes with no target sites (background). *P*-values were computed using the KS two-sample test.

Acknowledgments

We thank Jane Qiu for technical assistance. A.V. is grateful to Tyler Jacks and Robert Benezra for their generosity and support. This work was funded by the Sidney Kimmel Cancer Research Foundation and the Geoffrey Beene Cancer Research Foundation.

References

Adams JM, Harris AW, Pinkert CA, Corcoran LM, Alexander WS, Cory S, Palmiter RD, Brinster RL. 1985. The c-myc oncogene driven by immunoglobulin enhancers induces lymphoid malignancy in transgenic mice. *Nature* **318:** 533–538.

Baek D, Villén J, Shin C, Camargo FD, Gygi SP, Bartel DP. 2008. The impact of microRNAs on protein output. *Nature* **455:** 64–71.

Bagga S, Bracht J, Hunter S, Massirer K, Holtz J, Eachus R, Pasquinelli AE. 2005. Regulation by let-7 and lin-4 miRNAs results in target mRNA degradation. *Cell* **122:** 553–563.

Bartel DP. 2009. MicroRNAs: Target recognition and regulatory functions. *Cell* **136:** 215–233.

Betel D, Wilson M, Gabow A, Marks DS, Sander C. 2008. The microRNA.org resource: Targets and expression. *Nucleic Acids Res* **36:** D149–D153. doi: 10.1093/nar/gkm995.

Di Cristofano A, Pesce B, Cordon-Cardo C, Pandolfi PP. 1998. Pten is essential for embryonic development and tumour suppression. *Nat Genet* **19:** 348–355.

Fontana L, Fiori ME, Albini S, Cifaldi L, Giovinazzi S, Forloni M, Boldrini R, Donfrancesco A, Federici V, Giacomini P, et al. 2008. Antagomir-17-5p abolishes the growth of therapy-resistant neuroblastoma through p21 and BIM. *PLoS One* **3:** e2236. doi: 1371/journal.pone.0002236.

Grimson A, Farh KK, Johnston WK, Garrett-Engele P, Lim LP, Bartel DP. 2007. MicroRNA targeting specificity in mammals: Determinants beyond seed pairing. *Mol Cell* **27:** 91–105.

Hayashita Y, Osada H, Tatematsu Y, Yamada H, Yanagisawa K, Tomida S, Yatabe Y, Kawahara K, Sekido Y, Takahashi T. 2005. A polycistronic microRNA cluster, miR-17-92, is overexpressed in human lung cancers and enhances cell proliferation. *Cancer Res* **65:** 9628–9632.

He L, Thomson JM, Hemann MT, Hernando-Monge E, Mu D, Goodson S, Powers S, Cordon-Cardo C, Lowe SW, Hannon GJ, et al. 2005. A microRNA polycistron as a potential human oncogene. *Nature* **435:** 828–833.

John B, Enright AJ, Aravin A, Tuschl T, Sander C, Marks DS. 2004. Human microRNA targets. *PLoS Biol* **2:** e363. doi: 10.1371/journal.pbio.0020363.

Krek A, Grun D, Poy MN, Wolf R, Rosenberg L, Epstein EJ, MacMenamin P, da Piedade I, Gunsalus KC, Stoffel M, et al. 2005. Combinatorial microRNA target predictions. *Nat Genet* **37:** 495–500.

Lim LP, Lau N, Garrett-Engele P, Grimson A, Schelter J, Castle J, Bartel DP, Linsley PS, Johnson J. 2005. Microarray analysis shows that some microRNAs downregulate large numbers of target mRNAs. *Nature* **433:** 769–773.

Mendell JT. 2008. miRiad roles for the miR-17-92 cluster in development and disease. *Cell* **133:** 217–222.

O'Donnell KA, Wentzel EA, Zeller KI, Dang CV, Mendell JT. 2005. c-Myc-regulated microRNAs modulate E2F1 expression. *Nature* **435:** 839–843.

Ota A, Tagawa H, Karnan S, Tsuzuki S, Karpas A, Kira S, Yoshida Y, Seto M. 2004. Identification and characterization of a novel gene, C13orf25, as a target for 13q31-q32 amplification in malignant lymphoma. *Cancer Res* **64:** 3087–3095.

Podsypanina K, Ellenson LH, Nemes A, Gu J, Tamura M, Yamada KM, Cordon-Cardo C, Catoretti G, Fisher PE, Parsons R. 1999. Mutation of Pten/Mmac1 in mice causes neoplasia in multiple organ systems. *Proc Natl Acad Sci* **96:** 1563–1568.

Salmena L, Carracedo A, Pandolfi PP. 2008. Tenets of PTEN tumor suppression. *Cell* **133:** 403–414.

Schmidt-Supprian M, Rajewsky K. 2007. Vagaries of conditional gene targeting. *Nat Immunol* **8:** 665–668.

Selbach M, Schwanhausser B, Thierfelder N, Fang Z, Khanin R, Rajewsky N. 2008. Widespread changes in protein synthesis induced by microRNAs. *Nature* **455:** 58–63.

Suzuki A, de la Pompa JL, Stambolic V, Elia AJ, Sasaki T, del Barco Barrantes I, Ho A, Wakeham A, Itie A, Khoo W, et al. 1998. High cancer susceptibility and embryonic lethality associated with mutation of the PTEN tumor suppressor gene in mice. *Curr Biol* **8:** 1169–1178.

Tagawa H, Seto M. 2005. A microRNA cluster as a target of genomic amplification in malignant lymphoma. *Leukemia* **19:** 2013–2016.

Uziel T, Karginov FV, Xie S, Parker JS, Wang YD, Gajjar A, He L, Ellison D, Gilbertson RJ, Hannon G, et al. 2009. The miR-17~92 cluster collaborates with the Sonic Hedgehog pathway in medulloblastoma. *Proc Natl Acad Sci* **106:** 2812–2817.

Ventura A, Jacks T. 2009. MicroRNAs and cancer: Short RNAs go a long way. *Cell* **136:** 586–591.

Ventura A, Kirsch DG, McLaughlin ME, Tuveson DA, Grimm J, Lintault L, Newman J, Reczek EE, Weissleder R, Jacks T. 2007. Restoration of p53 function leads to tumour regression in vivo. *Nature* **445:** 661–665.

Ventura A, Young AG, Winslow MM, Lintault L, Meissner A, Erkeland SJ, Newman J, Bronson RT, Crowley D, Stone JR, et al. 2008. Targeted deletion reveals essential and overlapping functions of the miR-17 through 92 family of miRNA clusters. *Cell* **132:** 875–886.

Xiao C, Srinivasan L, Calado DP, Patterson HC, Zhang B, Wang J, Henderson JM, Kutok JL, Rajewsky K. 2008. Lymphoproliferative disease and autoimmunity in mice with increased miR-17-92 expression in lymphocytes. *Nat Immunol* **9:** 405–414.

ORIGINAL ARTICLE JCP09-0153(21843)

Journal of Cellular Physiology

Expression[Q1] of Angiogenic Regulators, VEGF and Leptin, Is Regulated by the EGF/PI3K/STAT3 Pathway in Colorectal Cancer Cells

SANDRA [Q3]CASCIO,[1] RITA FERLA,[1,2] ALECO D'ANDREA,[1] ALDO GERBINO,[3] BAZAN VIVIANA,[1] EVA SURMACZ,[2] AND ANTONIO RUSSO[1]*

[1]*Department of Surgical and Oncological Sciences, Section of Medical Oncology, Università di Palermo, Palermo, Italy*

[2]*Sbarro Institute for Cancer Research and Molecular Medicine, Temple University, Philadelphia, Pennsylvania*

[3]*Histological and Embriological Section, Department of Experimental Medicine, Institute of Pathology, Università di Palermo, Palermo, Italy*

Both leptin and vascular endothelial growth factor (VEGF) are growth and angiogenic cytokines that are upregulated in different types of cancer and have been implicated in neoplastic progression. Here we investigated the molecular mechanism by which leptin and VEGF expression are regulated in colon cancer by epidermal growth factor (EGF). In colon cancer cell line HT-29, EGF induced the binding of signal transducer and activator transcription 3 (STAT3) to STAT3 consensus motifs within the *VEGF* and *leptin* promoters and stimulated leptin and VEGF mRNA and protein synthesis. All these EGF effects were significantly blocked when HT-29 cells were treated with an inhibitor of the phosphoinositide 3-kinase (PI3K) pathway, LY294002, or with small interfering RNA (siRNA) targeting STAT3. Thus, our study identified the EGF/PI3K/STAT3 signaling as an essential pathway regulating VEGF and leptin expression in EGF-responsive colon cancer cells. This suggests that STAT3 pathways might constitute attractive pharmaceutical targets in colon cancer patients where anti-EGF receptor drugs are ineffective.

J. Cell. Physiol. 9999: 1–6, 2009.

Neoangiogenesis is a critical step for tumor growth and metastatic spread (Folkman, 1971). New blood vessels formation depends on the balance between positive and negative regulators and is induced when factors that promote angiogenesis are upregulated or those that inhibit angiogenesis are down-regulated (Ferrara and Kerbel, 2005).

Vascular endothelial growth factor (VEGF) plays a major role in tumor angiogenesis and its expression is inversely correlated with patient survival in many human cancers, including colon carcinomas (Logan-Collins et al., 2008; Zafirellis et al., 2008). VEGF expression is regulated by various signaling pathways induced by external stimuli (e.g., hypoxia, hormones, cytokines) and may depend on the cellular context (e.g., the presence of activated oncogenes) (Xu et al., 2005). Epidermal growth factor (EGF) receptor (EGFR) signaling pathway is commonly activated in colorectal cancer and has been investigated as a target for cancer therapy (Mendelsohn and Baselga, 2000). After ligand (EGF, transforming growth factor) binding to EGFR, a cascade of downstream signaling is activated, including activation of the Ras-MAP kinase and phosphoinositide 3-kinase (PI3K)/Akt pathways (Mendelsohn and Baselga, 2000). Moreover, in several cell lines, EGF as well as abnormal activation of EGFR signaling pathways induces VEGF expression (Maity et al., 2000; Zhong et al., 2000). Conversely, EGFR inhibition can decrease VEGF expression, and consequently angiogenesis, in many tumor types (Ciardiello and Tortora, 2001; Pore et al., 2006).

A less well-known factor with a strong neoangiogenic activity is leptin (Cao et al., 2001; Anagnostoulis et al., 2008). Leptin is a pleiotropic hormone whose major role is to regulate food intake and energy balance via hypothalamic effects. Leptin also affects many peripheral organs, behaving as a mitogen, survival factor, metabolic regulator, or angiogenic factor (Wauters et al., 2000; Cao et al., 2001; Misztal-Dethloff et al., 2004; Gonzalez et al., 2006). Furthermore, there is evidence that leptin promotes neoplastic processes in different cell types (Garofalo et al., 2006; Housa et al., 2006). In colorectal cancer, leptin can promote proliferation and invasiveness, and inhibit apoptosis (Attoub et al., 2000; Aparicio et al., 2004; Amemori et al., 2007; Jaffe and Schwartz, 2008). In addition, human colorectal cancers have been shown to overexpress leptin as well the leptin receptor (ObR) (Koda et al., 2007).

The *VEGF* and *leptin* gene promoters contain several regulatory motif as ERE, CRE, SP-1, AP-2, HRE, and SRE (STAT3-responsive element) (Finkenzeller et al., 1997; Mason et al., 1998; Brenneisen et al., 2003). STAT3 is a transcription factor activated through phosphorylation on a conserved tyrosine residue (Tyr705), leading to STAT3 dimerization, nuclear translocation and DNA binding to specific consensus sequence TT($N_{4/5}$)AA (Seidel et al., 1995; Frank, 2007). STAT3 has been identified as a major regulator of VEGF expression in glioblastoma and prostate cancer (Niu et al., 2002; Wei et al., 2003). *VEGF* induction by various oncogenic growth stimuli,

Cascio Sandra and Ferla Rita contributed equally to this work.

*Correspondence to: Antonio Russo, Department of Surgical and Oncological Sciences, Section of Medical Oncology, Università di Palermo, via del Vespro 127, 90127 Palermo, Italy.
E-mail: lab-oncobiologia@usa.net

Received 16 April 2009; Accepted 28 April 2009

Published online in Wiley InterScience (www.interscience.wiley.com.), 00 Month 2009.
DOI: 10.1002/jcp.21843

including IL-6, c-src, Her2/Neu can be abrogated by interruption of STAT3 signaling with dominant-negative STAT3 protein or STAT3 antisense nucleotide (Wei et al., 2003; Xu et al., 2005).

Recently data demonstrated that STAT3 is involved in colorectal cancer cells growth, survival, invasion, and migration (Klampfer, 2008), through upregulation of various genes, including *VEGF* (Xiong et al., 2008). However, the role of STAT3 in VEGF or leptin expression in colorectal cancer has never been assessed.

Because the growth of colorectal cancer cells can be regulated by the EGF/STAT3 pathway (Alvarez et al., 2006; Vigneron et al., 2008), we tested if this pathway can be involved in the activation of two angiogenic factors, VEGF and leptin. Here we demonstrated that in colorectal cancer cell line HT-29, EGF-induced leptin and VEGF expression is mediated by the recruitment of STAT3 to SRE motif in both *VEGF* and *leptin* gene promoters. EGF effects on VEGF and leptin expression were significantly blocked with small interfering RNA (siRNA) targeting STAT3.

Materials and Methods

Cell culture and treatments

HT-29 cells were grown in GIBCO^{TM} Leibovitz's L-15 Medium (Invitrogen, Carlsbad, CA) supplemented with 10% fetal bovine serum (FBS), 100 U/mL penicillin, and 50 μg/mL streptomycin. A total of 70% confluent cells were synchronized in serum-free medium (SFM) for 24 h and then stimulated with 10 ng/ml EGF (R&D Systems, Minneapolis, MN) for 24 h, with or without a 2 h pre-treatment of PI3K inhibitor LY294002 (Calbiochem, San Diego, CA) at 50 μM.

Quantitative real-time-PCR (qRT-PCR)

HT-29 cells were treated, as described above, or left untreated. Total cellular RNA was isolated using the RNeasy Mini Kit (Qiagen, Inc., Valencia, CA). A total of 5 μg of RNA was reverse transcribed using the High-Capacity cDNA Archive (Applied Biosystems, Foster City, CA) according to the manufacturer's protocol. Five microliters of the RT products were used to amplify leptin and VEGF sequences using respectively the Hs00174877_m1 Lep and the Hs00900054_m1 VEGF TaqMan Kit (Applied Biosystems), following vendor's instructions. To normalize qRT-PCR reactions, parallel reactions were run on each sample for cyclophilin A. Changes in the target mRNA content relative to cyclophilin A mRNA were determined using a comparative CT method to calculate changes in CT, and ultimately fold and percent change. An average CT value for each RNA was obtained for replicate reactions.

Leptin and VEGF detection by ELISA

A total of 3.6×10^7 HT-29 cells (or 1.8×10^7 for STAT3 siRNA) were treated, as above described. Secreted VEGF and leptin were measured in cell culture media using Human Quantikine ELISA Kits (R&D Systems) with the lowest detection limit of 5 pg/ml for VEGF and 7.8 pg/ml for leptin, intra-assay precision of <8.8% (VEGF) and <4.9% (leptin), and inter-assay precision <9.2% (VEGF) and <8.2% (leptin). All points were done in triplicate and the experiments were repeated three times. All leptin and VEGF concentrations were within the range of curve standard. Linear regression analysis was performed to create the curve standard.

Western blotting (WB)

Cytoplasmic and nuclear protein extraction was performed using NE-PER Extraction Reagents (Pierce Biotechnology, Inc., Rockford, IL). The expression of STAT3 was analyzed in 120 μg of cytoplasmic or nuclear cell lysates. The following antibodies were used for WB: anti-STAT3 (C-20 X), anti-C23 (MS-3), and anti-GAPDH (8C2). All above antibody were purchased from Santa Cruz (Santa Cruz Biotechnology, Santa Cruz, CA). Nuclear marker nucleolin and cytoplasmic marker GAPDH were used as loading controls.

Chromatin immunoprecipitation (ChIP)

ChIP was performed using the Chromatin Immunoprecipitation Assay kit (Upstate, Temecula, CA), according to manufacturer's instructions. Soluble chromatin was immunoprecipitated with STAT3 (C-20) pAb (Santa Cruz Biotechnology). The presence of leptin and VEGF promoter domains containing STAT3 motifs in immunoprecipitated DNA was identified by PCR using the following primers: for leptin (region from −1892 to −1403) forward 5′-TTG TGG TCA GAC CAG TTT TCT-3′, reverse 5′-GTT TGG TAA TGC CCA AAA GCT-3′, for VEGF (region −1041 from to −750) forward 5′-CAG GAA CAA GGG CCT CTG TCT-3′, reverse 5′-TGT CCC TCT GAC AAT GTG CCA TC-3′. The PCR conditions for leptin region were: 1 min at 94°C, 1 min at 60°C, 1 min at 72°C; for VEGF region: 1 min 94°C, 1 min at 64°C, 1 min at 72°C. The amplification of these regions was analyzed after PCR 35 cycles.

Knockdown of STAT3 using small interfering RNA (siRNA)

STAT3 knockdowns were achieved using siRNAs (Dharmacon, Inc., Lafayette, CO), according to manufacturer's instructions. Twenty-four hours following transfection, the cells were placed in SFM for 24 h, then stimulated with EGF 10 ng/ml for 24 h or left untreated. Non-specific siRNA (Dharmacon, Inc.) was used as a negative control.

Results

EGF upregulates VEGF and leptin expression

Since it is known that EGF regulates tumor-associated angiogenesis, we assessed EGF effects on the expression of VEGF and leptin. First, we measured the effects of EGF on VEGF and leptin mRNA levels. The treatment of HT-29 cells with EGF for 24 h induced VEGF mRNA production by 1.4-fold (Fig. 1a). Similarly, EGF stimulated leptin mRNA expression by 2.7-fold at 24 h relative to untreated cells (Fig. 1b). In parallel, EGF increased the levels of secreted VEGF and leptin by 2.6- and 1.7-fold, respectively (Fig. 1c,d). These results suggested that EGF upregulates VEGF and leptin at mRNA and protein levels.

EGF-induced STAT3 recruitment to VEGF and leptin promoters

Analysis of the *VEGF* promoter revealed a putative binding site for STAT3 at the −848 position (Niu et al., 2002). We also identified two binding sites for STAT3 within the *leptin* promoter at −1715 and at −1500 positions. Consequently, we investigated whether STAT3 could mediate EGF effects on VEGF and leptin expression in HT-29 colon cancer cell line.

We first examined the abundance of nuclear STAT3 in cells treated with EGF (Fig. 2a). In untreated cells, STAT3 was expressed in the nucleus at relatively low levels, while following EGF stimulation, nuclear accumulation of STAT3 was significantly increased (2.5-fold, relative to untreated cells); at the same time, the cytoplasmic STAT3 levels remained unchanged. Next, we assessed STAT3 binding to specific motifs in the *VEGF* and *leptin* promoters (Fig. 2b). Our results suggested that EGF increased STAT3 recruitment to both *VEGF* and *leptin* promoters by threefold.

Silencing of STAT3 expression reduces VEGF and leptin induction by EGF

To verify STAT3 involvement in EGF-induced VEGF and leptin mRNA production, we silenced STAT3 expression using RNA interference. The specific STAT3 siRNA down-regulated basal

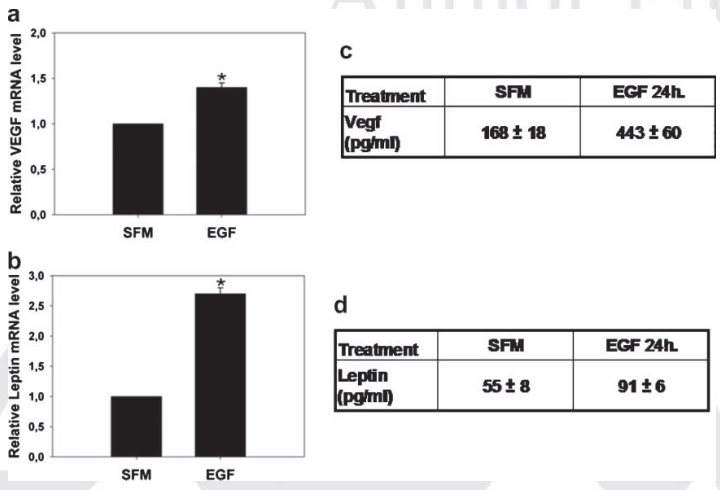

c

Treatment	SFM	EGF 24h.
Vegf (pg/ml)	168 ± 18	443 ± 60

d

Treatment	SFM	EGF 24h.
Leptin (pg/ml)	55 ± 8	91 ± 6

Fig. 1. Leptin and VEGF mRNA and protein expression increases in response to EGF stimulation. a,b: The abundance of VEGF and leptin mRNA were studied with qRT-PCR. HT-29 cells were synchronized in SFM for 24 h and then treated with 10 ng/ml EGF for 24 h or left untreated. To normalize qRT-PCR reactions, parallel reactions were run on each sample for cyclophilin A. The graphs represent increase of VEGF and leptin mRNA relative to SFM ± SD. *, $P < 0.05$, control versus EGF. c,d: The abundance of VEGF and leptin proteins were determined by ELISA assay. A total of 3.6×10^7 HT-29 cells were treated as previously described.

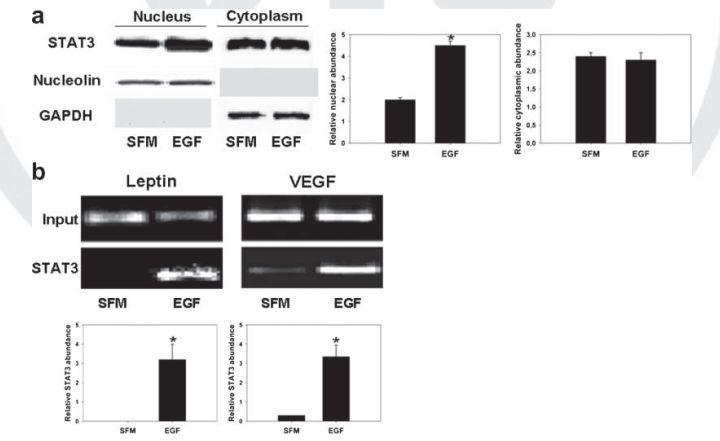

Fig. 2. EGF increases nuclear STAT-3 level and induces loading on the *VEGF* and *leptin* promoters. a: HT-29 cells at 70% confluence were synchronized in serum-free medium (SFM) for 24 h and then stimulated with 10 ng/ml EGF for 24 h. The expression of STAT3 was assessed by WB of 100 μg cytoplasmic and 120 μg nuclear proteins using specific Abs, as described in Material and Methods Section. Graphs represent relative STAT3 expression level normalized to nuclear marker nucleolin and cytoplasmic marker GAPDH; *Columns*, mean; *bars*, SD; *, $P < 0.05$ basal versus EGF. b: The binding of STAT-3 on both leptin and VEGF promoters was assessed by ChIP as described in Material and Methods Section. The graphs represent the abundance of STAT3 on *VEGF* and *leptin* promoters under different conditions ±SD; *, $P < 0.05$ basal versus EGF-treated *Columns*, mean; *bars*, SD.

STAT3 protein levels by 90%, whereas unrelated siRNA had no effects on this protein (Fig. 3a). STAT3 knockdown reduced by 16% and 48% EGF-induced VEGF and leptin mRNA levels respectively as well as down-regulated basal levels of both factors (Fig. 3b). Similarly, STAT3 siRNA reduced EGF-induced secreted VEGF and leptin proteins by 35% and 25%, respectively (Fig. 3c).

PI3K pathway is involved in EGF-dependent VEGF and leptin expression

The PI3K pathway can regulate VEGF and leptin expression in different cancer cell lines (Maity et al., 2000; Pore et al., 2003; Saxena et al., 2007). Using LY294002 inhibitor, we investigated whether this pathway is required for VEGF and leptin transcriptional regulation in HT-29 cells (Fig. 4c). Inhibition of the PI-3K pathway down-regulated EGF-dependent VEGF and leptin mRNA by 20%, LY294002 also blocked basal level of VEGF mRNA by 70%, whereas basal level of leptin was not affected (Fig. 4c).

Next, we studied whether inhibition of PI3K can affect EGF-induced recruitment of STAT3 to the *VEGF* and *leptin* promoters. First, we found that nuclear accumulation of STAT3 was inhibited by 30% under LY294002 treatment (Fig. 4a). This was followed by reduced EGF-dependent binding of STAT3 to the *VEGF* and *leptin* promoters by 30% and 50%, respectively (Fig. 4b).

Discussion

Angiogenesis is an essential process for the growth of primary tumor and metastasis formation and VEGF is a recognized critical factor involved in this process (Folkman, 1971). Tumor cells may produce VEGF in response to stimuli, such as cytokines and growth factors, such as EGF, or under hypoxic conditions. Angiogenesis might also be induced by leptin, directly, or indirectly through upregulation of VEGF (Cao et al., 2001; Misztal-Dethloff et al., 2004; Suganami et al., 2004; Anagnostoulis et al., 2008). Here we studied the molecular mechanism by which EGF can promote angiogenesis in colorectal cancer cells, focusing on EGF-dependent activation of pro-angiogenic factors, VEGF and leptin.

We found that in HT-29 colon cancer cell lines, VEGF and leptin levels were upregulated under EGF stimulation. Using qRT-PCR and ELISA assays, we documented increased

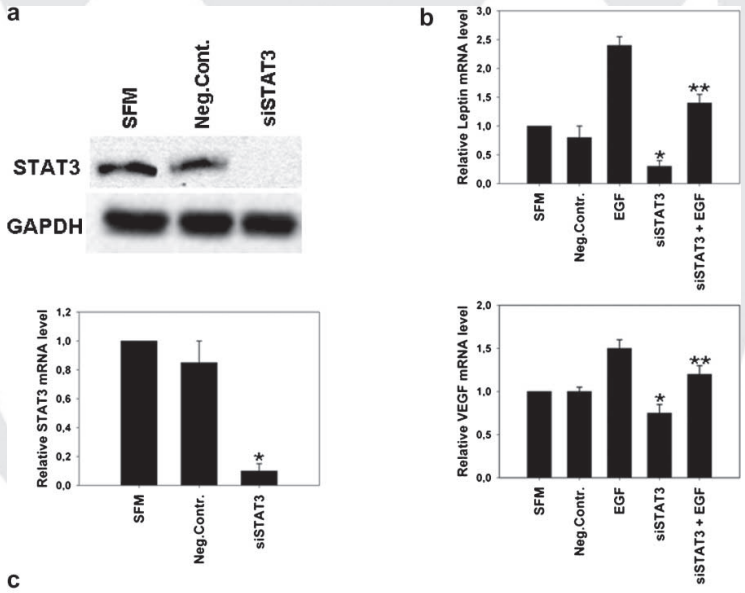

c

Treatment	SFM	neg.contr.	siSTAT3	EGF 24h.	siSTAT3+EGF 24h.
Vegf (pg/ml)	85 ± 10	90 ± 8	62 ± 4	220 ± 30	144 ± 10
Leptin (pg/ml)	25 ± 2	27 ± 3	15 ± 4	48 ± 4	36 ± 3

Fig. 3. Knockdown of STAT3 reduces VEGF and leptin expression. a: The expression of STAT3 was determined by WB. *Stat3* knockdowns were achieved using siRNAs as described in Material and Methods Section. After 24 h from transfection, cells were placed in SFM for 24 h then stimulated with EGF 10 ng/ml for 24 h or left untreated. Non-specific siRNA was used as a negative control. *Columns*, mean; *bars*, SD; *, $P < 0.05$ SFM versus treated cells. b: The expression of VEGF and leptin mRNA in STAT3 siRNA transfectants treated for 24 h with EGF or left untreated was studied by qRT-PCR. c: A total of 1.8×10^7 cells were treated as described above. The abundance of secreted leptin and VEGF (pg/ml) in conditioned medium was determined by ELISA. *Columns*, mean; *bars*, SD; * or **, $P < 0.05$ basal versus siSTAT3 trasfectant or EGF versus EGF + siSTAT3 trasfectant.

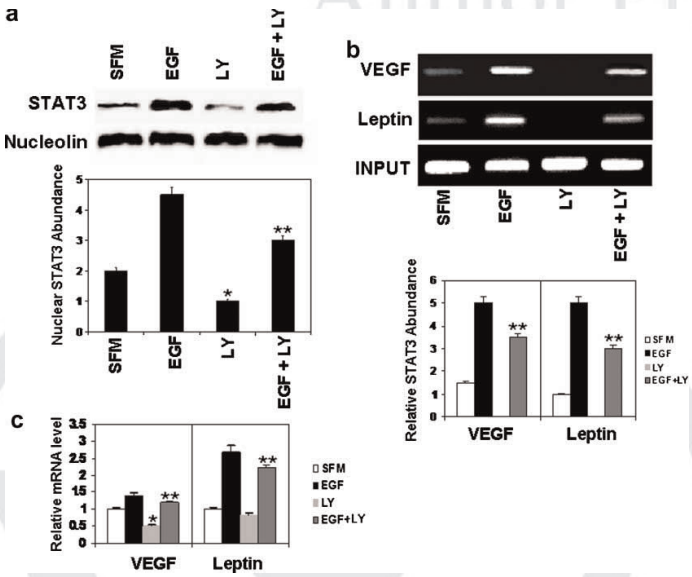

Fig. 4. EGF-induced VEGF and leptin expression is mediated by PI3K. a: HT-29 cells were treated for 24 h with 10 nM EGF for 24 h and/or 50 μM LY294002. The nuclear abundance of STAT3 was assessed by WB. b: The binding of STAT3 to *VEGF* and *leptin* promoter was determined by ChIP as described in material and Methods Section. c: The abundance of VEGF and leptin mRNA was studied with qRT-PCR in HT-29 cells untreated or treated with EGF, and/or LY294002. *Columns*, mean; *bars*, SD; * or **, $P < 0.05$ basal versus LY-treated or EGF versus EGF + LY-treated.

expression of both factors at mRNA and protein level. These data are in agreement with the observation that in glioblastoma and prostate cancer cells, EGF can induce VEGF expression (Maity et al., 2000; Zhong et al., 2000). However, direct mechanistic link between EGF and VEGF in colon cancer cells has not been described until now. Moreover, to our knowledge, our data provide the first mechanistic evidence on the role of EGF in the control of leptin expression in cancer cells.

It is known that VEGF promoter contains binding sites for STAT3. A recent study in mouse cerebral endothelial cells identified STAT3-mediated VEGF expression induced by ectopic decorin, a ligand for EGFR (Santra et al., 2008). The *leptin* promoter also contains two potential sites for STAT3 localized at −1715 and −1500 in the promoter. While it is known that STAT3 activation mediates many of the biological effects of leptin (Catalano et al., 2008), there are not evidences regarding STAT3 involvement in leptin gene transcription. Our study demonstrated for the first time that EGF-induced leptin and VEGF expression in colon cancer is mediated by and requires STAT3. Specifically, our results suggested that STAT3 binds both VEGF and leptin promoters under EGF stimulation in colon cancer cells and STAT3 down-regulation by RNA-interference significantly suppressed both VEGF and leptin expression.

Our previous study in cancer cells suggested that PI3K is involved in leptin expression (Bartella et al., 2008). PI3K involvement in leptin expression was also confirmed in other cell models (Cong et al., 2007; Tong et al., 2008). The PI3K/mTOR pathway has also been shown to play an important role in VEGF regulation (Zhong et al., 2000; Laughner et al., 2001; Kang et al., 2008). In agreement with these observations, we found that PI-3K is required for leptin and VEGF expression under EGF treatment, especially for STAT3 recruitment to both VEGF and leptin promoters, as demonstrated by ChIP assay.

In summary, we demonstrated that in colorectal cancer cells, EGF can upregulate the expression of two pro-angiogenic factors, VEGF and leptin via the PI3K signaling pathway. We report that the mechanism of this EGF-activity occurs at transcriptional level and it is mediated by the recruitment of STAT3 on *VEGF* and *leptin* promoters. The fact that EGF can stimulate leptin expression in colon cancer suggest that leptin and its receptor can become novel pharmaceutical targets in colorectal cancer. In addition, STAT3, which appears to play a major role in regulation of genes involved in angiogenesis might serve as alternative target in colon cancer patients in which anti-EGFR therapies are not effective.

Literature Cited

Alvarez JV, Greulich H, Sellers WR, Meyerson M, Frank DA. 2006. Signal transducer and activator of transcription 3 is required for the oncogenic effects of non-small-cell lung cancer-associated mutations of the epidermal growth factor receptor. Cancer Res 66:3162–3168.

Amemori S, Ootani A, Aoki S, Fujise T, Shimoda R, Kakimoto T, Shiraishi R, Sakata Y, Tsunada S, Iwakiri R, Fujimoto K. 2007. Adipocytes and preadipocytes promote the proliferation of colon cancer cells in vitro. Am J Physiol Gastrointest Liver Physiol 292:G923–G929.

Anagnostoulis S, Karayiannakis AJ, Lambropoulou M, Efthimiadou A, Polychronidis A, Simopoulos C. 2008. Human leptin induces angiogenesis in vivo. Cytokine 42:353–357.

Aparicio T, Guilmeau S, Goiot H, Tsocas A, Laigneau JP, Bado A, Sobhani I, Lehy T. 2004. Leptin reduces the development of the initial precancerous lesions induced by azoxymethane in the rat colonic mucosa. Gastroenterology 126:499–510.

Attoub S, Noe V, Pirola L, Bruyneel E, Chastre E, Mareel M, Wymann MP, Gespach C. 2000. Leptin promotes invasiveness of kidney and colonic epithelial cells via phosphoinositide 3-kinase-, rho-, and rac-dependent signaling pathways. FASEB J 14:2329–2338.

Bartella V, Cascio S, Fiorio E, Auriemma A, Russo A, Surmacz E. 2008. Insulin-dependent leptin expression in breast cancer cells. Cancer Res 68:4919–4927.

Brenneisen P, Blaudschun R, Gille J, Schneider L, Hinrichs R, Wlaschek M, Eming S, Scharffetter-Kochanek K. 2003. Essential role of an activator protein-2 (AP-2)/specificity

protein 1 (Sp1) cluster in the UVB-mediated induction of the human vascular endothelial growth factor in HaCaT keratinocytes. Biochem J 369:341–349.
Cao R, Brakenhielm E, Wahlestedt C, Thyberg J, Cao Y. 2001. Leptin induces vascular permeability and synergistically stimulates angiogenesis with FGF-2 and VEGF. Proc Natl Acad Sci USA 98:6390–6395.
Catalano S, Giordano C, Rizza P, Gu G, Barone I, Bonofiglio D, Giordano F, Malivindi R, Gaccione D, Lanzino M, De Amicis F, Ando S. 2008. Evidence that leptin through STAT and CREB signaling enhances cyclin D1 expression and promotes human endometrial cancer proliferation. J Cell[Q4] Physiol.
Ciardiello F, Tortora G. 2001. A novel approach in the treatment of cancer: Targeting the epidermal growth factor receptor. Clin Cancer Res 7:2958–2970.
Cong L, Chen K, Li J, Gao P, Li Q, Mi S, Wu X, Zhao AZ. 2007. Regulation of adiponectin and leptin secretion and expression by insulin through a PI3K-PDE3B dependent mechanism in rat primary adipocytes. Biochem J 403:519–525.
Ferrara N, Kerbel RS. 2005. Angiogenesis as a therapeutic target. Nature 438:967–974.
Finkenzeller G, Sparacio A, Technau A, Marme D, Siemeister G. 1997. Sp1 recognition sites in the proximal promoter of the human vascular endothelial growth factor gene are essential for platelet-derived growth factor-induced gene expression. Oncogene 15:669–676.
Folkman J. 1971. Tumor angiogenesis: Therapeutic implications. N Engl J Med 285:1182–1186.
Frank DA. 2007. STAT3 as a central mediator of neoplastic cellular transformation. Cancer Lett 251:199–210.
Garofalo C, Koda M, Cascio S, Sulkowska M, Kanczuga-Koda L, Golaszewska J, Russo A, Sulkowski S, Surmacz E. 2006. Increased expression of leptin and the leptin receptor as a marker of breast cancer progression: Possible role of obesity-related stimuli. Clin Cancer Res 12:1447–1453.
Gonzalez RR, Cherfils S, Escobar M, Yoo JH, Carino C, Styer AK, Sullivan BT, Sakamoto H, Olawaiye A, Serikawa T, Lynch MP, Rueda BR. 2006. Leptin signaling promotes the growth of mammary tumors and increases the expression of vascular endothelial growth factor (VEGF) and its receptor type two (VEGF-R2). J Biol Chem 281:26320–26328.
Housa D, Housova J, Vernerova Z, Haluzik M. 2006. Adipocytokines and cancer. Physiol Res 55:233–244.
Jaffe T, Schwartz B. 2008. Leptin[Q5] promotes motility and invasiveness in human colon cancer cells by activating multiple signal-transduction pathways. Int J Cancer.
Kang J, Rychahou PG, Ishola TA, Mourot JM, Evers BM, Chung DH. 2008. N-myc is a novel regulator of PI3K-mediated VEGF expression in neuroblastoma. Oncogene 27:3999–4007.
Klampfer L. 2008. The role of signal transducers and activators of transcription in colon cancer. Front Biosci 13:2888–2899.
Koda M, Sulkowska M, Kanczuga-Koda L, Cascio S, Colucci G, Russo A, Surmacz E, Sulkowski S. 2007. Expression of the obesity hormone leptin and its receptor correlates with hypoxia-inducible factor-1 alpha in human colorectal cancer. Ann Oncol 18:vi116–vi119.
Laughner E, Taghavi P, Chiles K, Mahon PC, Semenza GL. 2001. HER2 (neu) signaling increases the rate of hypoxia-inducible factor 1alpha (HIF-1alpha) synthesis: Novel mechanism for HIF-1-mediated vascular endothelial growth factor expression. Mol Cell Biol 21:3995–4004.
Logan-Collins JM, Lowy AM, Robinson-Smith TM, Kumar S, Sussman JJ, James LE, Ahmad SA. 2008. VEGF expression predicts survival in patients with peritoneal surface metastases from mucinous adenocarcinoma of the appendix and colon. Ann Surg Oncol 15:738–744.
Maity A, Pore N, Lee J, Solomon D, O'Rourke DM. 2000. Epidermal growth factor receptor transcriptionally up-regulates vascular endothelial growth factor expression in human glioblastoma cells via a pathway involving phosphatidylinositol 3'-kinase and distinct from that induced by hypoxia. Cancer Res 60:5879–5886.
Mason MM, He Y, Chen H, Quon MJ, Reitman M. 1998. Regulation of leptin promoter function by Sp1, C/EBP, and a novel factor. Endocrinology 139:1013–1022.
Mendelsohn J, Baselga J. 2000. The EGF receptor family as targets for cancer therapy. Oncogene 19:6550–6565.
Misztal-Dethloff B, Stepien H, Komorowski J. 2004. Effect of leptin on proliferative activity and vascular endothelial growth factor (VEGF) secretion from cultured endothelial cells HECa10 in vitro. Endocr Regul 38:161–166.
Niu G, Wright KL, Huang M, Song L, Haura E, Turkson J, Zhang S, Wang T, Sinibaldi D, Coppola D, Heller R, Ellis LM, Karras J, Bromberg J, Pardoll D, Jove R, Yu H. 2002. Constitutive Stat3 activity up-regulates VEGF expression and tumor angiogenesis. Oncogene 21:2000–2008.
Pore N, Liu S, Haas-Kogan DA, O'Rourke DM, Maity A. 2003. PTEN mutation and epidermal growth factor receptor activation regulate vascular endothelial growth factor (VEGF) mRNA expression in human glioblastoma cells by transactivating the proximal VEGF promoter. Cancer Res 63:236–241.
Pore N, Jiang Z, Gupta A, Cerniglia G, Kao GD, Maity A. 2006. EGFR tyrosine kinase inhibitors decrease VEGF expression by both hypoxia-inducible factor (HIF)-1-independent and HIF-1-dependent mechanisms. Cancer Res 66:3197–3204.
Santra M, Santra S, Zhang J, Chopp M. 2008. Ectopic decorin expression up-regulates VEGF expression in mouse cerebral endothelial cells via activation of the transcription factors Sp1, HIF1alpha, and Stat3. J Neurochem 105:324–337.
Saxena NK, Sharma D, Ding X, Lin S, Marra F, Merlin D, Anania FA. 2007. Concomitant activation of the JAK/STAT, PI3K/AKT, and ERK signaling is involved in leptin-mediated promotion of invasion and migration of hepatocellular carcinoma cells. Cancer Res 67:2497–2507.
Seidel HM, Milocco LH, Lamb P, Darnell JE, Jr., Stein RB, Rosen J. 1995. Spacing of palindromic half sites as a determinant of selective STAT (signal transducers and activators of transcription) DNA binding and transcriptional activity. Proc Natl Acad Sci USA 92:3041–3045.
Suganami E, Takagi H, Ohashi H, Suzuma K, Suzuma I, Oh H, Watanabe D, Ojima T, Suganami T, Fujio Y, Nakao K, Ogawa Y, Yoshimura N. 2004. Leptin stimulates ischemia-induced retinal neovascularization: Possible role of vascular endothelial growth factor expressed in retinal endothelial cells. Diabetes 53:2443–2448.
Tong KM, Shieh DC, Chen CP, Tzeng CY, Wang SP, Huang KC, Chiu YC, Fong YC, Tang CH. 2008. Leptin induces IL-8 expression via leptin receptor, IRS-1, PI3K, Akt cascade and promotion of NF-kappaB/p300 binding in human synovial fibroblasts. Cell Signal 20:1478–1488.
Vigneron A, Gamelin E, Coqueret O. 2008. The EGFR-STAT3 oncogenic pathway up-regulates the Eme1 endonuclease to reduce DNA damage after topoisomerase I inhibition. Cancer Res 68:815–825.
Wauters M, Considine RV, Van Gaal LF. 2000. Human leptin: From an adipocyte hormone to an endocrine mediator. Eur J Endocrinol 143:293–311.
Wei D, Le X, Zheng L, Wang L, Frey JA, Gao AC, Peng Z, Huang S, Xiong HQ, Abbruzzese JL, Xie K. 2003. Stat3 activation regulates the expression of vascular endothelial growth factor and human pancreatic cancer angiogenesis and metastasis. Oncogene 22:319–329.
Xiong H, Zhang ZG, Tian XQ, Sun DF, Liang QC, Zhang YJ, Lu R, Chen YX, Fang JY. 2008. Inhibition of JAK1, 2/STAT3 signaling induces apoptosis, cell cycle arrest, and reduces tumor cell invasion in colorectal cancer cells. Neoplasia 10:287–297.
Xu Q, Briggs J, Park S, Niu G, Kortylewski M, Zhang S, Gritsko T, Turkson J, Kay H, Semenza GL, Cheng JQ, Jove R, Yu H. 2005. Targeting Stat3 blocks both HIF-1 and VEGF expression induced by multiple oncogenic growth signaling pathways. Oncogene 24:5552–5560.
Zafirellis K, Agrogiannis G, Zachaki A, Gravani K, Karameris A, Kombouras C. 2008. Prognostic significance of VEGF expression evaluated by quantitative immunohistochemical analysis in colorectal cancer. J Surg Res 147:99–107.
Zhong H, Chiles K, Feldser D, Laughner E, Hanrahan C, Georgescu MM, Simons JW, Semenza GL. 2000. Modulation of hypoxia-inducible factor 1alpha expression by the epidermal growth factor/phosphatidylinositol 3-kinase/PTEN/AKT/FRAP pathway in human prostate cancer cells: Implications for tumor angiogenesis and therapeutics. Cancer Res 60:1541–1545.

Q1: Author: The Journal's copyeditors have taken care to format your authorship according to journal style (First name, Middle Initial, Surname). In the event a formatting error escaped their inspection, or there was insufficient information to apply journal style, please take a moment to review all author names and sequences to ensure the accuracy of the authorship in the published article. Please note that this information will also affect external indexes referencing this paper (e.g., PubMed).

Q2: Author: As per the journal style maximum limit of 45 characters (including space) is allowed for short title. Please reduce the short title accordingly.

Q3: Author: Please check the author names.

Q4: Author: Please provide the volume number and page range.

Q5: Author: Please provide the volume number and page range.

2010

GEOFFREY BEENE CANCER RESEARCH RETREAT

The Cancer Biology and Genetics Program (CBG)
&
The Human Oncology and Pathogenesis Program (HOPP)

April 8 - 9, 2010

Genetic Dissection of the miR-17~92 Cluster of microRNAs in Myc-induced B-cell Lymphomas

Ping Mu,[1,5] Yoon-Chi Han,[1,5] Doron Betel,[2] Evelyn Yao,[1] Massimo Squatrito,[1] Paul Ogrodowski,[1] Elisa de Stanchina,[3] Aleco D'Andrea,[1,4] Chris Sander,[2] and Andrea Ventura [1,6]

[1] Cancer Biology and Genetics Program, Memorial Sloan Kettering Cancer Center, New York, New York 10021, USA;
[2] Computational Biology Center, Memorial Sloan Kettering Cancer Center, New York, New York 10021, USA;
[3] Department of Molecular Pharmacology and Chemistry, Memorial Sloan Kettering Cancer Center, New York, New York 10021, USA;
[4] Department of Surgical and Oncological Sciences, Section of Medical Oncology, Universita` di Palermo, Palermo 90133, Italy

The miR-17~92 cluster is frequently amplified or overexpressed in human cancers and has emerged as the prototypical oncogenic polycistron microRNA (miRNA). miR-17~92 is a direct transcriptional target of c-Myc, and experiments in a mouse model of B-cell lymphomas have shown cooperation between these two oncogenes. However, both the molecular mechanism underlying this cooperation and the individual miRNAs that are responsible for it are unknown. By using a conditional knockout allele of miR-17~92, we show here that sustained expression of endogenous miR-17~92 is required to suppress apoptosis in Myc-driven B-cell lymphomas. Furthermore, we show that among the six miRNAs that are encoded by miR-17~92, miR-19a and miR-19b are absolutely required and largely sufficient to recapitulate the oncogenic properties of the entire cluster. Finally, by combining computational target prediction, gene expression profiling, and an in vitro screening strategy, we identify a subset of miR-19 targets that mediate its prosurvival activity.

[5]These authors contributed equally to this works
[6]Corresponding author

SOCIETÀ ITALIANA DI CITOMETRIA

XXVII CONFERENZA NAZIONALE DI CITOMETRIA
CENTRO CONGRESSI FIERA
FERRARA
14-17 OTTOBRE 2009

EFFECT OF EGF ON VEGF EXPRESSION IN COLON CANCER CELL LINE

Amodeo V.1, Insalaco L.1, Terrasi M.1, D'Andrea A.1, Fanale D.1, La Paglia L.1, Corsini L.R.1, Bazan V.1, Russo A. 1

1Department of Discipline chirurgiche ed Oncologiche, Università degli Studi di Palermo, Palermo, Italy
lab-oncobiologia@usa.net

Background: Epidermal growth factor (EGF) is a key regulating cell survival and several different studies confirmed this role in the pathogenesis of human cancer. Through its binding to epidermal growth factor receptor (EGFR), EGF activates an extensive network of signal transduction pathways. Moreover, this growth factor might be associated with synthesis and secretion of several different angiogenic growth factors, like vascular endothelial growth factor (VEGF). Infact, in several cancer cell lines EGF as well as abnormal activation of EGFR induce VEGF expression. VEGF plays a major role in tumor angiogenesis, infact it is up-regulated in different types of cancer and its expression is inversely correlated with patient survival in many human cancers, including colon carcinomas. Signal transducer and activator transcription 3 (STAT3) has been identified as a major regulator of VEGF expression in glioblastoma and prostate cancer.
Methods: We investigated whether the treatment with EGF in HT-29 cells could induce an increase of VEGF expression like in glioblastoma and prostate cancer cell line. We measured the effects of EGF on the VEGF mRNA levels by Quantitative Real Time-PCR (qRT-PCR) and in parallel we measured secreted VEGF levels by Enzime-Linked Immunosobent Assay (ELISA). Subsequently, we examined the abundance of nuclear STAT3 in HT-29 treated with EGF by Western Blotting and we conduced Chomatin Immunoprecipitation (ChIP) to assess STAT3 binding to specific motifs in the VEGF promoter. Finally, to confirm STAT3 involvement in EGF-induced VEGF mRNA production, we silenced STAT3 expression using RNA interference (siRNA). Moreover, using LY294002, an inhibitor of the phosphoinositide 3-kinase, we investigated whether PI3K pathway is required for VEGF transcriptional regulation.
Results: We found that EGF up-regulates VEGF expression. Our results suggested, also, that STAT3 binds consensus motifs within VEGF promoters under EGF stimulation in colon cancer cells. All these EGF effects were significantly blocked when HT-29 cells were treated with LY294002 or with small interfering RNA (siRNA) targeting STAT3.
Conclusions: This study identified the EGF/PI3K/STAT3 signaling as an essential pathway regulating VEGF expression in EGF-responsive colon cancer cells. This suggests that STAT3 pathways might constitute attractive pharmaceutical targets in colon cancer patients where anti-EGF receptor drugs are ineffective.

EGF DOWNREGULATES EXPRESSION OF CDC25A GENE IN BREAST CANCER CELL LINES

Corsini L.R.1, Fanale D., D'Andrea A., La Paglia L., Amodeo V., Terrasi M., Insalaco L., Perez M., Bazan V., Russo A.
1Department of Discipline Chirurgiche ed Oncologiche, Universita'degli Studi di Palermo, Palermo, Italy
lab-oncobiologia@usa.net

Background: The phosphatase Cdc25A is a major regulator of both G1/S and G2/M transitions during cell cycle progression.
This role appears consistent with the high incidence of its misregulation in cancer; it has been shown that Cdc25A is overexpressed in primary breast tumors and this overexpression is correlated with an increased cell proliferation and with a poor prognosis in patients with breast cancer.
In a previous work the authors have suggested that EGF treatment induced a modest effect on cell proliferation and a transitional G1 arrest in MCF-7 cells.
To evaluate this hypothesis, aim of our study was to identify, through the analysis of gene expression, the main factors involved in this process of cell cycle slowing in breast cancer cell lines.
Methods: A microarray analysis, using Affymetrix GeneChip expression arrays, are performed inMCF-7 and SKBR3 breast cancer cell lines stimulated with epidermal growth factor (EGF), to compare the differential gene expression profile of breast cancer cells treated and untreated controls.
This analysis allowed us to obtain a statistically significant (p-value < 0.05) differential
expression genes, and we selected a set of genes involved in cell cycle progression
and tumor pathogenesis.
Results: We found a down-regulation of *CDC25A* and *E1,E2,D3 cyclins* genes, known to be involved in the G1 phase, both MCF-7 and SKBR3 breast cancer cell lines.
Focusing on *CDC25A* gene, we showed a reduction of mRNA levels and of related protein, by Real-Time RT-PCR and Western Blotting, with a greater reduction in the gene expression and protein levels, higher in MCF-7 cells.
Conclusions: These data suggest that EGF treatment induced a reduction of *CDC25A* expression and, as previously demonstrated, we hypothesize a temporary cell cycle arrest in the G1 phase, that seems to depend on this downregulation.
Therefore, if our results are confirmed by subsequent cytofluorimetric analysis, in the future phosphatase *CDC25A* could be an important therapeutic target in breast cancer and play a key role in the new therapeutic strategies.

ANALYSIS OF GERMLINE GENE COPY NUMBER VARIANTIONS IN PATIENTS WITH SPORADIC PANCREATIC ADENOCARCINOMA

Fanale D.1, Corsini L. R.1, D'Andrea A.1, Terrasi M.1, La Paglia L.1, Amodeo V.1, Bronte G.1, Rizzo S.1, Bazan V.1, Calvo E. L.2, Iovanna J. L.3, Russo A.1

1Department of Discipline Chirurgiche ed Oncologiche, Università degli Studi di Palermo, Palermo, Italy. 2Molecular Endocrinology and Oncology Research Center, CHUL Research Center, Quebec, Canada. 3INSERM U.624, Stress Cellulaire, Parc Scientifique et Technologique de Luminy, Marseille, France.

ab-oncobiologia@usa.net

Background: The rapid fatality of pancreatic cancer is, in large part, the result of a diagnosis at an advanced stage in the majority of patients. Identification of individuals at risk of developing pancreatic adenocarcinoma would be useful to improve the prognosis of this disease. There is presently no biological or genetic indicator allowing detection of patients at risk of developing sporadic pancreatic cancer.

Methods: We analyzed gene copy number variations (CNVs) in leucocyte DNA from 31 patients (24 Europeans and 7 Japanese) with sporadic pancreatic adenocarcinoma and from 93 matched controls. Genotyping was performed with the use of the GeneChip Human Mapping 500K Array Set (Affymetrix). The HapMap database was used as the reference set.

Results: Our main goal was to identify CNVs common to all patients with sporadic pancreatic cancer. We identified 431 SNP probes with abnormal hybridization signal present in the DNA of all 31 patients. Of these SNP probes, 284 corresponded to 3 or more copies and 147 corresponded to 1 or 0 copies. Several cancer-associated genes such as CDC14B, CENPE, EIF2S2, FGF20, FZD10, GTF3C3, KLHL1, NOTCH3, RAB21, TULP3, VSNL1 and ZWINT were amplified in all patients. In addition, several genes supposed to oppose cancer development such as ASH1L, CD9, GRB14, IER3, LPXN, MAP3K7, MDC1, MINK1, SGPL1 and VRK1 were present as single copy in the genome of all 31 patients. Other genes involved in cancer such as BMP1, EGFL11, FLT4, FOSB, KIT, MAP4K4, MYB, PDGFRA, TGFA, AKT3 and KRAS were found amplified in almost all patients, whereas only one allele of the Myc inhibitor PAK2 and ARRB2 was detected in the majority of these patients. The set of the 431 SNP probes with abnormal hybridization signal of patients with sporadic pancreatic cancer was checked in the 93 control patients. None of them showed more than 5% match.

Conclusions: These data suggest that the set of 431 CNVs detected in the DNA of patients with sporadic pancreatic adenocarcinoma is associated to the disease. This CNV set could be used for early diagnosis of individuals with a genetic predisposition to develop a sporadic pancreatic cancer, for understanding the physiopathology of this disease and also to target these genes in a preventive strategy.

Oncology

Oncology 2009;77(suppl 1):132–162
DOI: 10.1159/000258505

EGF Induces STAT3-Dependent VEGF Expression in HT-29 Colon Cancer Cells

V. Amodeo [1], M. Terrosi [1], A. D'Andrea [1], L. Insalaco [1], D. Fanale [1], L. La Paglia [1], L.R. Corsini [1], M. Perez [1], M. Federico [1, 2], G. Bronte [1], S. Rizzo [1], S. Cimino [1], L. Bruno [1], V. Colò [1], V. Agnese [1], M. Messina [1], C.E. Symonds [2], F.P. Fiorentino [1, 2], N. Grassi [3], G. Pantuso [3], M. Frazzetta [4], V. Bazan [1], A. Russo [1, 2]

[1]Sezione di Oncologia Medica, [3]Sezione di Oncologia Chirurgica, [4]Sezione di Chirurgia Generale, Dipartimento di Discipline Chirurgiche ed Oncologiche, Università degli Studi di Palermo, Italy; [2]Sbarro Health Research Organization, Temple University, Philadelphia, USA

Background: Angiogenesis, the sprouting of blood vessels, is a fundamental biological process for tumor growth and metastatic spread. Vascular endothelial growth factor (VEGF) plays a major role in tumor angiogenesis, in fact it is up-regulated in different types of cancer and its expression is inversely correlated with patient survival in many human cancers, including colon carcinomas. In several cancer cell lines VEGF expression is induced by epidermal growth factor (EGF) as well as abnormal activation of epidermal growth factor receptor (EGFR). The VEGF gene promoter contains several regulatory motifs as ERE, CRE, SP-1, AP-2, HRE, and SRE (STAT3-responsive element). Signal transducer and activator transcription 3 (STAT3) has been identified as a major regulator of VEGF expression in glioblastoma and prostate cancer. **Methods:** We investigated the molecular mechanisms by which VEGF expression is regulated in colon cancer cells by EGF. First, we measured the effects of EGF on the VEGF mRNA levels by Quantitative real-time-PCR (qRT-PCR) and in parallel we measured secreted VEGF levels by Enzyme-Linked Immunosorbent Assay (ELISA). Secondary, by Western Blotting, we examined the abundance of nuclear STAT3 in HT-29 treated with EGF and then, to assess STAT3 binding to specific motifs in the VEGF promoter, we conducted Chromatin Immunoprecipitation (ChIP). Finally, to confirm STAT3 involvement in EGF-induced VEGF mRNA production, we silenced STAT3 expression using RNA interference (siRNA). Moreover, using LY294002, an inhibitor of the phosphoinositide 3-kinase, we investigated whether PI3K pathway is required for VEGF transcriptional regulation. **Results:** We found that EGF up-regulates VEGF expression. Our results suggested, also, that STAT3 binds consensus motifs within VEGF promoters under EGF stimulation in colon cancer cells. All these EGF effects were significantly blocked when HT-29 cells were treated with LY294002 or with small interfering RNA (siRNA) targeting STAT3. **Conclusions:** This study identified the EGF/PI3K/STAT3 signaling as an essential pathway regulating VEGF expression in EGF-responsive colon cancer cells. This suggests that STAT3 pathways might constitute attractive pharmaceutical targets in colon cancer patients where anti-EGF receptor drugs are ineffective.

BRCA 1 and BRCA2 Variants of Uncertain Clinical Significance and Their Implications for Genetic Counseling

L. Bruno [1], V. Calò [1], V. Schirò [1], L. La Paglia [1], V. Agnese [1], D. Colcara [1], S. Cimino [1], D. Fanale [1], A. D'Andrea [1], L.R. Corsini [1], V. Amodeo [1], S. Rizzo [1], M. Terrasi [1], G. Bronte [1], D. Bruno [1], D. Piazza [1], E.S. Symonds [2], M. Federico [1, 2], F.P. Fiorentino [1, 2], N. Grassi [3], G. Pantuso [3], M. Frazzetta [4], V. Bazan [1], A. Russo [1, 2]

[1]Sezione di Oncologia Medica, [3]Sezione di Oncologia Chirurgica, [4]Sezione di Chirurgia Generale, Dipartimento di Discipline Chirurgiche ed Oncologiche, Università degli Studi di Palermo, Italy; [2]Sbarro Health Research Organization, Temple University, Philadelphia, USA

Background: Germline mutations in BRCA1/2 genes are responsible for a large proportion of hereditary breast and/or ovarian cancers (HBOC). About one-third of the genetic variant in BRCA1 and 50% of those found in BRCA2, reported by the Breast Cancer Information Core are considered variants of unknown clinical significance, also known as unclassified variants (UVs), because of the uncertainty about their cancer risk. This is often the case for missense variations or when the nucleotide change affects or creates a putative splice-site. In families affected by HBOC syndrome with only an unknown variant identified, it is difficult to determine whether the variant is or not causally linked to predisposition and so it is uninformative for genetic counselling and predictive testing purposes. Presyntomatic testing is not possible in family with an UV, and surveillance can only be based upon the severity of the cancer family history. Actually the methods to discriminate deleterious/high-risk from neutral/low-risk unclassified variants are based on informations about the cosegregation in families of the UVs, comparison of sequence conservation across multiple species, loss of heterozigosity in the tumor, histopathologic characteristic and functional assay, in addiction to biochemical and epidemiological criteria. **Methods:** 141 Sicilian patients with Breast and/or Ovarian Cancer were submitted to both counselling and genetic testing. 121 of these patients were screened for BRCA1 and 86 of them also for BRCA2 mutations in all coding exons and exon-intron boundaries of the genes by automatic direct sequencing. Moreover, we collected a control population consisting of 50 index cases without a familial history of cancer and we analysed this control group for the presence of UVs. **Results:** During these mutational screening we identified five variants of BRCA1 gene (Y179C, F486L, A521T, N550H, V740L) and ten of BRCA2 gene (A22T, Y42C, A2466V, T3013I, T200I, IVS24–16T>C, R2034C, IVS25–12T>G, IVS 2–7T>A, P2639A), classified in BIC database as UVs. Fifty healthy individuals were analyzed but any UVs did not found, suggesting no association of UVs with HBOC. **Conclusions:** We identified fifteen UVs in the BRCA1/2 genes that could contribute to the early onset of breast and/or ovarian cancer. The study of this variants in fifty healthy individuals confirms this hypothesis. For this reason it is difficult to inform carriers about the finding of UVs because of the actual lack of clinical significance. Classification of UVs into deleterious/high risk or neutral/low clinical significance is essential to identify individuals with high risk to develope a breast and/or ovarian tumor. Likely some of UVs detected may have a functional relationship with breast/ovarian cancer development, but this remains to be further explored.

BRCA1 and *BRCA2* Germline Mutations in Sicilian Breast and/or Ovarian Cancer Families and Their Association with Familial Profiles

V. Calò [1], L. Bruno [1], L. La Paglia [1], V. Schirò [1], V. Agnese [1], D. Calcara [1], S. Cimino [1], D. Fanale [1], A. D'Andrea [1], L.R. Corsini [1], V. Amodeo [1], S. Rizzo [1], M. Terrasi [1], G. Bronte [1], D. Bruno [1], D. Piazza [1], Fiorentino F.P. [1, 2], N. Grassi [3], G. Pantuso [3], M. Frazzetta [4], C.E. Symondi [2], M. Federico [1, 2], V. Bazan [1], A. Russo [1, 2]

[1]Sezione di Oncologia Medica, [2]Sezione di Oncologia Chirurgica, [4]Sezione di Chirurgia Generale, Dipartimento di Discipline Chirurgiche ed Oncologiche Università degli Studi di Palermo, Italy; [2]Sbarro Health Research Organization-Temple University-Philadelphia, USA

Background: Germline mutations in *BRCA1* and *BRCA2* genes account for the majority of familial and hereditary cases of breast and/or ovarian cancer (BC and OC). Many highly penetrant predisposition alleles have been identified and include frameshift or nonsense mutation which lead to the translation of a truncated protein. Other alleles contain missense mutations which result in amino acid substitution and intronic variant with splicing effect. The features that indicate increased likelihood of having BRCA mutations are multiple cases of early onset BC, OC (with family history of BC or OC), BC and OC in the same woman, bilateral BC and male BC. We evaluate the contribution of germline *BRCA1/2* mutations in the incidence of hereditary and familial BC and/or OC in Sicilian patients and identify a possible association between the higher frequency of *BRCA1/2* mutations and a specific familial profile. **Methods:** One hundred and forty one BC and OC families were screened for germline mutations in *BRCA1* and eighty-six for germline mutations in *BRCA2* at the 'Regional Reference Center for the Characterization and Genetic Screening of Hereditary Tumors' at the University of Palermo. Each case was selected for personal and/or familial tumoral history according to selection criteria for genetic testing of American Society of Clinical Oncology. In our study we performed a molecular analysis complete coding sequence and the exon-intron boundaries of *BRCA* genes using automatic direct sequencing. **Results:** 141 patients were selected. 121 of them had BC (among which 7 were bilateral), 10 had OC and 5 both tumors. We detected eight pathological mutations (C61G, Y101X, 633delC, 916delTT, R1443X, 5083de19, 4843delC, 5149del4) that lead not functional truncated proteins, identified in 13/141 (9%) families. In eighty-six patients analyzed for *BRCA2* gene we found 8 *BRCA2* pathological mutations (IVS 14 + 6G/A, 6079del4, Q2042X, IVS11–19delAT, 9254del5, V211T, 6079del4, 6310del5) identified in 9/86 (10%) families. The frequency of *BRCA1/2* mutations is 25% (22/86) in our Sicilian population group. According to the analysis of the different familial profiles and also taking into consideration the II degree, the HBOC profile had a major frequency (61%) in 8/13 of *BRCA1* mutation carriers families. 56% (5/9) of *BRCA2* mutation carriers families had HBC profile and 33% (3/9) had MBC profile. **Conclusions:** This is the first study that analyzes the incidence of germinal mutations in *BRCA1/2* gene in patients with familial/hereditary of BC/OC in Sicilian population. Both genes contribute to identify 25% of families with HBOC syndrome. From familial profile analysis it result that family history of BC and OC would be a good predictor to identify *BRCA1* mutation carriers in the Sicilian population, but identification of specific features should address BC/OC patients and their families to genetic counseling and *BRCA1/2* mutational analysis.

Downregulated Expression of Cdc25A Gene in MCF-7 Breast Cancer Cell

L.R. Corsini [1], D. Fanale [1], A. D'Andrea [1], L. La Paglia [1], D. Calcara [1], V. Amodeo [1], M. Terrasi [1], L. Insalaco [1], M. Perez [1], S. Cimino [1], L. Bruno [1], V. Calò [1], V. Agnese [1], V. Schirò [1], G. Bronte [1], S. Rizzo [1], M. Federico [1-3], C.E. Symonds [2], N. Grassi [4], G. Pantuso [4], M. Frazzetta [5], V. Bazan [1], A. Russo [1,2]

[1]Sezione di Oncologia Medica, [4]Sezione di Oncologia Chirurgica, [5]Sezione di Chirurgia Generale, Dipartimento di Discipline Chirurgiche ed Oncologiche, Università degli Studi di Palermo, [3]U.O Radioterapia M. Ascoli Palermo, Italy; [2]Sbarro Health Research Organization, Temple University, Philadelphia, USA

Background: The phosphatase Cdc25A plays an important role in cell cycle regulation both in G1/S and G2/M transitions. This role appears consistent with the high incidence of its misregulation in cancer; it has been shown that Cdc25A is overexpressed in primary breast tumors and that this overexpression is correlated with biological behaviour of breast tumors and with poor survival. A previous work suggests that EGF induced a modest effect on cell proliferation and a transitional G1 arrest in MCF-7 cells. Therefore aim of our study was to identify, through the analysis of gene expression, the main factors involved in the process of cell cycle slowing. **Methods:** We performed a microarray analysis in MCF-7 breast cancer cells, using Affymetrix GeneChip expression arrays, to compare the gene expression profile of MCF-7 treated with epidermal growth factor (EGF) and untreated controls. This analysis allowed us to obtain a statistically significant (p value < 0.05) differential expression of 706 genes, and we selected a set of genes involved in cell cycle progression and tumor pathogenesis. **Results:** We found a down-regulation of *CDC25A*, *E1,E2,D3 cyclins* genes, known to be involved in the G1 phase. Focusing on *CDC25A* gene, we showed a reduction of mRNA level and of related protein by Real-Time RT-PCR and Western Blotting. **Conclusions:** These data suggest that EGF treatment induced a reduction of *CDC25A* expression and, as previously demonstrated, we hypothesize a temporary cell cycle arrest in the G1 phase, that seems to depend on this downregulation. Therefore this indicates that in the future phosphatase *CDC25A* could be an important therapeutic target in breast cancer and play a key role in the new therapeutic strategies.

Analysis of Germline Gene Copy Number Variants of Patients with Sporadic Pancreatic Adenocarcinoma Reveals Specific Variations

D. Fanale [1], L.R. Corsini [1], A. D'Andrea [1], M. Terrasi [1], L. La Paglia [1], V. Amodeo [1], G. Bronte [1], S. Rizzo [1], L. Insalaco [1], M. Perez [1], S. Cimino [1], L. Bruno [1], V. Calò [1], V. Agnese [1], C.E. Symonds [2], M. Federico [1, 4], N. Grassi [5], G. Pantuso [5], M. Frazzetta [6], V. Bazan [1], E.L. Calvo [2], J.L. Iovanna [3], A. Russo [1, 4]

[1]Sezione di Oncologia Medica, [5]Sezione di Oncologia Chirurgica, [6]Sezione di Chirurgia Generale, Dipartimento di Discipline Chirurgiche ed Oncologiche, Università degli Studi di Palermo, Italy; [2]Molecular Endocrinology and Oncology Research Center, CHUL Research Center, Quebec, Canada; [3]INSERM U.624, Stress Cellulaire, Parc Scientifique et Technologique de Luminy, Marseille, France; [4]Sbarro Health Research Organization, Temple University, Philadelphia, USA

Background: The rapid fatality of pancreatic cancer is, in large part, the result of a diagnosis at an advanced stage in the majority of patients. Identification of individuals at risk of developing pancreatic adenocarcinoma would be useful to improve the prognosis of this disease. There is presently no biological or genetic indicator allowing detection of patients at risk of developing sporadic pancreatic cancer. **Methods:** We analyzed gene copy number variations (CNVs) in leucocyte DNA from 31 patients (24 Europeans and 7 Japanese) with sporadic pancreatic adenocarcinoma and from 93 matched controls. Genotyping was performed with the use of the GeneChip Human Mapping 500K Array Set (Affymetrix). The HapMap database was used as the reference set. **Results:** Our main goal was to identify CNVs common to all patients with sporadic pancreatic cancer. We identified 431 SNP probes with abnormal hybridization signal present in the DNA of all 31 patients. Of these SNP probes, 284 corresponded to 3 or more copies and 147 corresponded to 1 or 0 copies. Several cancer-associated genes such as CDC14B, CENPE, EIF2S2, FGF20, FZD10, GTF3C3, KLHL1, NOTCH3, RAB21, TULP3, VSNL1 and ZWINT were amplified in all patients. In addition, several genes supposed to oppose cancer development such as ASH1L, CD9, GRB14, IER3, LPXN, MAP3K7, MDC1, MINK1, SGPL1 and VRK1 were present as single copy in the genome of all 31 patients. Other genes involved in cancer such as BMP1, EGFL11, FLT4, FOSB, KIT, MAP4K4, MYB, PDGFRA, TGFA, AKT3 and KRAS were found amplified in almost all patients, whereas only one allele of the Myc inhibitor PAK2 and ARRB2 was detected in the majority of these patients. The set of the 431 SNP probes with abnormal hybridization signal of patients with sporadic pancreatic cancer was checked in the 93 control patients. None of them showed more than 5% match. **Conclusions:** These data suggest that the set of 431 CNVs detected in the DNA of patients with sporadic pancreatic adenocarcinoma is associated to the disease. This CNV set could be used for early diagnosis of individuals with a genetic predisposition to develop a sporadic pancreatic cancer, for understanding the physiopathology of this disease and also to target these genes in a preventive strategy.

The Proximal Leptin Gene Promoter is Regulated by Pparγ Agonist in MCF-7 and MDA-MB-231 Breast Cancer Cells

M. Terrasi [1], A. D'Andrea [1], V. Amodeo [1], L.R. Corsini [1], D. Fanale [1], L. Insalaco [1], L. La Paglia [1], M. Perez [1], M. Federico [1, 2], C.E. Symonds [2], V. Bazan [1], E. Surmacz [2], A. Russo [1, 2]

[1]Sezione di Oncologia Medica, Dipartimento di Discipline Chirurgiche ed Oncologiche, Università degli Studi di Palermo, Italy; [2]Sbarro Health Research Organization, Temple University, Philadelphia, USA

Background: The obesity hormone leptin, initially discovered as a cytokine controlling food intake and energy balance, has recently emerged as a potent regulator of different physiological and pathological processes, including cancer development and progression. The importance of leptin signaling in breast tumorigenesis has been confirmed by the fact that breast tumors overexpress both leptin and its receptor, both of which correlate with higher tumor grade and worse prognosis. In vitro studies demonstrated that breast cancer cells are able to synthesize leptin in response to obesity-related stimuli, like hyperinsulinemia and hypoxia. This process is mediated through interactions of Sp-1, a nuclear factor that mediates the effects of insulin and/or HIF-1, the master transcription factor in cellular response to oxygen deficiency, with specific motifs within the leptin gene promoter. Considering that in adipocytes leptin promoter is regulated by the activation of peroxisome proliferator activated receptor (PPAR) γ, we studied whether or not ciglitazone, a PPAR-γ ligand, used for treatment of patients with diabetes and obesity and a potential anti-neoplastic agent, can modulate the expression of leptin mRNA in breast cancer cells. **Methods:** We used chromatin immunoprecipitation (ChIP), to treat of MCF-7 and MDA-MB-231 breast cancer cells with submolar concentrations of ciglitazone. Real Time PCR, Western blotting as well as growth experiments were used to confirm previous experiments. **Results:** Using chromatin immunoprecipitation (ChIP), we found that treatment of MCF-7 and MDA-MB-231 breast cancer cells with submolar concentrations of ciglitazone induced binding of PPAR-γ to the proximal portion of the leptin promoter, while it decreased the association of Sp-1 with this DNA region. Results obtained with Real Time PCR, Western blotting as well as growth experiments confirmed that these effects coincided with elevated leptin mRNA expression, protein synthesis and increased cell proliferation. The mitogenic effects of ciglitazone were not observed when higher doses of the drug were used. **Conclusions:** These data suggest that one of the mechanisms of leptin overexpression in breast tumors might involve activation of PPAR-γ with submolar concentrations of ciglitazone.

Index